THE INHIBITORY IMPACT OF GERANYLGERANIOL ON THE DIFFERENTIATION OF MURINE 3T3-F442A PREADIPOCYTES

A DISSERTATION

SUBMITTED IN PARTIAL FULFILLMENT OF THE REQUIREMENTS

FOR THE DEGREE OF DOCTOR OF PHILOSOPHY

IN THE GRADUATE SCHOOL OF THE

TEXAS WOMAN'S UNIVERSITY

DEPARTMENT OF NUTRITION AND FOOD SCIENCE

COLLEGE OF HEALTH SCIENCES

BY

MANAL ELFAKHANI, B.S., M.S.

DENTON, TEXAS

MAY 2013

DEDICATION

This dissertation is dedicated to my mother, Hana, whose support, encouragement and constant love has sustained me throughout mylife.

I also dedicate this work to my sweet daughters, Lana and Sarah, whose births have lit up my life and inspired me to be the best at whatever I do.

ACKNOWLEDGMENTS

So many people have helped me throughout these past six years, without whom this doctoral journey would not have been so rewarding, enjoyable, and even possible. First and foremost, I thank God for the numerous blessings He has bestowed upon me throughout my life and for giving me this opportunity and the perseverance to fully benefit from it, personally and professionally.

I would like to express my sincere gratitude to my advisor Professor Huanbiao Mo for the continuous support he has given me throughout my doctoral study and research; for his supervision, motivation, enthusiasm, and vast knowledge. His mentorship was paramount to providing me with a well-rounded and stimulating research experience. I would like to thank the rest of my dissertation committee: Dr. Nancy DiMarco, Dr. Parakat Vijayagopal and Dr. Dianna Hynds for their valuable comments and insightful suggestions. I particularly thank Dr. Nathaniel Mills for his support during these years; his guidance helped me tremendously with the experimental procedures and the analysis of the results.

I would like to express my deepest thanks to the faculty and staff in the Department of Nutrition and Food Sciences at Texas Woman's University for all your help and support these past few years, the Department Chair Mr. Ronald Hovis for his support and the Department Staff, Estee Easley and Marcella Ettinger for their assistance and for always being such a pleasure to work with. Warm thanks to Dr. Dibyendu Dutta

for always going out of his way to help me with my procedures; his guidance will not be forgotten. I especially thank my dear friend, Dr. Deema Hussein, for the endless support she has given me over the years. Her advice was always so insightful and caring; I will forever cherish our friendship.

I thank my fellow lab mates, Sonia, Anureet, Hoda and Sheida, for the enjoyable group work, stimulating discussions and fun times in the lab. Also, I would like to acknowledge my previous lab mates, Nicolle, Rajshekar, Praveen, Jegghna, Renee, Ivan, Rachelle, Sarah and Sara; we had some really great times and I will always treasure them. Among friends at TWU, I would like to thank Kathleen, Mindy, Casey, Affifa, Kasturi, Shivani,, Chelsea, Rebecca, Melanie, Shamali and Shradha. And my loving cousins Dania, Dana, Wisam, Mona, Halah, Eman, Noor, Nissreen and Zana and my caring aunts Hiam and Beth and dear uncle Basem, I graciously thank you all for your words of encouragement over the years.

I thank my parents, Said and Hana, for their faith in me and encouraging me to be as ambitious as I could be. It was with their love and faith that I developed the drive to tackle challenges head on. My dear brothers, Mohamed, Mazen and Mostafa, your love and wise words were always such an inspiration and I truly thank you for always being there for me and lending an ear. And my loving sister-in-law Maha and my sweet niece Dalia and precious nephew Saeed, I thank you for all of the joy you have brought to my life. Also, I thank my mother-in-law, Najat, for her constant love and support she has shown me throughout these years of study. Her continuous words of kindness and

encouragement have been so uplifting and I will forever be grateful for all of the assistance that she has provided our family during the times of difficulty. I also thank my husband's aunt, Fatima, and his siblings, Bilal, Rouba and Wissam for their endless motivation throughout this journey.

Finally, and most importantly, I would like to thank my loving, supportive, motivating and patient husband Wael, whose faithful support throughout this doctoral degree, especially during its final stages, is so appreciated. Wael and my children, Lana and Sarah have been such an inspiration to me. Especially my sweet Lana, you have been my best friend and the greatest source of joy during this journey. My precious Sarah, you have been our little angel, joining us near the completion of this degree. I give my deepest expression of love and appreciation for the encouragement that you gave and the sacrifices you made during this graduate program. Thank you for the support and company during late nights of work. Your support, encouragement, quiet patience and unwavering love are so dear to my heart.

ABSTRACT

MANAL ELFAKHANI

THE INHIBITORY IMPACT OF GERANYLGERANIOL ON THE DIFFERENTIATION OF MURINE 3T3-F442A PREADIPOCYTES

MAY 2013

The use of statins, competitive inhibitors of 3-hydroxy-3-methylglutaryl coenzyme A (HMG-CoA) reductase, is possibly associated with insulin resistance. This potential effect of statins is presumably due to the impaired differentiation and diminished glucose utilization of adipocytes. The role of HMG-CoA reductase inhibition and mevalonate deprivation is not clear in the statin-mediated inhibition of adipocyte differentiation. There is also a need to evaluate the effect of other HMG-CoA reductase suppressors, particularly phytochemicals, on adipocyte differentiation.

Mevalonate depletion is hypothesized to mediate the effect of lovastatin on adipocyte differentiation. In addition, geranylgeraniol, a diterpene shown to accelerate the degradation of HMG-CoA reductase, mimics the impact of lovastatin in adipocytes by suppressing adipocyte differentiation and adipogenic gene expression.

The impact of lovastatin and geranylgeraniol, on the differentiation of murine 3T3-F442A adipocytes, were evaluated. Adipo-Red assay and oil Red O staining showed that a 7 day incubation with 1.25 - 10 μmol/L lovastatin and 2.5 - 20 μmol/L geranylgeraniol reduced the intracellular triglyceride content of the cells in a dose-

dependant manner. Concomitantly, lovastatin and geranylgeraniol each down-regulated the expression of peroxisome proliferator-activated receptor γ (*Pparγ*), a key regulator of adipocyte differentiation; as analyzed by real-time qPCR. The expression of adipocyte marker genes including sterol regulatory element-binding protein 1 (SREBP1), adiponectin, leptin, and fatty acid binding protein 4 was suppressed by lovastatin. Mevalonate (500 μmol/L) reversed the effect of lovastatin on intracellular triglyceride content and gene expression. The expression of SREBP1, adiponectin, leptin, fatty acid binding protein 4, fatty acid synthase, glycerol-3-phosphate dehydrogenase and glucose transporter 4 was also suppressed by geranylgeraniol. Mevalonate-derived metabolites have essential roles in promoting adipocyte differentiation and adipogenic gene expression. Dietary mevalonate suppressors may have potential as anti-adipogenic compounds.

TABLE OF CONTENTS

LIST OF TABLES

Table Page

LIST OF FIGURES

Figure Page

CHAPTER I

INTRODUCTION

Adipogenesis involves a number of transcriptional factors. Complex interactions of these factors control the expression of hundreds of adipogenic genes (Morrison andFarmer, 1999). These transcription factors include, but are not limited to peroxisome proliferator-activated receptor γ (*Pparγ*), the CCAAT enhancer-binding protein (C/EBP) family (Farmer, 2006) and adipocyte determination and differentiation factor-1 (ADD1)/sterol regulatory element-binding protein 1c (*SREBP1c*) (Rosen andSpiegelman, 2000). Mature adipocytes are also characterized by the presence of lipoprotein lipase (*LPL*), insulin induced gene 1 (*INSIG1*), and fat specific genes (fatty acid binding protein 4 (*Fabp4*), stearoyl CoA desaturase 1 (SCD-1), glycerol-3-phosphate dehydrogenase (*GPDH*)), insulin-mediated glucose uptake and metabolism and markers of terminal differentiation (glucose transporter type 4 (*GLUT4*), fatty-acid synthase (*Fasn*)) (Krapivner et al., 2008). The only commonly recognized marker for preadipocytes is preadipocyte factor 1 (Pref-1) (Villena et al., 2002).

Due to the complexity of studying adipocyte differentiation *in vivo*, a great part of our knowledge of the process of adipocyte differentiation and the factors involved have been acquired from the extensive work done on *in vitro* models of adipogenesis. Among

the different *in vitro* models of adipogenesis, the 3T3 preadipocyte cell line is one of the most well-established and dependable models (Wood, 2008).

The differentiation of fibroblasts to adipocytes is a complex process requiring the activation of signaling pathways including those mediated by insulin, insulin like growth factor (IGF)-1, Ras protein and *Pparγ*2 (Fernyhough et al., 2007). Insulin is an important activator of preadipocyte differentiation. The activation of Ras proteins is followed by the activation of *Pparγ* which promotes preadipocyte differentiation and insulin sensitivity and suppresses adipocyte lipolysis. The cross-activation of *Pparγ*2 and *C/EBPα* up-regulates preadipocyte differentiation by activating the expression of various genes required for acquiring the preadipocyte phenotype such as *Fabp4*, *GLUT4*, *LPL* and leptin (Tontonoz et al., 1994a). Further stimulation of *Pparγ* can occur through an indirect manner with SREBP/ADD1 which stimulates even more genes associated with adipogenesis including SCD-1 and *Fasn* (Brown andGoldstein, 1997). *INSIG1*, a *Pparγ* target gene, is an important regulator in the processing of the SREBPs and is regulated by *Pparγ* (Kast-Woelbern et al., 2004).

Another SREBP responsive enzyme is 3-hydroxy-3-methylglutaryl coenzyme A (HMG-CoA) reductase, a vital component of the mevalonate pathway. The mevalonate pathway produces sterol (cholesterol) and non-sterol (isoprenoid) products that have various functions in the human body. There are two specific enzymes in the mevalonate pathway that are important for the function of the insulin signaling pathway consequently leading to adipocyte differentiation. HMG-CoA reductase and geranylgeranyl-

pyrophosphate (GGPP) synthetase activities provide prenyl pyrophosphates in the form of GGPP and farnesyl pyrophosphate (FPP) that are required for the modification and biological activity of the IGF-1 receptor and Ras, respectively (Goldstein andBrown, 1990), ultimately leading to the activation of *Ppar*γ2 and adipogenesis. Insulin stimulates the mevalonate pathway which modifies p21Ras in fibroblasts (Goalstone andDraznin, 1996). When fibroblasts undergo differentiation to mature adipocytes, the mRNA expression of GGPP synthetase increases by more than 20-fold and fatty acid synthase expression increases by 80% (Vicent et al., 2000).

The mevalonate pathway can be suppressed by the use of HMG-CoA reductase inhibitors (mevalonate suppressors). It is believed that by down regulating HMG-CoA reductase activity, pools of FPP and GGPP will be limited, thereby attenuating preadipocyte differentiation into adipocytes (Figure 1). Mevalonate suppressors including the statins are competitive inhibitors of HMG-CoA reductase and synthesis of isoprenoids. Statins, widely prescribed cholesterol-lowering drugs, clearly suppress preadipocyte differentiation in a dose-dependent manner (Mauser et al., 2007; Nakata et al., 2006; Nicholson et al., 2007; Nishio et al., 1996). However, it is unclear whether the statin effect is due to mevalonate depletion or other properties of statins. In addition, emerging evidence suggests that statins may have adverse side effects such as elevated liver enzymes, muscle problems, cognitive loss, pancreatic dysfunction, hepatic dysfunction and neuropathy (Golomb andEvans, 2008). In addition, a recent study

shows an increased risk of developing diabetes for patients taking statins compared to those given a placebo (Sattar et al., 2010).

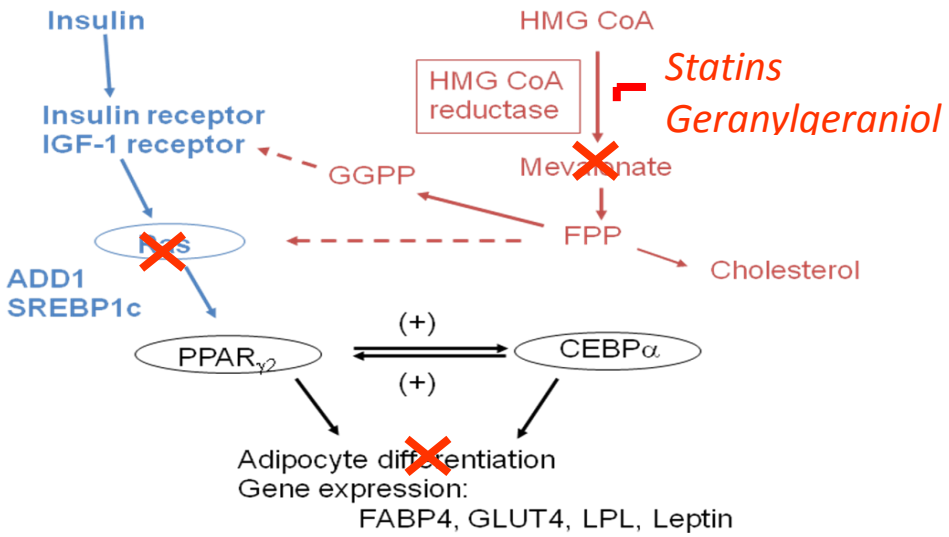

Figure 1: The mevalonate pathway provides essential intermediates for the signaling pathway in adipocyte differentiation. Inhibition of the mevalonate pathway by statins and geranylgeraniol leads to suppression of adipogenesis.

Isoprenoids are plant products that are derived from the mevalonate pathway that down-regulate HMG-CoA reductase and block the synthesis of FPP and GGPP, products that play important roles in preadipocyte differentiation. Geranylgeraniol is a diterpene alcohol found in linseed and peanut oil (Fedeli et al., 1966). Geranylgeraniol has been shown to down-regulate HMG-CoA reductase (Katuru et al., 2011). However, the potential role of geranylgeraniol in down-regulating HMG-CoA reductase or the insulin signaling pathway is still unclear and either or both may consequently disrupt preadipocyte differentiation.

Purpose of the Study

The purpose of this study was to evaluate the effect of geranylgeraniol on adipocyte differentiation. Moreover, underlying mechanisms of the impact of geranylgeraniol was to be examined through adipogenic gene expression.

Statement of Hypothesis

Geranylgeraniol suppresses the differentiation of murine 3T3-F442A preadipocytes by down regulating the expression of adipogenic transcriptional factors associated with the mevalonate pathway and the insulin signaling pathway, pathways that promote adipogenesis, thus decreasing lipid accumulation and inhibiting adipocyte maturation.

Scope of the Study

Adipogenesis of murine 3T3-F442A preadipocytes, characterized by triglyceride accumulation, was measured by Oil Red O staining and the AdipoRed assay. The expression of genes involved in adipogenesis was determined by reverse transcription quantitative real-time polymerase chain reaction (qRT-PCR). In addition, cell viability and apoptosis were measured by CellTiter 96® Aqueous One Solution MTS (3-(4,5-dimethylthiazol-2-yl)-5-(3-carboxymethoxyphenyl)-2-(4-sulfophenyl)-2H-tetrazolium) assay and the acridine orange/ethidium bromide (AO/EB) dual staining assay, respectively. We also investigated the effect of geranylgeraniol on (1) the mevalonate

pathway, (2) the insulin signaling pathway, and (3) fatty acid metabolism by examining the mRNA levels of key enzymes involved in these pathways.

Limitations of the Study

Further examination of specific mechanisms of action involved in the impact of geranylgeraniol on suppressing preadipocyte differentiation may be necessary. Western Blot analysis of the geranylgeraniol treated preadipocytes would provide useful insight into the detection of specific proteins involved in the adipogenesis process. Also, assessment of the potential reversal of the effect of geranylgeraniol by mevalonate, at physiologically acceptable levels, warrants additional investigation.

Other limitations of this study are those related to *in vitro* research, including: the finite doubling potential of normal cells and the propensity of some cultured cells to change their morphology**,** functions or array of genes that they express (Hunter-Cevera, 1996). Moreover, it can sometimes be difficult to extrapolate from the results of an *in vitro* study to the biology of a whole organism (Rothman, 2002), requiring future studies to examine the impact of geranylgeraniol on animal adipose tissue regulation *in vivo*.

Significance of the Study

To our knowledge, no research has explored the potential role of geranylgeraniol as an anti-adipogenic compound. This study will help to understand the role of geranylgeraniol in down-regulating HMG-CoA reductase and the insulin signaling pathway and the subsequent effect on preadipocyte differentiation. The results from this

study offer insight into the impact of geranylgeraniol on the expression of genes involved in the adipogenic process.

CHAPTER II

REVIEW OF LITERATURE

The Obesity Epidemic

Obesity has become a worldwide epidemic and one of the major public health concerns in developed countries (Caballero, 2007). In 2008, the World Health Organization reported that there are 1.4 billion overweight adults with 500 million of them considered obese. As of 2011, there are more than 40 million children under the age of five who are classified as overweight (WHO) . Many industrialized countries have experienced these increases, but the United States by far, has the greatest prevalence of obesity among its population with 68.8% of adults (Flegal et al., 2012) and 31.8% of children (Ogden et al., 2012) being overweight or obese . If this trend persists, it is projected that by 2015, 75% of adults in the United States will be considered overweight while 41% will be deemed obese (Wang andBeydoun, 2007).

Medical risk is positively associated with the degree of obesity (Kissebah andKrakower, 1994; Romero-Corral et al., 2006). Being classified as overweight or obese is associated with an increased risk of a variety of metabolic diseases such as coronary heart disease, type 2 diabetes, cancer (endometrial, breast, and colon), hypertension, dyslipidemia, stroke, liver and gallbladder disease, sleep apnea and respiratory problems, osteoarthritis and gynecological problems (Badman andFlier, 2007; NIH, 1998). Worldwide, obesity is one of the leading preventable causes of deaths and is

believed toclaim 111,909 to 365,000 lives a year (Allison et al., 1999; Haslam andJames, 2005). Overweight and obesity and their accompanying health complications constitute a substantial economic toll on the U.S. health care system (USDHHS, 2001). In 2008, medical care costs attributable to obesity were estimated to be as high as $147 billion in the United States (Finkelstein et al., 2009) .

The Etiology of Obesity

Obesity is defined as a medical condition that involves the development of an overabundance of excess body fat (Badman andFlier, 2007). While the notion that obesity simply occurs when energy input exceeds energy expenditure is widely perceived, in reality, bodily energy reserves are directed by complex systems that control food intake and energy expenditure (Badman andFlier, 2007). The development of obesity involves noticeable changes in adipocyte gene expression that affects several pathways and secretory functions thus dysregulating cellular homeostasis (Rajala andScherer, 2003).

Fundamental to the pathology of obesity is the occurrence of hypertrophy and hyperplasia of adipocytes. Hypertrophy signifies increased cell size whereas hyperplasia refers to the mobilization and proliferation of preadipocytes and their subsequent differentiation to adipocytes (Gesta et al., 2007). Modulation of body fat storage through adipogenesis and adipocyte lipolysis ultimately controls the number and size of adipocytes (Flier, 2004). The most important health concerns associated with adipocyte

development are due to the extreme abnormality in adipocyte cell number that occurs (Ntambi andYoung-Cheul, 2000).

In recent years, there has been a strong research interest in the area of adipocyte development. Since adipocytes play an important role in various physiological and pathological pathways, they can no longer be perceived as inert cells whose solitary function is to store lipids (Morrison andFarmer, 1999). Adipose tissue is an important target in preventing and treating common diseases (Kawada et al., 2008; Ntambi andYoung-Cheul, 2000). Fat accumulation and adipocyte differentiation are closely associated with the occurrence and advancement of several metabolic diseases including obesity, diabetes mellitus (type 2), cardiovascular disease, hypertension, sleep apnea and muscular-skeletal issues (Ahima andFlier, 2000; Otto andLane, 2005). A comprehensive understanding of the progression of adipocyte differentiation is needed to manipulate adipocyte cell number to control certain diseases (Gesta et al., 2007).

To recognize and control the mechanisms that lead to obesity, we must study the molecular events that regulate preadipocyte differentiation to adipocytes since they are the major cellular component of adipose tissue.

Adipose Tissue and the Adipocyte

Adipose tissue is specialized connective tissue that is situated underneath the skin (subcutaneous fat) to provide insulation from extreme hot and cold and conserve body temperature (Fonseca-Alaniz et al., 2007). It can also be found intra-abdominally surrounding internal organs (visceral fat) for protective padding, in bone marrow (yellow

bone marrow) and within breast tissue. Regions where adipose tissue is located are described as “adipose depots”. Under ordinary circumstances, adipose depots supply feedback for hunger to the brain. The location of the fat and its distribution plays an important role in metabolic risk. Excess intra-abdominal/visceral fat (central or above the waist obesity) leads to a high risk of metabolic disease, but increased subcutaneous fat in the thighs and hips (peripheral or below the waist obesity) poses little or no risk (Kissebah andKrakower, 1994; Romero-Corral et al., 2006).

Adipose tissue has many small blood vessels and is composed of conjunctive tissues (collagen and reticular fibers), nerve fibers, lymph nodes, vascular stroma (mesenchymal stem cells), immune cells (leukocytes and macrophages) and endothelial cells (Ahima andFlier, 2000). These numerous cell types compose nearly 50% of the total cellular content (Trayhurn, 2007). Adipose tissue also contains fibroblasts and preadipocytes—undifferentiated adipocytes—but its primary and most abundant component are the fat-containing adipocytes (Ahima andFlier, 2000; Trayhurn, 2007).

In mammals, there are two distinct types of adipose tissue: white adipose tissue and brown adipose tissue. Mature white adipocytes store triglycerides in one large lipid droplet in the cell core accounting for 85-90% of the mass of the cell and pushing the cytoplasm, nucleus and other organelles to the sides where they reside in a thin layer of cytosol (Fonseca-Alaniz et al., 2007). During development, young adipocytes enclose multiple small lipid droplets. However, as the cell matures, these droplets join together to form a single large lipid droplet whose size can change vastly depending on the

magnitude of triglyceride accumulated (Pond, 2001). Even though there are many cell types all over the body which accumulate lipid, adipocytes are morphologically distinct due to their large lipid droplets coated by the protein, perilipin (Greenberg et al., 1991).

The main function of white adipose tissue is to be a primary storage site for lipid in the human body in the form of triglycerides in the adipocyte (Kawada et al., 2001). Adipose tissue is the body's largest energy reservoir (Otto andLane, 2005). When necessary, white adipose tissue resupplies energy by mobilizing lipids through lipolysis, leading to the release of free fatty acids and glycerol (Ahima andFlier, 2000). Lipids can be burned to meet the energy needs of the body. Humans, like many other members of the animal kingdom, have developed methods to store energy through times of extra caloric intake for future necessity (Gesta et al., 2007), which makes the adipose tissue the most important buffer system for energy balance (Fonseca-Alaniz et al., 2007). On the other hand, brown adipose tissue is specialized to metabolize fatty acids (Park et al., 2008) and has highly developed thermogenic functions (Kawada et al., 2001). Brown adipose tissue is believed to be non-existent in the adult human but can be found in fetuses and newborn infants (Fonseca-Alaniz et al., 2007). However, emerging research demonstrates that defined regions of functional brown adipose tissue have been detected in adult humans and that it was inversely correlated with Body Mass Index (BMI) (Cypess et al., 2009).

Adipose tissue is a highly active metabolic and endocrine organ playing a key role in the regulation of metabolism and homeostasis via paracrine and endocrine functions

(Otto andLane, 2005). Adipose tissue secretes important factors termed adipokines (adipocytokines) that circulate in the blood and act on distal tissues influencing food intake, energy expenditure, carbohydrate and lipid metabolism, reproductive function and insulin secretion and sensitivity (Flier, 2004; Otto andLane, 2005). Some examples of these cytokines (cell to cell signaling proteins) include: adiponectin and resistin (glucose metabolism), leptin (feeding behavior), chemerin and cholesteroyl ester transfer protein (CETP; lipid metabolism), apelin (insulin signaling), retinol binding protein 4 (RBP4; insulin resistance), visfatin (insulin sensitivity), tumor necrosis factor-alpha (TNFα) and Interleukin-6 (IL-6) (inflammation), plasminogen activator inhibitor-1 (PAI-1) (coagulation) and angiotensinogen and angiotensin II (blood pressure) (Boucher et al., 2005; Bozaoglu et al., 2007; Fukuhara et al., 2005; Otto andLane, 2005). The dysregulation of adipokine expression is considered to be an important factor in the pathogenesis of obesity (Waki andTontonoz, 2007).

Two adipokines particularly important for adipose tissue and adipocyte development are adiponectin and leptin. Adiponectin is the most abundant protein produced by the adipose tissue. The gene for adiponectin (AdipoQ, apM1, ACRP30) was first identified in 1995. Adiponectin is a 30kDa protein and increased levels are associated with improved insulin sensitivity, alteration of the effects of nuclear factor Kappa B (NFκB) and inhibition of tumor necrosis factor alpha (TNF-α). An inverse correlation has been observed between levels of adiponectin in circulation and insulin resistance, cardiovascular disease and obesity risk. Circulating levels of adiponectin are

negatively correlated with the degree of obesity and increasing concentrations are observed with weight loss. Low adiponectin levels have been associated with increased insulin resistance and hyperinsulinemia. Thiazolidinediones (TZDs), a class of drugs used in the treatment of Diabetes Mellitus type 2, stimulate the secretion of adiponectin. Two adiponectin receptors have been recognized. Adiponectin Receptor 1 (ADP-R1) is mainly expressed in muscle whereas adiponectin receptor 2 (ADP-R2) is largely expressed in the liver. The biological effects of the protein depend on circulating blood concentrations and the particular tissue (Fonseca-Alaniz et al., 2007). Adiponectin in circulation (2 – 10μg/mL) does not greatly fluctuate which implies that it is regulated by long term metabolic changes (Fonseca-Alaniz et al., 2007; Park et al., 2004). Women have been observed to have higher levels compared to men, (Fonseca-Alaniz et al., 2007) despite their higher body fat percentages (Snijder et al., 2006). The correlation between low adiponectin levels and increased risk of metabolic syndrome, howevever, might be stronger in women compared to men (Eglit et al., 2012).

Leptin, another important adipokine, is a 16 kDa protein with a central role in the regulation of energy balance, acting on the hypothalamus of the brain to induce satiety. It was discovered in 1994 when a strain of obese mice termed ob/ob demonstrated a genetic defect which prevented the production of this protein (Trayhurn, 2007). It was originally thought that leptin functioned as a signal that prevented obesity because leptin-deficient ob/ob mice and leptin-resistant db/db mice are obese (Fried et al., 2000). Serum leptin levels are positively correlated with body mass index, percentage of body fat and body fat

mass (Considine et al., 1996). Levels of leptin are typically elevated in obese individuals (Considine et al., 1996). The positive association between total body fat mass and serum leptin can be explained by the fact that large fat cells release more leptin compared to small fat cells (Lonnqvist et al., 1997). Leptin secretion is up to seven times higher in obese subjects compared to lean subjects mainly because fat cell size is typically 2 – 4 times larger in the former (Fried et al., 2000). A lean individual typically has 5-15 ng/ml of leptin in circulation (Yang andBarouch, 2007). However, some obese subjects have markedly lower or higher leptin levels than what would be presumed from their body fat, which implies that there are other mechanisms regulating serum leptin (Fried et al., 2000).

Leptin notifies the brain about body fat accumulation to alter feeding behavior (Yang andBarouch, 2007). It stimulates satiety by binding to leptin receptors (Ob-R) in the basomedial region of the hypothalamus, inducing neurons to synthesize pro-opiomelanocortin (POMC). POMC is cleaved to generate α-melanocyte stimulating hormone (αMSH), which binds downstream melanocortin receptors (MC-3 and MC-4) and ultimately inhibits nutritional intake and reducing body fat mass (Schwartz et al., 2000). Leptin inhibits the expression of neuropeptide Y (NPY) and the agouti peptide (AgRP), both of which are involved in enhancing nutritional intake and reducing energy consumption while triggering lipogenic enzymes in the adipose tissue and liver (Schwartz et al., 2000). Leptin also activates adenylcyclase which in turn increases the oxidation of lipids in the skeletal muscles and decreases the synthesis of triglycerides in the liver

(Fonseca-Alaniz et al., 2007). Leptin expression is stimulated by overfeeding, insulin, glucocorticoids, cytokines, TNFα, estrogens and CCAAT/enhancer-binding protein-α (*C/EBP*α) and decreased by fasting, 3-adrenergic activity, androgens, free fatty acids, growth hormone, peroxisome proliferator-activated receptor-γ (*Ppar*γ) agonists, thyroid hormone and cold weather (Margetic et al., 2002; Yang andBarouch, 2007).

Adipose Tissue: Origin and Transcriptional Regulation

Adipose tissue, similar to bone and muscle, is considered to be of mesodermal origin. The initial step in the formation of the mesoderm during gastrulation—one of the early phases of embryonic development—is the migration of a layer of germ cells between the primitive endoderm and ectoderm cell layers. A large part of our knowledge of these events is taken from studies using a multipotent stem cell line, C3H10T1/2, isolated from 14 - 17 day old C3H mouse embryos (Gesta et al., 2007). Bone morphogenetic protein-2 (BMP2) and Bone morphogenetic protein-4 (BMP4) and some of the transforming growth factor β superfamily are cytokines shown to induce the commitment of C3H10T1/2 stem cells to adipocyte lineage (Huang et al., 2009).

Mesenchymal stem cells have the ability to differentiate into adipocytes, osteoblasts, chondrocytes, myoblasts, and connective tissue. They give rise to a common early precursor termed ‘adipoblast’ that sequentially develops into committed white and brown preadipocytes. Under suitable conditions, these preadipocytes are stimulated to differentiate into mature adipocytes of distinct type: subcutaneous white fat, visceral white fat and brown fat. No unique markers have been identified for these precursor cells

thus making it unclear if there are separate adipoblasts and/or preadipocytes for brown and white fat or if there are different white preadipocytes for different white adipose tissue (Gesta et al., 2007).

Adipogenesis, the process in which preadipocytes differentiate into mature adipocytes, entails four stages: growth arrest, clonal expansion, early differentiation and terminal differentiation (Gesta et al., 2007). This transition involves a number of transcriptional factors, which through complex interactions, control the expression of hundreds of adipogenic genes required for glucose metabolism, insulin sensitivity, changing cell morphology, expression/secretion of adipogenic products and the emergence of lipid droplets in the cytoplasm (Morrison andFarmer, 1999). These transcription factors include, but are not limited to, peroxisome proliferator-activated receptor γ (*Pparγ*), the CCAAT enhancer-binding protein (C/EBP) family (Farmer, 2006; Morrison andFarmer, 1999) and adipocyte determination and differentiation factor-1 (ADD1)/sterol regulatory element-binding protein 1c (SREBP1c) (Rosen andSpiegelman, 2000). Mature adipocytes are characterized by the presence of these transcription factors and several different indicators such as leptin, lipoprotein lipase (*LPL*), insulin induced gene 2 (INSIG-2), fat specific genes [fatty acid binding protein 4 (*Fabp4*), stearoyl CoA desaturase 1 (SCD-1), glycerol-3-phosphate dehydrogenase (*GPDH*)], insulin-mediated glucose uptake and metabolism and markers of terminal differentiation (glucose transporter type 4 (*GLUT4*), fatty-acid synthetase,) (Dani et al., 1989; Krapivner et al., 2008; Rosen andMacDougald, 2006; Tontonoz et al., 1994b).

On the contrary, preadipocytes are quite similar to other fibroblast-like cells, making them difficult to identify and study (Gesta et al., 2007). The only commonly recognized marker is preadipocyte factor 1 (Pref-1) also known as Drosophila Homolog-like 1 (DLK-1) (Villena et al., 2002). They are members of the Notch/Delta/Serrate family that have epidermal growth factor-like repeats responsible for inhibiting adipocyte differentiation. They are transmembrane proteins cleaved to produce a soluble 50 kDa form. They are greatly expressed in undifferentiated preadipocytes and diminished during the differentiation process into mature adipocytes. Pref-1 deficient mice have rapid fat deposition, while mice with greater Pref-1 levels have decreased fat mass and adipogenic gene expression (Gesta et al., 2007).

The role of *Pparγ* in adipogenesis has been extensively studied. *Pparγ* is a member of the nuclear hormone receptor subfamily which binds to the peroxisome proliferator response elements on the DNA sequence controlling the transcription of genetic information from DNA to mRNA (Latchman, 1997). Other members of the *Ppar* family include *Pparα* and *Pparδ*. *Pparα* induced adipogenesis occurs at a slower pace and leads to a lesser percentage of differentiated cells compared to *Pparγ* and cells expressing *Pparδ* did not differentiate (Brun et al., 1996). Pparγ is transcribed from the *Pparγ* gene and through alternative splicing and promoter usage, two isoforms (*Pparγ*1 and *Pparγ*2) are produced (Berger andMoller, 2002; Farmer, 2006; Gesta et al., 2007). *Pparγ*1 is expressed in many tissues including adipose tissue, yet *Pparγ*2 expression is almost exclusively found in adipose tissue making it a specific marker of fat (Farmer,

2006). However, knockout of *Pparγ*2 in mice shows that they still have some white adipose tissue, signifying that *Pparγ*1 can have the ability to compensate for *Pparγ*2 loss (Rosen andSpiegelman, 2006). Ectopic expression of *Pparγ* in non-adipogenic murine fibroblasts can initiate adipogenesis, producing mature adipocytes (Tontonoz et al., 1994c) and that *Pparγ* is necessary in maintaining differentiated adipocytes in their terminal state (Gesta et al., 2007).

All Ppar receptors have a specific endogenous ligand (Brun et al., 1996) and these include free fatty acids and eicosanoids (Marlow et al., 2009). Synthetic and naturally occurring ligands for *Pparγ* have been recognized and are capable of binding and activating *Pparγ*, subsequently leading to adipocyte differentiation (Forman et al., 1995). *Pparγ* induces adipocyte differentiation in reaction to numerous *Pparγ* activators, even those which only vaguely trigger its transcriptional activity (Brun andSpiegelman, 1997). Ligand activation of *Pparγ* leads to the transcriptional up regulation and down regulation of target genes that modulate biological functions. Its transcriptional activity can be distorted by ligand-receptor interactions interfering in the process (Morrison andFarmer, 1999). Both *Pparγ*1 and *Pparγ*2 form heterodimers with the retinoid X receptor (RXR) and then bind to promoters of various target genes (Walkey andSpiegelman, 2008). This *Pparγ*-RXR complex binds to different ligands, including fatty acids, 9-cis-retinoic acid and 15d-PGJ2 (anti-inflammatory prostaglandin) in the hydrophobic pocket of the C-terminal domain (Hamm et al., 2001; Sarruf et al., 2005; Walkey andSpiegelman, 2008).

However, it is suggested that ligand binding may not be necessary for *Ppar*γ function during adipose differentiation (Walkey andSpiegelman, 2008).

The C/EBP family also has an important part in the process of adipogenesis. They are basic-leucine zipper (bZIP) transcription factors comprised of six distinct members characterized as α, β, δ, γ, ε and ζ. The C/EBPs have a basic-leucine zipper domain, composed of an α-helix structure, at the C-terminus that is important in binding to DNA sequences and for dimer formation. They also have activation domains at the N-terminus and regulatory domains. All C/EBPs can form hetero- and homodimers with other C/EBPs and transcription factors, which may or may not have the leucine zipper domain. Subsequently, they bind to various gene promoters to modify gene expression. *C/EBP*α, β and δ, in particular, have been studied at length with regards to their association with adipogenic regulation (Hamm et al., 2001; Morrison andFarmer, 1999; Rosen et al., 2000). *C/EBP*β and *C/EBP*δ are expressed early in adipocyte differentiation, where they induce the expression of *C/EBP*α and *Ppar*γ (Farmer, 2006; Zuo et al., 2006). Some suggest that adipose tissue is not formed in *C/EBP*β and *C/EBP*δ deficient mice (Tanaka et al., 1997), while others claim that mice lacking both *C/EBP*β and -δ can produce adipose tissue (Gesta et al., 2007). *C/EBP*α, however, is necessary for adipogenesis of white adipose tissue (Gesta et al., 2007). Ectopic expression of *C/EBP*α in many different fibroblastic cells can stimulate adipocyte differentiation (Freytag et al., 1994) while ectopic expression of *C/EBP*β can stimulate adipogenesis in non-adipogenic fibroblasts (Farmer, 2006). Knockout of *C/EBP*α has demomonstrated its

necessity for white adipose tissue formation but not brown adipose tissue formation (Linhart et al., 2001). *C/EBP*δ does not seem to have any adipogenic activity but with the presence of *C/EBP*β, it can play an important role in the induction of *C/EBP*α (Cao et al., 1991).

The adipocyte phenotype is dependent on the mutual interaction between *Ppar*γ and the C/EBPs. While both *C/EBP*α and *Ppar*γ direct adipocyte differentiation, *Ppar*γ appears to be the dominant factor. *Ppar*γ expression can induce adipocyte differentiation in *C/EBP*α deficient mouse embryonic fibroblasts, but expression of *C/EBP*α does not stimulate adipocyte differentiation in those lacking *Ppar*γ (Gesta et al., 2007) suggesting that *C/EBP*α is upstream of *Ppar*γ. Also, *C/EBP*β has been shown to be ineffective at stimulating the expression of *C/EBP*α when lacking *Ppar*γ (Zuo et al., 2006). Once activated, *C/EBP*α and *Ppar*γ then promote their own gene expression through feedback mechanisms, even after *C/EBP*β and *C/EBP*δ levels have declined (Morrison andFarmer, 1999). Subsequently, they activate the expression of numerous adipogenic genes including *Fabp4*, also known as Adipocyte Protein 2 (aP2). Fabp4 is a carrier protein for fatty acids whose expression is mainly in adipocytes and macrophages. Inhibition of this protein has been implicated in the treatment of obesity (Baxa et al., 1989; Maeda et al., 2005).

Another family of transcription factors, the SREBPs, has been identified as essential in modulating the gene expression of proteins crucial in fatty acid biosynthesis (SREBP-1a, SREBP-1c) and cholesterol metabolism (SREBP-2). SREBPs have two

trans-membrane domains that bind the protein to the endoplasmic reticulum. When low levels of sterol are present, the N-terminal portions of the SREBP protein are released into the cytoplasm and translocated to the nucleus where they bind to the promoters of various genes. (Morrison andFarmer, 1999).

When SREBP is bound to ADD1 (ADD1/SREBP1), it is highly expressed in adipose tissue and seems to be involved in early adipocyte differentiation (Kim andSpiegelman, 1996). A part of the basic helix–loop–helix transcription factor family, ADD1/SREBP1 is capable of binding two unique DNA sequences: E-boxes (CANNTG) and the sterol regulatory element (SRE) (Briggs et al., 1993; Kim et al., 1995). The expression of ADD1/SREBP1 stimulates *Pparγ* expression by promoting ligand production for *Pparγ*; this may explain the influence of ADD1/SREBP1 on adipocyte differentiation (Kim et al., 1998).

ADD1/SREBP1 may be largely involved in coordinating the different pathways involved in lipid metabolism (Kim et al., 1995). Many genes are responsive to the presence of SREBP including *LPL* and SCD-1 (Kim andSpiegelman, 1996). The mRNA expression of *LPL* has repeatedly been refered to as an early sign of adiopocyte differentiation (Ailhaud, 1996). *LPL* is secreted by mature adipocytes and has as a vital role in controlling lipid accumulation (Goldberg, 1996). A key enzyme in fatty acid metabolism, SCD1 catalyzes the synthesis of unsaturated fatty acids. Other SREBP responsive genes are involved in cholesterol metabolism (3-Hydroxy-3-methylglutaryl coenzyme A (HMG-CoA) synthase, HMG-CoA reductase, farnesyl diphosphate

synthase, squalene synthase, low density lipoprotein (LDL) receptor) and fatty acid synthesis (fatty acid synthase) (Brown andGoldstein, 1997; Sato et al., 1996).

3T3-F442A preadipocytes: A Model for the Mechanism of Adipogenesis

Manipulating adipocyte differentiation *in vivo* can be a complex process and ex-vivo experimentation requires large amounts of animal fat tissue to get a sufficient amount of adipocytes to study (Geloen et al., 1989). Collection of animal fat tissue can be tedious since it consists of blood vessels, nerve tissue, fibroblasts and preadipocytes whereas only a third of the composition is mature adipocytes. Therefore, part of the process of adipocyte differentiation and the factors involved has been acquired from the extensive work in *in vitro* models of adipogenesis. Among the different in-vitro models of adipogenesis, the 3T3 preadipocyte cell line is one of the most well-established and dependable models (Wood, 2008). Differentiated 3T3-L1 and 3T3-F442A preadipocytes possess a large amount of the ultra-structural properties of adipocytes found in animal tissue. Subcutaneous injection of 3T3-F442A cells in nude mice produces an entirely differentiated fat pad (Green andKehinde, 1979).

Generally, 3T3-F442A cells are believed to not have the capability of differentiating into other cell types, however, insulin mediated adipocyte differentiation can be inhibited by BMP2 which stimulates the expression of differentiation markers attributed to osteoblasts. Serial analysis of gene expression (SAGE) of 3T3-F442A cells responding to BMP2 has shown that 3T3-F442A cells are biopotential cells meaning that they are capable of differentiating into both adipocytes and osteoblasts (Ji et al., 2000).

The process of terminal adipocyte differentiation during which preadipocytes mature into adipocytes, has been extensively studied in mouse 3T3-L1 and 3T3-F442A cell lines (Rosen andSpiegelman, 2000). The 3T3-L1 and 3T3-F442A preadipocyte cell lines have the morphology of fibroblasts. They are cloned cell lines derived from Swiss 3T3 mouse embryos that are capable of differentiating into cells similar to adipocytes (Green andKehinde, 1976). They are committed to an adipocyte lineage and differentiate in a predictable sequential pattern. They begin as spindle-shaped fibroblast-like cells and eventually differentiate to round mature adipocytes (Wood, 2008). Once the cells have reached confluency and have begun the process of adipogenesis, they instinctively undergo growth arrest and begin differentiation into white adipocytes (Green andKehinde, 1979).

The differentiation of 3T3-L1 cells requires the addition isobutylmethylxanthine, dexamethasone, insulin and fetal bovine serum (FBS) whereas 3T3-F442A cells only require the supplementation of insulin and FBS to induce differentiation. The growth arrested 3T3-F442A cells enter the cell cycle process once again, in the presence of insulin and FBS, and undertake numerous rounds of cell division known as mitotic clonal expansion (Hamm et al., 2001; Sarruf et al., 2005). This mitotic clonal expansion is similar to the process of hyperplasia which is seen in the development of obesity (Farmer, 2006). Chromatin modification during mitosis has been implicated as essential for the transcription of genes responsible for the adipocyte phenotype (Farmer, 2006; Otto andLane, 2005). The transcription factor signaling cascade begins when *C/EBP*β attains

DNA-binding activity (Tang et al., 2003) and terminal differentiation is sustained by *C/EBP*α and *Ppar*γ expression.

Insulin-Ras Signaling Pathway: Modulator of Adipogenesis

The differentiation of fibroblasts to adipocytes is a complex process which involves the occurrence of several crucial events that require the activation of signaling pathways (see figure 2) including those mediated by insulin, insulin like growth factor (IGF)-1, Ras protein and *Ppar*γ2 (Fernyhough et al., 2007; Ntambi andYoung-Cheul, 2000).

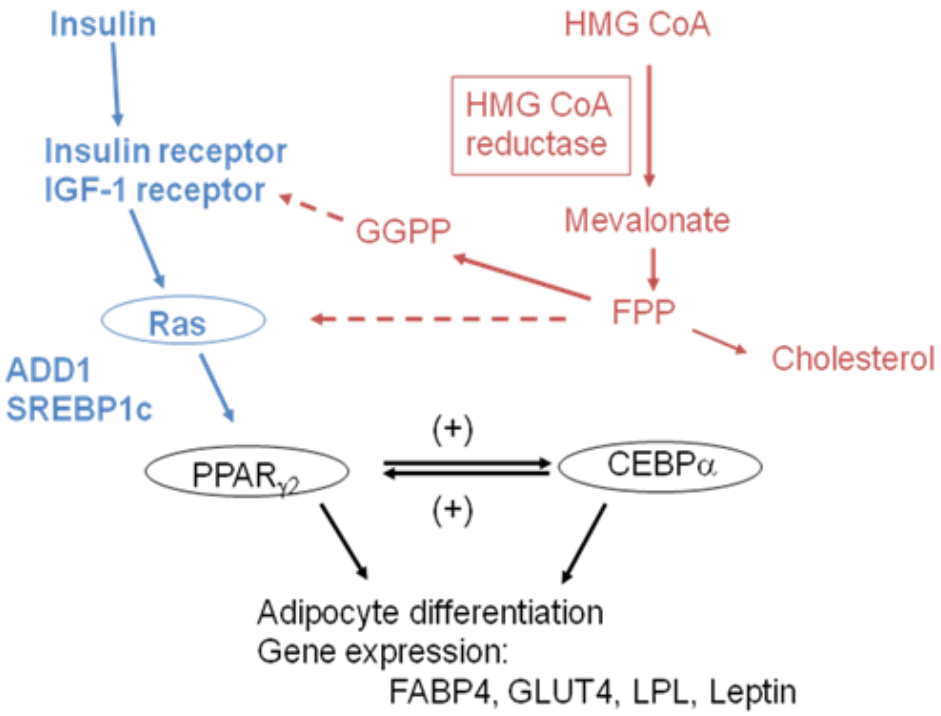

Figure 2: The mevalonate pathway provides essential intermediates for the signaling pathway in adipocyte differentiation. Insulin like growth factor 1 (IGF-1) receptor and Ras protein mediate the insulin-induced activation of *Ppar*γ2, a key regulator that cross-activates *C/EBP*α. IGF-1 receptor and Ras are modified with geranylgeranyl- (GGPP) and farnesyl- (FPP) pyrophosphates, respectively (dotted lines).

Insulin is an important activator of preadipocyte differentiation. Insulin action is initiated when it binds to its specific cell surface receptor (Olefsky, 1990) that promotes many intracellular intermediates leading to the response of insulin targeted cells (Rhodes andWhite, 2002). The insulin receptor undergoes a conformation change in response to the ligand binding causing phosphorylation of the β subunit and activation of the intrinsic tyrosine kinase leading to intracellular insulin signaling. Insulin receptor substrate (IRS) and Shc proteins with phosphotyrosine binding (PTB) domains, carry out key functions such as interacting with phosphorylated tyrosine residues motifs located on the insulin receptor (Sharma et al., 1997). Interfering with the PTB domains of these proteins hinders the ability of insulin to produce cellular responses (Goalstone et al., 2001).

The phosphorylation of IRS and Shc proteins leads to further downstream insulin signaling (Rhodes andWhite, 2002). The IRS insulin signaling pathway mediates the metabolic effects of insulin while Shc insulin signaling mediates the nuclear effects of insulin (Sutherland et al., 1998). Shc proteins can bind to growth receptor binding protein 2 (Grb2), which in turn is bound to SOS, a guanine nucleotide exchange factor (Sasaoka et al., 1994). This Shc–Grb2–SOS complex leads to the activation of Ras proteins through binding of guanosine triphosphate (Campbell et al., 1998). The Ras superfamily of proteins is composed of five major subfamilies: Ras, Rho/Rac, Sarl/Arf, Rab, and Ran (Rajalingam et al., 2007; Takai et al., 2001). They are small G proteins, also known as guanosine 5' triphosphatases (GTPases) and can be found on the inner segment of the plasma membrane. They are involved in cellular signal transduction

pathways that influence growth, migration, adhesion, cytoskeletal integrity, cell survival, and cell cycle progression, differentiation and survival (Rajalingam et al., 2007).

The activation of Ras proteins initiates a cascade of phosphorylation and activation of serine/threonine kinases (Raf, MEK, and MAP kinase) (Macdonald et al., 1993). Activation of p21 Ras and MAP kinase by insulin is fast and continuous, relative to the number of insulin receptors activated (Marshall, 1995). This sequence of events is followed by the activation of *Pparγ* by Ras which promotes preadipocyte differentiation and insulin sensitivity and suppresses adipocyte lipolysis. *Pparγ*2 and *C/EBPα* are over-expressed during the preliminary stages of adipocyte differentiation. The cross-activation of these proteins up-regulates preadipocyte differentiation by activating the expression of various genes encoding essential proteins required for acquiring the preadipocyte phenotype such as *Fabp4*, *GLUT4*, *LPL* and leptin (Tontonoz et al., 1994a).

Further stimulation of *Pparγ* can occur through an indirect manner with SREBP/ADD1. Over-expression of SREBP/ADD1 can activate *Ppar γ* by stimulating the production of an endogenous ligand for this nuclear receptor (Kim et al., 1998). Ectopic expression of ADD-1/SREBP-1 in 3T3-L1 cells was shown to induce endogenous *Pparγ* mRNA levels (Fajas et al., 1999). Inducing differentiation in 3T3-L1 preadipocytes was shown to increase SREBP-1a levels close to 8.2 fold (Shimomura et al., 1997). The presence of SREBP stimulates even more genes associated with adipogenesis including *LPL*, SCD-1 and fatty acid synthase (Brown andGoldstein, 1997; Sato et al., 1996). Another SREBP responsive enzyme is HMG-CoA reductase, a vital

component of the mevalonate pathway, whose activity provides prenyl pyrophosphates for the modification and biological activities of Ras and growth and differentiation factors (Brown andGoldstein, 1997).

The Mevalonate Pathway

The mevalonate pathway, also known as the cholesterol biosynthetic pathway, produces sterol (cholesterol) and non-sterol (isoprenoid) products (figure 2) that have various necessary functions in the human body. Cholesterol is an important constituent of the cell membrane and a precursor for lipoproteins, vitamin D, steroid hormones and bile acids. The isoprenoid products of the pathway include heme A and ubiquinone (part of the electron transport chain), dolichol (co-translational and post-transcriptional modification of proteins), FPP, GGPP, dolichylphosphate (post-translational modification of the Ras and Rho proteins), isopentyladenine (a component of some transfer RNA (tRNA) useful for protein synthesis) and intercellular messengers (plant cytokines) (Goldstein andBrown, 1990; Laufs andLiao, 2000; Mo andElson, 2004).

Two sequential enzymes of the mevalonate pathway, HMG-CoA synthase and HMG-CoA reductase, play an important role in maintaining a balance in the production of mevalonate and cholesterol through feedback regulation (Goldstein andBrown, 1990). The first reaction of the mevalonate pathway is freely reversible and involves acetoacetyl-coenzyme A (CoA) thiolase. HMG-CoA synthase catalyzes the condensation of acetyl-CoA with acetoacetyl-CoA in the formation of HMG-CoA; the second reaction in the mevalonate pathway (Theisen et al., 2004). HMG-CoA reductase is the rate-

limiting enzyme of the mevalonate pathway and is subject to inhibition by sterols (cholesterol) at the transcriptional level and non-sterol metabolites (geranylgeraniol, farnesol) at post transcriptional levels via feedback regulation. This subsequently blocks the translation and accelerates degradation of the enzyme (Goldstein andBrown, 1990). The strict control of the progression of the mevalonate pathways provides a continuous supply of mevalonate products while avoiding over production of cholesterol. Surplus cholesterol can be fatal since it initiates the process of atherosclerosis in blood vessels and forms plaques inside the cell (Small andShipley, 1974).

The direct product of HMG-CoA reductase is mevalonate and by combining 5 carbon precursors, several isoprenoid products are formed including: geranyl pyrophosphate (10 carbons), farnesyl pyrophosphate (15 carbons) and geranylgeranyl pyrophosphate (20 carbons). Combining two farnesyl pyrophosphate groups can generate squalene, the precursor used for the production of cholesterol. Since the enzyme HMG-CoA reductase is necessary for the synthesis of cholesterol and isoprenoids, HMG-CoA reductase inhibitors, such as statins, can inhibit their production (Boyartchuk et al., 1997).

Isoprenylation, also known as prenylation, refers to the covalent addition of hydrophobic isoprenoid molecules to proteins, resulting in post-translational modification. The isoprenoid intermediates are in the pyrophosphate form; thus they must be converted to isoprenoid diphosphates before they can be added to cellular proteins. The isoprenoid groups bind to the carboxyl-terminal of proteins, composed of

cysteine and an aliphatic amino acid, forming a highly stable thioether bond acting as a membrane anchor for proteins. The proteins are farnesylated or geranylgeranylated depending on the amino acid present (Boyartchuk et al., 1997). Prenylation is catalyzed by one of three protein-prenyl transferases: protein farnesyltransferase (FTase), protein geranylgeranyltransferase type I (GGTase I), and geranylgeranyl transferase type II (GGTase II). FTase transfers a farnesyl group from FPP while GGTase I transfers a geranylgeranyl group from GGPP to the cysteine component of the carboxyl-terminal of the specific protein (Adjei, 2001; Goldstein andBrown, 1990). Farnesylation is observed in all members of the Ras family of proteins, allowing them to migrate to the proper location on cellular membranes and interact with other signaling molecules to control cell proliferation, differentiation and survival (Goldstein andBrown, 1990; Mo andElson, 2004). Geranylgeranylation, on the other hand, can be detected in the lipid anchoring of the Rho family, a subfamily of Ras proteins.

HMG-CoA Reductase Regulation: Transcriptional and Post-Transcriptional Regulation of the Mevalonate Pathway

Cells are capable of endogenously synthesizing cholesterol by way of the mevalonate pathway. The mevalonate pathway is repressed when cells have acquired their sterol and non-sterol requirements and stimulated once lack of exogenous cholesterol is detected. HMG-CoA reductase is securely bound to the endoplasmic reticulum (ER) and has a C-terminal catalytic domain that dwells in the cytosol and a N-terminal trans-membrane domain. The latter domain includes the sterol-sensing domain

needed for sterol feedback regulation which is regulated by SREBP (Hampton, 2002). HMG-CoA Reductase is greatly responsive to SREBP activity (Brown andGoldstein, 1997). SREBPs are also bound to a protein named sterol regulatory element binding protein cleavage-activating protein (SCAP), which is also related to HMG-CoA Reductase since it has five regions on its membrane that are similar to the sterol-sensing domain of HMG-CoA reductase (Hua et al., 1996).

When sterol levels are low, SCAP senses this change in cholesterol levels and is pushed to guide the SREBPs to the Golgi apparatus for activation to endure a two-step proteolytic process. The first step involves sterol regulated cleavage in the luminal loop which breaks the covalent bond connecting the two trans-membrane domains of SREBP-2. The second step is non-sterol regulated and takes place inside the first trans-membrane domain releasing the water soluble NH_2-terminal fragment (Sakai et al., 1996). Once activated, SREBP moves to the nucleus and binds to the sterol regulatory element (SRE-1) in the 5'-flanking region/promoter region of the reductase gene, activating transcription (Sato et al., 1994) and up-regulating enzymes related to sterol biosynthesis (Wang et al., 1994). Genes involved in encoding other enzymes of cholesterol synthesis (HMG-CoA synthase, farnesyl diphosphate synthase, LDL receptors) are activated (Brown andGoldstein, 1997; Goldstein andBrown, 1990). Conversely, when high levels of sterols are sensed SCAP is modified and bound to INSIG1 (Yang et al., 2002) disallowing it from crossing into the nucleus thus hindering the transcription of genes

related to cholesterol synthesis, *LPL* endocytosis, fatty acid and phospholipid synthesis (Brown andGoldstein, 1997; Hampton, 2002).

The activity of HMG-CoA reductase is tightly regulated, partially due to post-transcriptional mechanisms that are controlled by the non-sterol and sterol products of mevalonate metabolism (Goldstein andBrown, 1990; Petras et al., 1999). Many studies have explored the rate at which mRNA translation of HMG-CoA reductase takes place by incorporating HMG-CoA Reductase inhibitors. Blocking mevalonate production with the use of a HMG-CoA reductase inhibitor shows a subsequent rapid translation of mRNA despite the presence of sterols (Goldstein andBrown, 1990). This augmentation in mRNA translation is decreased fivefold when non-sterol needs are met thus indicating that cells move according to their need for non-sterol isoprenoids (Goldstein andBrown, 1990). In cultured cells, inhibiting the mevalonate pathway, triggers a 200-fold increase in the HMG-CoA reductase activity just within a few hours (Nakanishi et al., 1988). The degradation of HMG-CoA reductase has been evaluated by measuring the decline in HMG-CoA reductase degradation upon the addition of an inhibitor. Its degradation has been shown to increase or decrease depending on the amount of sterol and non sterol products (Straka andPanini, 1995).

It has also been shown that farnesylated proteins may also contribute to the feedback control of HMG-CoA reductase. The effect of these proteins is believed to be at the post-transcriptional level because even when farnesylation is inhibited, sterol input decreases the transcription of HMG-CoA reductase (Nakanishi et al., 1988). When

mevalonate is inhibited, proteins which are normally farnesylated start to build up in the unfarnesylated form and modify HMG-CoA reductase either in a positive or negative manner, effecting translation or degradation (Goldstein andBrown, 1990; Repko andMaltese, 1989). Farnesol, a FFP derivative of the mevalonate pathway, has been shown to stimulate reductase degradation (Correll et al., 1994). Numerous farnesyl derivatives and farnesyl homologs inhibit the synthesis of HMG-CoA reductase and accelerate its degradation (Mo andElson, 2004).

Mevalonate Pathway: Modulation of Adipogenesis

There are two specific enzymes in the mevalonate pathway that are implicated in the function of the insulin signaling pathway consequently leading to adipocyte differentiation. HMG-CoA reductase and GGPP synthetase activity provide prenyl pyrophosphates in the form of GGPP and FPP that are required for the modification and biological activity of the IGF-1 receptor and Ras, respectively, (Goldstein andBrown, 1990) ultimately leading to the activation of *Ppar*γ2 and the adipogenic process (Figure 2). In fibroblasts, insulin stimulates the mevalonate pathway activity necessary for the modification of p21 Ras (Goalstone andDraznin, 1996).

When fibroblasts undergo differentiation into mature adipocytes, the expression of GGPP synthetase was increased by more than 20-fold. To explore the effect of insulin on the regulation of GGPP synthetase expression, 3T3-L1 adipocytes were cultured with or without insulin for 24 hours followed by the measurement of mRNA expression. Insulin did not induce GGPP synthetase mRNA expression; however, fatty acid

synthetase expression increased by 80% (Vicent et al., 2000). During the differentiation of the 3T3-L1 cells, there were large increases in the mRNA levels of LDL receptor and HMG-CoA synthetase and smaller increases in the levels of *LPL*. HMG-CoA reductase was markedly increased at day 3 of differentiation (Shimomura et al., 1997).

The mevalonate pathway can be suppressed by the use of HMG-CoA reductase inhibitors (mevalonate suppressors) which inhibit the enzyme HMG-CoA reductase thus ultimately lowering circulating levels of cholesterol. It is believed that by down regulating HMG-CoA reductase activity, pools of FPP and GGPP will be limited, thereby attenuating preadipocyte differentiation into adipocytes (Figure 3).

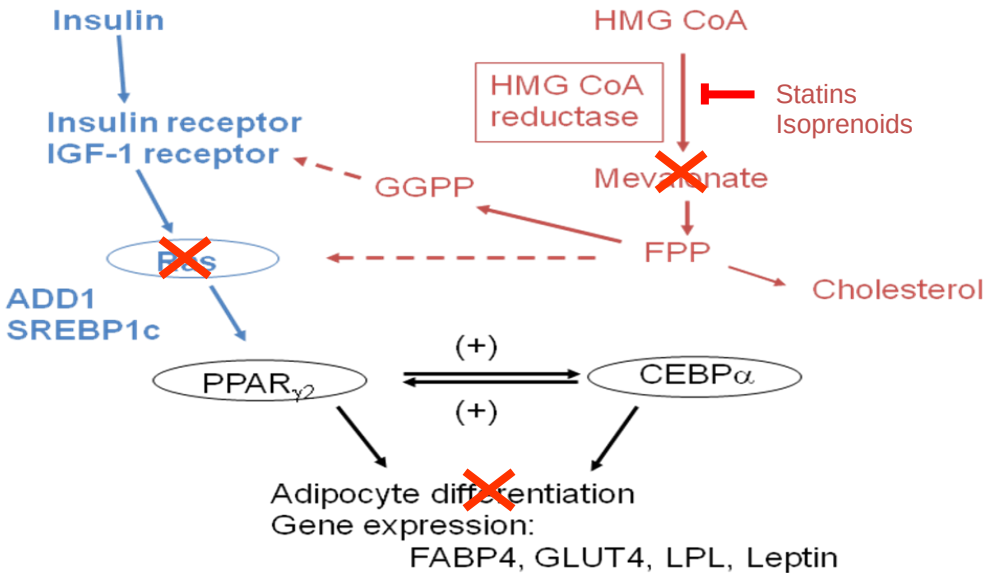

Figure 3: Statins and isoprenoids suppress HMG-CoA reductase (rectangle), the key enzyme in the syntheses of FPP and GGPP. This leads to the inactivation of Ras and *Ppar*γ which may consequently inhibit adipocyte differentiation.

Lovastatin: Role in Preadipocyte Differentiation

Mevalonate suppressors including the statins, competitive inhibitors of HMG-CoA reductase activity have been shown to play an important role in preadipocyte differentiation. Lovastatin, a widely prescribed cholesterol-lowering drug, competitively inhibits HMG-CoA reductase activity, the rate-limiting step in cholesterol biosynthesis (see figure 3).

Lovastatin-containing red yeast rice suppresses lipid accumulation, down-regulates the expression of adipogenic transcriptional factors including *Pparγ*2, and inhibits adipocyte differentiation (Jeon et al., 2004). A new-generation statin, atorvastatin, inhibits adipocyte maturation, *C/EBP*α expression, insulin signaling (Nakata et al., 2006) and lipid accumulation (Mauser et al., 2007) in differentiating 3T3-L1 cells, effects reversed by mevalonate and GGPP (Nakata et al., 2006). Statin treatment in 3T3-L1 cell differentiation leads to disruption of insulin signaling, IGF-1 and Ras (Siddals et al., 2004). Inhibition of isoprenoid synthesis is associated with reduced expression of *GLUT4*. Lovastatin's inhibition of adipocyte differentiation was reversed with the addition of mevalonate, FPP and GGPP, but not by cholesterol, confirming the requirement of the mevalonate-derived prenyl intermediates for insulin signaling (Nishio et al., 1996). Pitavastatin decreased the expression of adipogenic genes including *Pparγ*, *Fabp4*, adipsin and *GLUT4* but not *C/EBP*α. Most importantly, it induced pref-1 expression in preadipocytes and maintained the expression of pref-1 at high levels in differentiated cells which suggests that pitavastatin inhibits adipocyte differentiation by

blocking *Pparγ* expression and activating pref-1 expression. This study showed no reversal with the addition of mevalonate (Nicholson et al., 2007).

Several studies have examined the effect of incorporating statins at different time points throughout the differentiation process on triglyceride accumulation and gene expression. Others have looked at the issue of dose dependency. Pitavastatin was shown to inhibit adipocyte differentiation in a time dependent fashion. When it was added at the early stages of differentiation, no triglyceride accumulated within cells. Significant amounts of triglycerides were present when pitavastatin was added on day 1 or more after the induction of differentiation (Nicholson et al., 2007). Also, it has been demonstrated that statins clearly suppress preadipocyte differentiation in a dose-dependent manner (Mauser et al., 2007; Nakata et al., 2006; Nicholson et al., 2007; Nishio et al., 1996).

Statins have a strong inhibitory impact on the adipogenic process. Unfortunately, the potential for the long-term application of statins in obesity prevention and treatment is unknown by their dose-limiting toxicities (Thibault et al., 1996). Emerging evidence suggests that statins may have adverse side effects such as elevated liver enzymes, muscle problems, cognitive loss, pancreatic dysfunction, hepatic dysfunction and neuropathy (Golomb andEvans, 2008). In addition, a recent study shows an increased risk of developing diabetes for patients taking statins compared to those given a placebo (Sattar et al., 2010).

Isoprenoids: Role in Preadipocyte Differentiation

Isoprenoids, also termed terpenoids, are plant products that are derived from the mevalonate pathway. There are more than 23,000 individual isoprenoids that have been characterized (Sacchettini andPoulter, 1997). They are derived from the 5 carbon molecule isopentenyl pyrophosphate (IPP), an important intermediate in the mevalonate pathway. They are considered pure when they are made of 5 or more carbon units (X) and mixed when only part of their structure is derived from the mevalonate pathway (Elson et al., 1999). Some examples include: monocyclic monoterpenes (2X; d-limonine, perillyl alcohol, perillaldehyde, carvacrol, and thymol), acyclic monoterpenes (2X; geraniol), sesquiterpenes (3X; farnesol), diterpenes (4X; geranylgeraniol), triterpenes (6X; lupeol) and tetraterpenes (8X; lycopene). When isoprenoids contain a large number of isoprene units, they are called polyterpenes (Mo andElson, 1999). Mixed isoprenoids include tocotrienols, prenylated coumarins, flavones, flavanols, isoflavones, chalcones, quinones, chromanols, and menaquinone-3 (Elson et al., 1999; Mo andElson, 1999). At levels adequate to suppress HMG-CoA reductase, isoprenoids have shown no toxicity to normal cells and animals, and as dietary ingredients, are considered safe for human consumption (Mo andElson, 2006).

Similar to the statins, isoprenoids are mevalonate suppressors which act as down-regulators of HMG-CoA reductase blocking of the pathway leading to synthesis of isoprenoids, which are downstream products of mevalonic acid. Thus, they also have the potential of playing an important role in preadipocyte differentiation. Geranylgeraniol is

a diterpene alcohol found in linseed and peanut oil (Fedeli et al., 1966) which has been shown to inhibit HMG-CoA reductase (Katuru et al., 2011). It is derived from GGPP and is an intermediate in the biosynthesis of dicyclic and tricyclic diterpenes.

Little research has been done on the mevalonate suppressive activity of geranylgeraniol and its effect on human health. No research has explored the potential role of geranylgeraniol in inhibiting the insulin signaling pathway and consequently preadipocyte differentiation by way of down regulation of the mevalonate pathway. We hypothesize that geranylgeraniol is effective in suppressing the differentiation of murine 3T3-F442A preadipocytes by down regulating the expression of adipogenic transcriptional factors associated with the mevalonate pathway and the insulin signaling pathway and decreasing lipid accumulation.

CHAPTER III

MATERIALS AND METHODS

Study Design

The impact of geranylgeraniol on adipocyte differentiation was determined by measuring intracellular triglyceride (TG) content in 3T3-F442A cells using Oil Red O staining and the AdipoRed Assay. Cell viability and apoptosis of the cells were assessed to evaluate any potential cytotoxicity of the treatment. The impact of geranylgeraniol on the mRNA levels of *Pparγ*2 and *C/EBPα*, two key regulators in adipocyte differentiation, using qRT-PCR was then measured and the expression of other adipogenic genes including: *SREBP1, ADD-1, INSIG1, Fabp4, LPL, GPDH, GLUT4, SCD-1*, leptin (*Lep*), *pref-1, Fasn* and Adiponectin (*AdipoQ*) were also examined. To further test our hypothesis that the geranylgeraniol impact stems from the suppression of HMG-CoA reductase, the mRNA levels of HMG-CoA reductase were examined (Figure 3). Lovastatin, a known inhibitor of preadipocyte differentiation, was used as a positive control. Mevalonate (5 and 500μM) was added to the culture medium to evaluate its attenuation of the treatment effect (Figure 4).

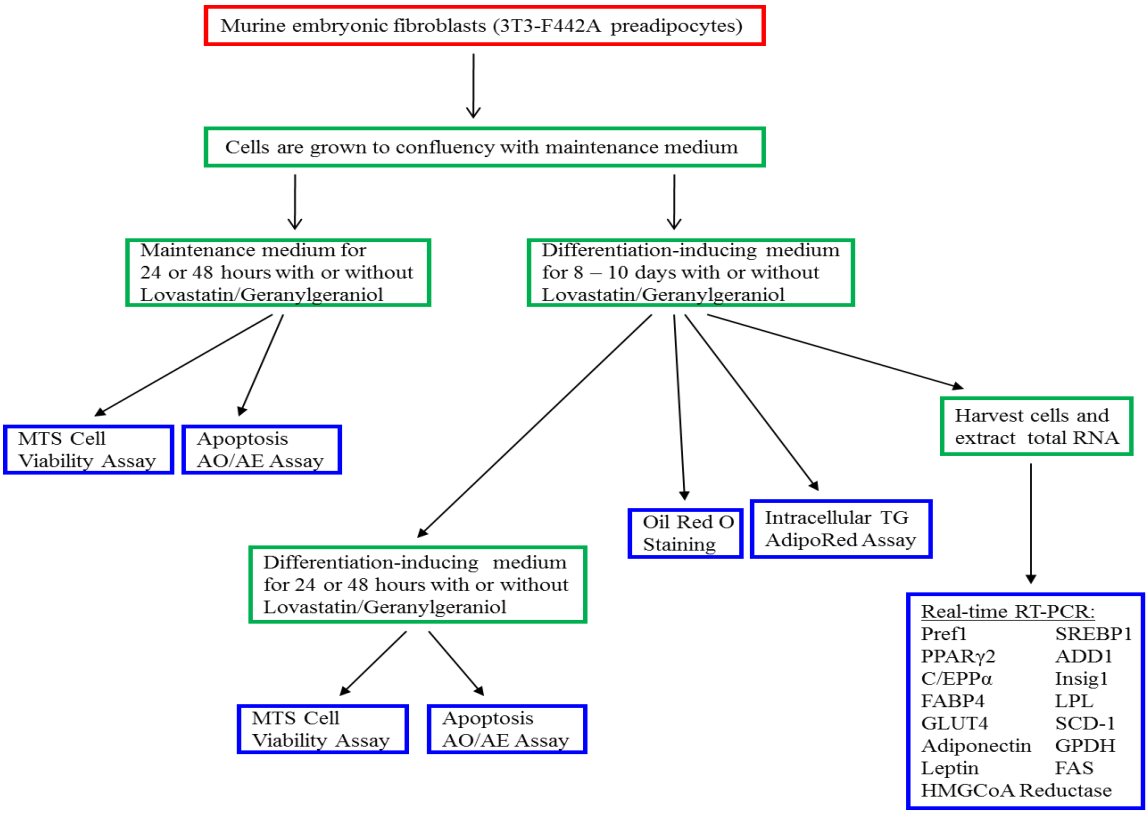

Figure 4: Study design to evaluate the effect of geranylgeraniol on adipocyte differentiation in murine 3T3-F442A preadipocytes.

Cell Culturing and Adipocyte Differentiation

Murine 3T3-F442A preadipocytes were purchased from Dr. Howard Green (Harvard Medical School) and grown and maintained in Dulbecco's Modified Eagle's Media (DMEM) with 4 mmol/L L-glutamine adjusted by American Type Culture Collection (ATCC, Manassas, VA) to contain 1.5 g/L sodium bicarbonate and 4.5 g/L glucose and supplemented with 10% bovine calf serum (BCS, Fisher Scientific Company LLC, Houston, TX) and 1% penicillin/streptomycin (GIBCO, Grand Island, NY) at 37^{o}C in a humidified atmosphere of 10% CO_2. Upon reaching confluency, cells were seeded

in 96-well plates at a density of 2.5 x 10^3 or 5 x 10^3 cells per well, 24 well plates (1 x 10^4 cells/well), 6-well plates (4 x 10^4 cells/well) and in tissue culture dishes (100 mm x 20 mm, Corning Life Sciences, Wilkes Barre, PA) at 2 x 10^5 per dish. For the experiments using well plates, cells were cultured in at least 3 separate wells for each treatment concentration, for each experiment executed. For the tissue culture plates, cells were cultured in at least two plates for each treatment concentration for each experiment that was implemented. At least three independent experiments, performed in duplicate or triplicate, were completed for each experimental procedure.

3T3-F442A preadipocytes were cultured for 2 days and then differentiation was induced according to the protocol recommended by the lab of Dr. Howard Green (Harvard Medical School). Differentiation was achieved by maintenance in DMEM supplemented with 10% fetal bovine serum (FBS, Fisher Scientific Company) and 1% penicillin/streptomycin (GIBCO) for 8 days; in the presence of 5µg/mL insulin (Sigma Aldrich, St. Louis, MO) the first 4 days, until the differentiation of adipocytes. For days 0 – 8 of adipogenesis, geranylgeraniol (2.5 - 20µmol/L) or lovastatin (1.25 - 5µmol/L) were added to the differentiation medium of experimental groups, and the control cells were incubated in medium containing the vehicle; known solvents for the treatments [dimethyl sulfoxide (DMSO, ATCC) or ethanol (0.1%, v/v)]. Supplemental mevalonate (5 and 500 µmol/L), was added to some of the groups to assess possible reversal. The medium was changed every two days. On days 8 - 10, experiments were performed with the treated cells.

Cell Viability

Preadipocytes

Cultures of 3T3-F442A preadipocytes were seeded (2500 cells/well) in 100µL maintenance medium in 96-well plates and incubated for 48 hours at 37°C in a humidified atmosphere of 10% CO_2. The medium was then aspirated from each well and replaced with 100µL of fresh medium containing DMSO, ethanol or increasing concentrations of lovastatin (1.25 - 10µmol/L) and geranylgeraniol (20 - 200µmol/L). The cells continued to be incubated for an additional 24 or 48 hours. Cell populations were determined using the CellTiter 96® Aqueous One Solution MTS assay (Promega, Madison, WI) procedure. Cells were then washed once with Hank's Balanced Salt Solution (HBSS). Subsequently, 100µL of serum free medium and 20µL of 3-(4,5-dimethythizol-2-yl)-5-(3-carboxymethoxyphenyl)-2-(4-sulfophenyl)-2H-tetrazolium salt solution were added to each well. Cells were incubated for 2 hours at 37 °C. The absorbance was measured at 490 positioned in a Tecan Infinite M200 micro plate reader (Tecan Systems Inc., Salzburg, Austria**)** to verify the formazin concentration, which is relative to the number of live cells. The mean absorbance from wells containing cell-free medium was used as the baseline and was deducted from the absorbance of other cell-containing wells.

Mature Adipocytes

Cultures of 3T3-F442A preadipocytes were seeded (5000 cells/well) in 100µL maintenance medium in 96-well plates and incubated for 48 hours at 37°C in a

humidified atmosphere of 10% CO_2. Cells were then induced to differentiate, as described above, and grown to maturation. On day 8 – 10 of differentiation, the medium was aspirated from each well and replaced with 100µL of fresh medium containing DMSO or ethanol or increasing concentrations of lovastatin (1.25 - 10µmol/L) and geranylgeraniol (20 - 200µmol/L). The cells continued to incubate for an additional 24 or 48 hours. Cell populations were determined using the CellTiter 96® Aqueous One Solution (Promega, Madison, WI) procedure as described above.

Apoptosis

Preadipocytes

For detection of apoptotic cells, cultures of 3T3-F442A preadipocytes were seeded (2500 cells/well) in 100µL maintenance medium in 96-well plates and incubated for 48 hours at 37°C in a humidified atmosphere of 10% CO_2. The medium was aspirated from each well and replaced with 100µL of fresh medium containing DMSO, ethanol or increasing concentrations of lovastatin (1.25 - 10µmol/L) and geranylgeraniol (20 - 200µmol/L). The cells continued to incubate for an additional 24 or 48 hours. The cells were processed for Acridine Orange/Ethidium Bromide (AO/EB) dual staining assay. Cells were washed with PBS twice and treated with 500µL of trypsin and collected with 500µL FBS and centrifuged to get a cell pellet. Cells were re-suspended in 500µL media and dye mixture containing 50µg/mL acridine orange (Becton, Dickinson and Company, Sparks, MD). 50µg/mL ethidium bromide (Sigma) was added to each cell suspension. The cell suspension was loaded on a glass slide and observed

under an Axiovert 200 M microscope (Carl Zeiss MicroImaging Inc., Thornwood, NY) equipped with a FluoArc lamp, a AxioCam MRm digital camera system (Carl Zeiss), and AxioVision Rel. 4.3 program (Carl Zeiss).

Mature Adipocytes

For detection of apoptotic cells, these cells were processed for AO/EB Assay. Cultures of 3T3-F442A preadipocytes were seeded (5000 cells/well) in 100µL maintenance medium in 96-well plates and incubated for 48 hours at 37°C in a humidified atmosphere of 10% CO_2. Cells were then induced to differentiate, as described above, and grown to maturation. On day 8 – 10 of differentiation, the medium was aspirated from each well and replaced with 100µL of fresh medium containing DMSO or ethanol or increasing concentrations of lovastatin (1.25 - 10µmol/L) and geranylgeraniol (20 - 200µmol/L). The cells were then processed for AO/EB Assay using the procedure as described above.

Oil Red O Staining

On day 8 – 10 of preadipocytes differentiation to mature adipocytes, 3T3-F442A adipocytes were stained with Oil Red O. In brief, cell monolayers were washed twice with phosphate buffer solution (PBS) and fixed in 0.2mL (24-well plate) or 1mL (6-well plate) of 10% formalin per well at room temperature for 1 hour. Cells were then rinsed with deionized water and stained with 0.1mL (24-well) 0.5mL (6-well) of 0.3% freshly filtered Oil Red O working solution per well at room temperature for 30 minutes (Ramirez-Zacarias et al., 1992). The cells were then rinsed with 0.2mL (24-well) or 1mL

(6-well) deionized water before photomicrographs of representative fields of monolayer cells were taken with a Nikon Eclipse TS 100 microscope (Nikon Corporation, Tokyo, Japan) equipped with a Nikon Coolpix 995 digital camera (Nikon Corporation) to visualize cellular neutral lipids.

Triglyceride Measurement

Around 8 - 10 days after the induction of differentiation, lipid content was quantified using an AdipoRed™ Assay kit (Lonza, Walkersville, MD) according to manufacturer's instructions. AdipoRed is a reagent that contains the hydrophilic Nile Red stain and allows the quantification of intracellular lipid droplets (Greenspan et al., 1985). Differentiated cells were rinsed with 2mL HBSS and to each well, 5 mL HBSS and 140µL of AdipoRed reagent were added. After 10 - 15 minutes of incubation, the plates were positioned in a Tecan Infinite M200 micro plate reader (Tecan Systems Inc., Salzburg, Austria**)** and fluorescence was measured with an excitation wavelength of 485 nm and an emission wavelength of 572 nm.

Quantitative Real-time Polymerase Chain Reaction

On day 8 - 10 of preadipocyte differentiation to mature adipocytes, total cellular RNA was extracted from the 3T3-F442A adipocytes using TRIZOL reagent (Invitrogen) according to the manufacturer's protocols. The concentration and purity of the isolated total RNA was determined spectrophotometrically by running the samples in a spectrum of 230 - 400 nm at 10 nm intervals and using the OD260:280 ratio. The quality of the purified total RNA was verified by detecting a 2:1 ratio for the 28s:18s ribosomal RNA

(rRNA) using gel electrophoresis. Samples were run on a 1.5% agarose gel (Tris-acetate (TAE) buffer) at 80 volts for 90 min. and visualized by Chemi Doc XRS imaging system (Bio-Rad, Hercules, CA) following the addition of 0.5 μg/ml ethidium bromide. The level of mRNA expression of *Pparγ*, SREBP-1c, *INSIG1*, *Fabp4*, leptin, adiponectin, *Fasn*, *GLUT4* and *GPDH* was analyzed by reverse transcription (RT) followed by quantitative real-time polymerase chain reaction (qPCR). 2 μg of total RNA in a 20 μl reaction buffer was reverse transcribed into cDNA using an Oligo $(dT)_{20}$ primer and SuperScript® III First-Strand kit (Invitrogen, Grand Island, NY) following the manufacturer's instructions. The cDNA was diluted by 25-fold with 25μg/ml solution of acetylated bovine serum albumin (BSA) and 6 μl of diluted cDNA was amplified in a 25 μl PCR reaction which included 250 nM of both forward and reverse primers of the gene and iQ™ SYBR® Green Supermix (Bio-Rad Laboratories). The cDNA was denatured at 95°C for 3 minutes followed by 40 cycles of PCR (94°C for 30 s, 60°C for 25 s, 72°C for 25 s, and 78°C for 9 s) by means of an iQ™5 multi-color Real-Time PCR Detection System (Bio-Rad) with Bio-Rad iQ5 Optical System Software (version 2.1). The mRNA levels of all the genes were normalized using ribosomal protein L22 (*RPL22*) as internal control (de Jonge et al., 2007) by using the ΔC_T method. Fold changes of gene expression were calculated by the $2^{-\Delta\Delta CT}$ method.

Primer Design

Before PCR was executed, a pair of primers that selectively bind to the target DNA sequence were designed for each gene of interest. The primers were designed to

have a sequence which is the reverse complement of a region of template or target DNA to which we require the primer to anneal. To retrieve the genetic sequences of the relevant genes, the official webpage of the National Center for Biotechnology Information (NCBI) was utilized. The sequences for the primers are listed in Table 1. To design the primer sequences, we used the Primer 3 Output version 4.0 online software (Massachusetts Institute of Technology (MIT)) (Rozen, 2000).

Table 1

Primer Sequences (forward and reverse) and GenBank Accession Numbers used in the Real-Time qPCR

Gene	Accession#	Primer Sequence
AdipoQ	NM_009605	5'-CGGCAGCACTGGCAAGTTCTACTGC-3'
		5'-TTGTGGTCCCCATCCCCATACACCT-3'
ADD1	NM_001024458	5'-ACCGACGAGAGGTGGAGCGGA-3'
		5'-TGTCGGCTCCTGGGGAAGGTCT-3'
C/EBPα	NM_007678	5'-GGCCCCCGATGAGCAGTCACCT-3'
		5'-TTGAAGGCGGCCGGGTCGAT-3'
Fabp4	NM_024406	5'-GTGTGATGCCTTTGTGGGAACCTGG-3'
		5'-TGCGGTGATTTCATCGAATTCCACG-3'
Fasn	NM_007988	5'-CCCAGGCCTTGCCGTGCAGT-3'
		5'-GCTCAGGACTGCGTGGGGCT-3'
GLUT4	NM_009204	5'-GAACCCCCTCGGCAGCGAGT-3'
		5'-ATCCGGTCCCCCAGGACCTTGC-3'
GPDH	NM_010271	5'-GGGGGTAGACGAGGCCCCAA-3'
		5'-GCCGGGTCCTTGCAGCCGAT-3'
HMG-CoAR	NM_008255	5'-GCCAGTGGTGCGTCTTCCACG-3'
		5'-CATGCCCATGGCGTCCCCCG-3'
INSIG1	NM_153526	5'-GCACGAGCTATTCCGGAGAAGGGTTC-3'
		5'-GGACCAACGACTGTGTCAGGAGGTCAG-3'
Lep	NM_008493	5'-TGGAGGTGAGCGGGATCAGGTTTTG-3
		5'-TGGCACGTGGGATCTTTCAGAAGCC-3'
LPL	NM_008509	5'-TCCCTTCACCCTGCCCGAGGT-3'
		5'-CGATGACGAAGCTGGGGCTGCT-3'
Pparγ	NM_001127330	5'-AGAGGGCCAAGGATTCATGACCAGG-3'
	NM_011146	5'-TTCAGCTTGAGCTGCAGTTCCAGGG-3'
Pref1	NM_001190703	5'-CCGTGCCAGAACGGGGGCAC-3'
		5'-CGGGGGTCAGGCGGTAGGTGA-3'
RPL22	NM_009079	5'-GCGACTTTAACTGGGCTGCTGCT-3'
		5'-GCCCACCACCCAGCCTCTCG-3'
SCD1	NM_009127	5'-CCGGAACCGAAGTCCACGCTCG-3'
		5'-TCCAGGTGGAGGGGCACCGT-3'
SREBP-1	NM_011480	5'-TGGCACCCTCTTGCTCTGTAGGCAC-3
		5'-GCTGAGGCAGACATCTGCCTACCCA-3'

Primer Verification

Primer blast. After the primers were designed, they were tested for specificity by using the "BLAST' tool on the NCBI website. The primers were BLAST against the genome to see if they were specific to the region that we wanted to amplify (Table 2) and to guarantee that the sequence chosen did not match any other gene.

Table 2.
Primer Blast Results

Gene	**Result**
LPL	1 match
Pref1	1 match to Dlk1, NM_010052.5; this is also the suggested primer 1 if NM_001190703 is entered.
Lep	1 match
AdipoQ	1 match
Pparγ	2 matches: *Pparγ*1 (NM_001127330) and *Pparγ*2 (NM_011146.3)
Fabp4	1 match
C/EBPα	1 match
RPL22	1 match
Fasn	1 match
GPDH	2 matches: NM_010271.2 (Gpd1) and NM_033526.2 (Ubqin4), ubiquilin 4
HMGR	1 match
Glut4	1 match
SCD1	1 match
ADD1	1 match
INSIG1	1 match

Melting profile. Purity of the double stranded DNA (dsDNA) was determined by analyzing the melt peak charts of the PCR products generated from each primer and it was ensured that a single gene-specific product was amplified.

DNA sequencing. Subsequent to the completion of PCR, products of the reaction were collected and stored in -20^{o}C. The specific PCR products were purified with HT ExoSAP-IT® (mixture of Exonuclease I and Shrimp Alkaline Phosphatase, Recombinant (rSAP)) High Throughput PCR Product Clean-Up (USB® Products, Affymetrix Inc., Cleveland, Ohio, USA). To confirm specificity and rule out the possibility of two products being generated by RT-PCR, primers used to generate the PCR products were used as sequencing primers to sequence both strands. For sequencing preparation, primer solutions were prepared from 100µM stock solutions of upstream (Up+) and downstream (Dn-) primer sequences for each relevant gene. We formulated 10µM solutions for each sequencing primer with upstream (up+) and downstream (dn-) sequences prepared separately, each in one tube.

One PCR product was collected for each gene of interest. The samples were purified according to the manufacturer's instructions. The purifying reaction requires 4µL of HT ExoSAP-IT for 20µL of PCR product. The PCR products were incubated at 37^{o}C for 30 minutes to degrade remaining primers and nucleotides (dNTPs). The purified double-stranded DNA was kept at 80°C for 30 minutes to inactivate the ExoSAP-IT and was then quickly chilled on ice. For each PCR product, 10µL were pipetted into two separate tubes and 5µL of up+ primer was added to one tube and 5µL of Dn- primer was added to the other. All samples were sealed and labeled and sent for DNA sequencing at GENEWIZ, Inc (South Plainfield, New Jersey).

.

Statistics

One-way ANOVA was performed using Prism® 4.0 software (GraphPad Software Inc, San Diego, CA, USA) to assess the treatment-mediated effects on preadipocyte differentiation. Differences in means were analyzed by Dunnett's multiple comparison test. Values with $P < 0.05$ are considered statistically significant.

CHAPTER IV

THE INHIBITORY IMPACT OF GERANYLGERANIOL ON THE DIFFERENTIATION OF MURINE 3T3-F442A PREADIPOCYTES

A Paper To Be Submitted For Publication

In The Journal of Expermential Biology and Medicine

Manal Elfakhani, Hoda Yeganehjoo, Anureet Shah, Huanbiao Mo

Abbreviations: **ADD1:** adipocyte determination- and differentiation-dependent factor 1; ***AdipoQ***: Adiponectin; ***Fabp4***: fatty acid-binding protein 4; ***Fasn***: Fatty acid synthase; ***GLUT-4***: glucose transporter type 4**;** ***GPDH***: Glycerol-3-phosphate dehydrogenase ***HMG-CoA***: 3-hydroxy-3-methylglutaryl coenzyme A; **IDI**: adipogenic inducers (isobutylmethylxanthine, dexamethasone, and insulin); ; ***INSIG1***: Insulin-induced gene 1; ***Lep***: Leptin; ***Pparγ***: peroxisome proliferator-activated receptor γ; ***SREBP1***: sterol regulatory element binding protein

Supported by Texas Department of Agriculture Food and Fiber Research Program and Texas Woman's University Research Enhancement Program.

Abstract

The use of statins, competitive inhibitors of 3-hydroxy-3-methylglutaryl coenzyme A (HMG-CoA) reductase, is possibly associated with insulin resistance. This potential effect of statins is presumably due to the impaired differentiation and diminished glucose utilization of adipocytes. The role of HMG-CoA reductase inhibition

and mevalonate deprivation is not clear in the statin-mediated inhibition of adipocyte differentiation. There is also a need to evaluate the effect of other HMG-CoA reductase suppressors, particularly phytochemicals, on adipocyte differentiation. Geranylgeraniol, a phytochemical (diterpene) shown to accelerate the degradation of HMG-CoA reductase, is hypothesized to mimic the impact of lovastatin in adipocytes by suppressing adipocyte differentiation and adipogenic gene expression. The impact of lovastatin and geranylgeraniol on the differentiation of murine 3T3-F442A adipocytes was evaluated. Adipo-Red assay and oil Red O staining showed that a 7 day incubation with 1.25 - 10 μmol/L lovastatin and 2.5 - 20 μmol/L geranylgeraniol reduced the intracellular triglyceride content of the cells in a dose-dependent fashion. Concomitantly, lovastatin and geranylgeraniol down-regulated the expression of peroxisome proliferator-activated receptor γ (*Pparγ*), a key regulator of adipocyte differentiation as analyzed by real-time qPCR. The expression of adipocyte marker genes including SREBP1, adiponectin, leptin, and fatty acid binding protein 4 was suppressed by lovastatin. The expression of SREBP1, adiponectin, leptin, fatty acid binding protein 4, fatty acid synthase, glycerol-3-phosphate dehydrogenase and glucose transporter 4 was also suppressed by geranylgeraniol. Mevalonate-derived metabolites have essential roles in promoting adipocyte differentiation and adipogenic gene expression. Dietary mevalonate suppressors may have potential as anti-adipogenesis compounds.

Key words: geranylgeraniol, adipocyte, differentiation, mevalonate, *Pparγ*, SREBP-1c, leptin, adiponectin, *Fabp4*, *GPDH*, INSIG1, *GLUT4*, *Fasn*

Introduction

Obesity has become a worldwide epidemic and one of the major public health concerns in developed countries [1]. The degree of obesity [2, 3] is directly associated with an increased risk of a variety of metabolic diseases such as coronary heart disease, type 2 diabetes, cancer, hypertension, dyslipidemia and stroke [4, 5]. Fundamental to the pathology of obesity is the occurrence of hypertrophy and hyperplasia of adipocytes differentiating from fibroblastic preadipocytes and their over-accumulation [6]. Modulation of body fat storage by regulating adipocyte differentiation and adipocyte lipolysis ultimately controls the number and size of adipocytes; [7] therefore, suppressing adipogenesis may be a plausible approach to obesity prevention.

Due to the complexity of studying adipocyte differentiation *in vivo*, a great part of our knowledge of the process has been acquired from the extensive work done on *in vitro* models of adipogenesis, the 3T3 preadipocyte cell line being one of the most well-established and dependable [8, 9]. Differentiated 3T3-L1 and 3T3-F442A preadipocytes possess a large amount of the ultra-structural properties of adipocytes found in animal tissue. Mature 3T3-L1 cells have analogous characteristics with adipocytes in adipose tissues [10]. Once the cells are differentiated, the fat droplets formed are similar in appearance to adipose tissue *in vivo*. Subcutaneous injection of 3T3-F442A cells into nude mice produces an entirely differentiated fat pad [11].

Adipogenesis involves a number of transcriptional factors. Complex interactions of these factors control the expression of hundreds of adipogenic genes [12]. The

differentiation of fibroblasts to adipocytes requires the activation of signaling pathways including those mediated by insulin, insulin like growth factor (IGF)-1, Ras protein and peroxisome proliferator-activated receptor γ (*Pparγ*) [13]. The activation of Ras proteins is followed by the activation of *Pparγ* which promotes preadipocyte differentiation and insulin sensitivity and suppresses adipocyte lipolysis. *Pparγ* is one of the central regulators of adipocyte differentiation and is crucial to adipose tissue formation *in vivo* [14]. The cross-activation of *Pparγ*2 and CCAAT enhancer-binding protein α (*C/EBPα*) up-regulates preadipocyte differentiation by activating the expression of various genes required for acquiring the preadipocyte phenotype such as adiponectin, adipocyte fatty acid-binding protein 4 (*Fabp4*), glucose transporter type 4 (*GLUT4*), and leptin [15] which all play important roles in fatty acid metabolism and adipocyte function. Mature adipocytes are also characterized by glycerol-3-phosphate dehydrogenase (*GPDH*) [16].

Further stimulation of *Pparγ* can occur through an indirect manner with adipocyte determination and differentiation factor-1/sterol regulatory element (SRE) binding protein 1c (ADD1/SREBP1) [17, 18]. ADD1/SREBP1 promotes adipocyte differentiation by increasing the availability of ligands for *Pparγ* [19] and stimulates more genes associated with adipogenesis including fatty-acid synthase (*Fasn*) [20]. Furthermore, SREBP-1c binds to the SRE of adiponectin promoter and stimulates adiponectin expression [21]. Insulin-induced gene 1 (*INSIG1*), a *Pparγ* target gene, is an important regulator in the processing of the SREBPs and is regulated by *Pparγ* [22].

Another SREBP responsive enzyme is 3-hydroxy-3-methylglutaryl coenzyme A (HMG-CoA) reductase, a vital component of the mevalonate pathway. The mevalonate pathway produces sterol (cholesterol) and non-sterol (isoprenoids) products that have various functions in the human body [23]. There are two specific enzymes in the mevalonate pathway that are important for the function of the insulin signaling pathway, consequently leading to adipocyte differentiation. HMG-CoA reductase and geranylgeranyl-pyrophosphate (GGPP) synthetase activities provide prenyl pyrophosphates in the form of GGPP and farnesyl pyrophosphate (FPP) that are required for the modification and biological activity of the IGF-1 receptor and Ras, respectively [23], ultimately leading to the activation of *Ppar*γ2 and adipogenesis. Insulin stimulates the mevalonate pathway which modifies p21Ras in fibroblasts [24].

The mevalonate pathway can be suppressed by the use of HMG-CoA reductase inhibitors. It is believed that by down regulating HMG-CoA reductase activity, pools of FPP and GGPP will be limited, thereby attenuating preadipocyte differentiation into adipocytes. Statins are competitive inhibitors of HMG-CoA reductase and have been shown to inhibit 3T3-L1 preadipocyte differentiation; however, emerging evidence suggests that statins may have adverse side effects such as elevated liver enzymes, muscle problems, cognitive loss, pancreatic dysfunction, hepatic dysfunction and neuropathy [25]. Isoprenoids are plant products derived from the mevalonate pathway that are believed to act similarly to the statins. They down-regulate HMG-CoA reductase and block the synthesis of FPP and GGPP, products that play important roles in

preadipocyte differentiation. Geranylgeraniol, a diterpene alcohol found in linseed and peanut oil [26], has been shown to down-regulate HMG-CoA reductase activity [27]. No research has explored the potential role of geranylgeraniol in suppressing the insulin signaling pathway and preadipocyte differentiation. The effect of geranylgeraniol has also never been studied with 3T3-F442A cells.

In this study, the effect of geranylgeraniol on 3T3-F442A preadipocyte differentiation was evaluated. A possible mechanism for the impact of geranylgeraniol was examined by measuring the expression of adipogenic marker genes including *Pparγ, SREBP-1c, INSIG1, Fabp4, Fasn, GLUT4, GPDH, AdipoQ* and *Lep.*

Materials and Methods

Chemicals

Murine 3T3-F442A cells were purchased from Dr. Howard Green (Harvard Medical School). Geranylgeraniol was purchased from Sigma Aldrich (St. Louis, MO). Lovastatin was a gift from Merck Research Laboratories (Rahway, NJ).

Adipocyte Differentiation

Murine 3T3-F442A preadipocytes were grown and maintained in Dulbecco's Modified Eagle's Media (DMEM) with 4 mmol/L L-glutamine adjusted by American Type Culture Collection (ATCC, Manassas, VA) to contain 1.5 g/L sodium bicarbonate and 4.5 g/L glucose and supplemented with 10% bovine calf Serum (BCS, Fisher Scientific Company LLC, Houston, TX) and 1% penicillin/streptomycin (GIBCO, Grand Island, NY) at 37oC in a humidified atmosphere of 10% CO2.. The cells were seeded in

96-well plates at a density of 2.5 x 103 or 5 x 103 cells per well, 24 well plates (1 x 104 cells/well), 6-well plates (4 x 104 cells/well) or in tissue culture dishes (100 mm x 20 mm, Corning Life Sciences, Wilkes Barre, PA) at 2 x 105 per dish, contingent on the experimental procedure to be carried out. Upon reaching ~70% confluency, 3T3-F442A cells were cultured for 2 days and differentiation was achieved by maintenance in DMEM supplemented with 10% fetal bovine serum (FBS, Fisher Scientific Company), 1% penicillin/streptomycin (GIBCO) and 5µg/mL insulin (Sigma Aldrich). Geranylgeraniol (2.5 - 20µmol/L) or lovastatin (1.25 - 5µmol/L) was added to the differentiation medium of experimental groups, and the control cells were incubated in medium containing the vehicle [dimethyl sulfoxide (DMSO, ATCC) or ethanol (0.1%, v/v)]. Following a 2-day incubation the cells were then cultured in DMEM supplemented with 10% FBS and 5 µg/mL insulin for additional 2 days. Cells were continued in medium without insulin for additional 5-7 days until the differentiation of adipocytes.

Oil Red O staining

Differentiated 3T3-F442A cells were washed twice with phosphate buffer solution (PBS) and fixed in 0.2 mL (24-well plate) or 1mL (6-well plate) of 10% formalin per well at room temperature for 1 hour. Cells were then rinsed with deionized water and stained with 01.mL (24-well) 0.5 mL (6-well) of 0.3% freshly filtered Oil Red O working solution per well at room temperature for 30 minutes [28]. The cells were then rinsed with 0.2mL (24-well) or 1mL (6-well) deionized water before photomicrographs of representative fields of monolayer cells were taken with a Nikon Eclipse TS 100

microscope (Nikon Corporation, Tokyo, Japan) equipped with a Nikon Coolpix 995 digital camera (Nikon Corporation) to visualize cellular neutral lipids.

AdipoRed™ Assay for Measuring Intracellular Triglyceride Content

The lipid content of the differentiated cells was quantified using an AdipoRed™ Assay kit (Lonza, Walkersville, MD) according to manufacturer's instructions. AdipoRed is a reagent that contains the hydrophilic Nile Red stain and allows the quantification of intracellular lipid droplets [29]. Differentiated cells were rinsed with 2 mL Hank's Balanced Salt Solution (HBSS) and to each well, 5 mL HBSS and 140 µL of AdipoRed reagent were added. After 10 - 15 minutes of incubation, the plates were positioned in a Tecan Infinite M200 micro plate reader with Magellan™ software version 6.3 (Tecan Systems Inc., Salzburg, Austria) and fluorescence was measured with an excitation wavelength of 485 nm and an emission wavelength of 572 nm.

Cell Viability Assay

Cultures of 3T3-F442A preadipocytes were seeded (2500 cells/well) in 100µL maintenance medium in 96-well plates and incubated for 48 hours at 37°C in a humidified atmosphere of 10% CO2. The medium was then aspirated from each well and replaced with 100µL of fresh medium containing DMSO or ethanol or increasing concentrations of geranylgeraniol (20 - 200µmol/L) or lovastatin (1.25 – 10µmol/L). The cells continued to incubate for an additional 24 or 48 hours. Cell populations were determined using the CellTiter 96® Aqueous One Solution MTS assay (Promega, Madison, WI) procedure. Cells were then washed once with HBSS. Subsequently,

100µL of serum free medium and 20µL of 3-(4,5-dimethythizol-2-yl)-5-(3-carboxymethoxyphenyl)-2-(4-sulfophenyl)-2H-tetrazolium salt solution were added to each well. Plates were incubated at 37°C in the dark for two hours and then absorbance was measured at 490 nm with a Tecan infiniteM200 plate reader with Magellan™ software version 6.3 (Tecan Systems Inc., Salzburg, Austria) to verify the formazin concentration, which is relative to the number of live cells. The mean absorbance from wells containing cell-free medium was used as the baseline and was deducted from the absorbance of other cell-containing wells. Cell viability was also measured in mature adipocytes. Cultures of 3T3-F442A preadipocytes were seeded (5000 cells/well) and incubated as described above. Cells were then induced to differentiate as described above and grown to maturation. On day 8 – 10 of differentiation, the medium was aspirated from each well and replaced with 100µL of fresh medium containing DMSO or ethanol or increasing concentrations of geranylgeraniol (20 - 200µmol/L) or lovastatin (1.25 - 10µmol/L). The cells continued to incubate for an additional 24 or 48 hours. Cell populations were determined using the CellTiter 96® Aqueous One Solution procedure as described above.

Quantitative Real-time Polymerase Chain Reaction

Total cellular RNA of mature 3T3-F442A adipocytes was extracted using TRIZOL reagent (Invitrogen) according to the manufacturer's protocols. The concentration and purity of the isolated total RNA was determined spectrophotometrically by running the samples in a spectrum of 230 - 400 nm at 10 nm

intervals and using the OD260:280 ratio. The quality of the purified total RNA was verified by detecting a 2:1 ratio for the 28s:18s ribosomal RNA (rRNA) using gel electrophoresis. Samples were run on a 1.5% agarose gel (Tris-acetate (TAE) buffer) at 80 volts for 90 min. and visualized by Chemi Doc XRS imaging system (Bio-Rad, Hercules, CA) following the addition of 0.5 μg/ml ethidium bromide. The level of mRNA expression of *Pparγ, SREBP-1c, INSIG1, Fabp4, Lep, AdipoQ, Fasn, GLUT4* and *GPDH* was analyzed by reverse transcription (RT) followed by quantitative real-time polymerase chain reaction (qPCR). 2 μg of total RNA in a 20 μl reaction buffer was reverse transcribed into cDNA using an Oligo (dT)20 primer and SuperScript® III First-Strand kit (Invitrogen, Grand Island, NY) following the manufacturer's instructions. The cDNA was diluted by 25-fold with 25μg/ml solution of acetylated bovine serum albumin (BSA) and 6 μl of diluted cDNA was amplified in a 25 μl PCR reaction which included 250 nM of both forward and reverse primers of the gene and iQTM SYBR® Green Supermix (Bio-Rad Laboratories). The cDNA was denatured at 95oC for 3 minutes followed by 40 cycles of PCR (94oC for 30 s, 60oC for 25 s, 72oC for 25 s, and 78oC for 9 s) by means of an iQTM5 multi-color Real-Time PCR Detection System (Bio-Rad) with Bio-Rad iQ5 Optical System Software (version 2.1). The mRNA levels of all the genes were normalized using ribosomal protein L22 (*RPL22*) as internal control [30] by using the ΔCT method. Fold changes of gene expression were calculated by the 2-ΔΔCT method.

Primer Design and Verification

Primers were designed using Primer 3 Output version 4.0 online software (Massachusetts Institute of Technology (MIT)) [31]. The sequences were determined for the genes of interest in this study (Table 1). To ensure that a single gene was amplified, the melting profile of double stranded DNA product of PCR generated from each primer was analyzed. The specific PCR products were purified with HT ExoSAP-IT® High Throughput PCR Product Clean-Up (USB® Products, Affymetrix Inc., Cleveland, Ohio, USA) and incubated at 37oC for 30 minutes to degrade remaining primers and nucleotides (dNTPs). The purified double-stranded DNA was kept at 80°C for 30 minutes to inactivate the ExoSAP-IT and was then quickly chilled on ice. To confirm specificity, PCR primers were used to sequence both strands of DNA.

Statistics

One-way analysis of variance (ANOVA) and Tukey's post hoc tests were performed to assess the differences between groups using Prism® 4.0 software (GraphPad Software Inc., San Diego, CA). Levels of significance were designated as $P < 0.05$.

Results

Figure 1 shows the impact of geranylgeraniol on the differentiation of murine 3T3-F442A cells. When differentiated cells were stained with Oil Red O, overall lipid accumulation was noticeably less in the cells that were treated with geranylgeraniol (0 – 20 μmol/L) compared to the control (Figure 1A). Furthermore, there was a clear dose

dependent reduction in the number of lipid droplets observed. A decrease in lipid content was also visible with the cells treated with lovastatin (1.25µmol/L), a known inhibitor of adipocyte differentiation.

The suppression of adipocyte differentiation was confirmed when intracellular triglyceride accumulation was measured by AdipoRed™ Assay (Figure 1B). A concentration-dependent decrease in triglyceride levels was evident with the geranylgeraniol treated cells. Compared with control, the level of adipocyte triglycerides was lower in 3T3-F442A cells treated with 5µmol/L ($P < 0.01$) and 10µmol/L ($P < 0.0001$) of geranylgeraniol. Lovastatin also induced a decrease in triglyceride accumulation in comparison to the control but it was not significant.

To ensure that the decreased intracellular triglyceride was not attributable to cytotoxicity, cell viability was measured with 3T3-F442A preadipocytes prior to the induction of differentiation (Figure 2, A & B) and subsequent to the differentiation process (Figure 2, C & D) differentiation process. When 3T3-F442A preadipocytes were incubated with 20 – 200 µmol/L of geranylgeraniol for 24 (Figure 2A) or 48 hours (Figure 2B) no reduced cell viability was observed at any of the concentrations. Similar findings were observed when mature, fully-differentiated 3T3-F442A cells were incubated with the same concentrations of geranylgeraniol for the same time lengths (Figure 2, C & D). Conversely, decreased cell viability was observed when preadipocytes were incubated with 10 µmol/L of lovastatin for 48 hours (data not shown).

The same concentration of lovastatin (10 μmol/L) also reduced the viability of mature, fully-differentiated 3T3-F442A cells.

We then examined the effect of geranylgeraniol on the genetic expression of *Pparγ* and *SREBP-1c*, two important transcription factors whose interplay is crucial in the early phase of adipogenesis. The mRNA levels of *Pparγ* in the geranylgeraniol treated cells were significantly decreased in a dose dependent manner in comparison with the control ($P < 0.0001$). As anticipated, the preadipocytes grown without adipogenic inducers (IDI-) had lower *Pparγ* levels compared to the control but this was not considered statistically significant (Figure 3A). The mRNA expression of *SREBP-1c* among the geranylgeraniol treated cells mimicked the pattern that was observed with *Pparγ* (Figure 3B); a decreased expression of the gene which is concentration dependent ($P < 0.0001$). INSIG1, a key regulator in the processing of the SREBPs, also showed similar results of mRNA expression when induced by geranylgeraniol ($P < 0.001$). *INSIG1* expression is controlled by *Pparγ* so levels are expected change when *Pparγ* expression is compromised. This outcome is in accordance with geranylgeraniol-mediated reduction in intracellular triglyceride levels that we observed and further supports the claim that all three genes have a critical function in the early process of adipocyte differentiation.

Subsequently, we observed the genes which are under the regulation of *Pparγ* and *SREBP-1c.* The differentiation of the 3T3-F442A preadipocytes in the presence of geranylgeraniol induced a consistent dose-dependent decrease in the mRNA expression

of several adipogenic marker genes: *AdipoQ, Lep, Fabp4, Fasn, GPDH* and *GLUT4* (Figure 3D – I). In comparison to the untreated differentiated cells (control), preadipocytes (IDI-) had a much lower mRNA expression of *AdipoQ, Lep, Fasn, GPDH* and *GLUT4* ($P < 0.0001$). The decreased expression of the leptin mRNA induced by geranylgeraniol is in accordance with the lower levels of *Pparγ* and SREBP-1c that were observed. *Lep* is an established marker of adipocyte differentiation and is involved in the expression of *Pparγ* and *SREBP-1c*. Furthermore, two important markers of terminal differentiation, *GLUT4* and *Fasn*, both experienced markedly lower mRNAs levels due to geranylgeraniol mediated suppression of adipocyte differentiation in the earlier stages. ADD1/SREBP1 is known to stimulate the expression of *Fasn*.

Lovastatin at 1.25μmol/L also suppressed the mRNA levels of *SREBP* and *INSIG1* as well other crucial adipogenic genes including *Lep, Fasn, GPDH* and *GLUT4* an observation consistent with the role of statins in inhibiting adipocyte differentiation.

Table 1.

Primer sequences (forward and reverse) and GenBank accession numbers used in the Real-Time qPCR

Gene	Accession#	Primer Sequence
Pparγ	NM_001127330 & NM_011146	5'-AGAGGGCCAAGGATTCATGACCAGG-3' 5'-TTCAGCTTGAGCTGCAGTTCCAGGG-3'
SREBP-1	NM_011480	5'-TGGCACCCTCTTGCTCTGTAGGCAC-3 5'-GCTGAGGCAGACATCTGCCTACCCA-3'
INSIG1	NM_153526	5'-GCACGAGCTATTCCGGAGAAGGGTTC-3' 5'-GGACCAACGACTGTGTCAGGAGGTCAG-3'
Fabp4	NM_024406	5'-GTGTGATGCCTTTGTGGGAACCTGG-3' 5'-TGCGGTGATTTCATCGAATTCCACG-3'
Lep	NM_008493	5'-TGGAGGTGAGCGGGATCAGGTTTTG-3 5'-TGGCACGTGGGATCTTTCAGAAGCC-3'
AdipoQ	NM_009605	5'-CGGCAGCACTGGCAAGTTCTACTGC-3' 5'-TTGTGGTCCCCATCCCCATACACCT-3'
Fasn	NM_007988	5'-CCCAGGCCTTGCCGTGCAGT-3' 5'-GCTCAGGACTGCGTGGGGCT-3'
GPDH	NM_010271	5'-GGGGGTAGACGAGGCCCCAA-3' 5'-GCCGGGTCCTTGCAGCCGAT-3'
GLUT4	NM_009204	5'-GAACCCCCTCGGCAGCGAGT-3' 5'-ATCCGGTCCCCCAGGACCTTGC-3'
RPL22	NM_009079	5'-GCGACTTTAACTGGGCTGCTGCT-3' 5'-GCCCACCACCCAGCCTCTCG-3'

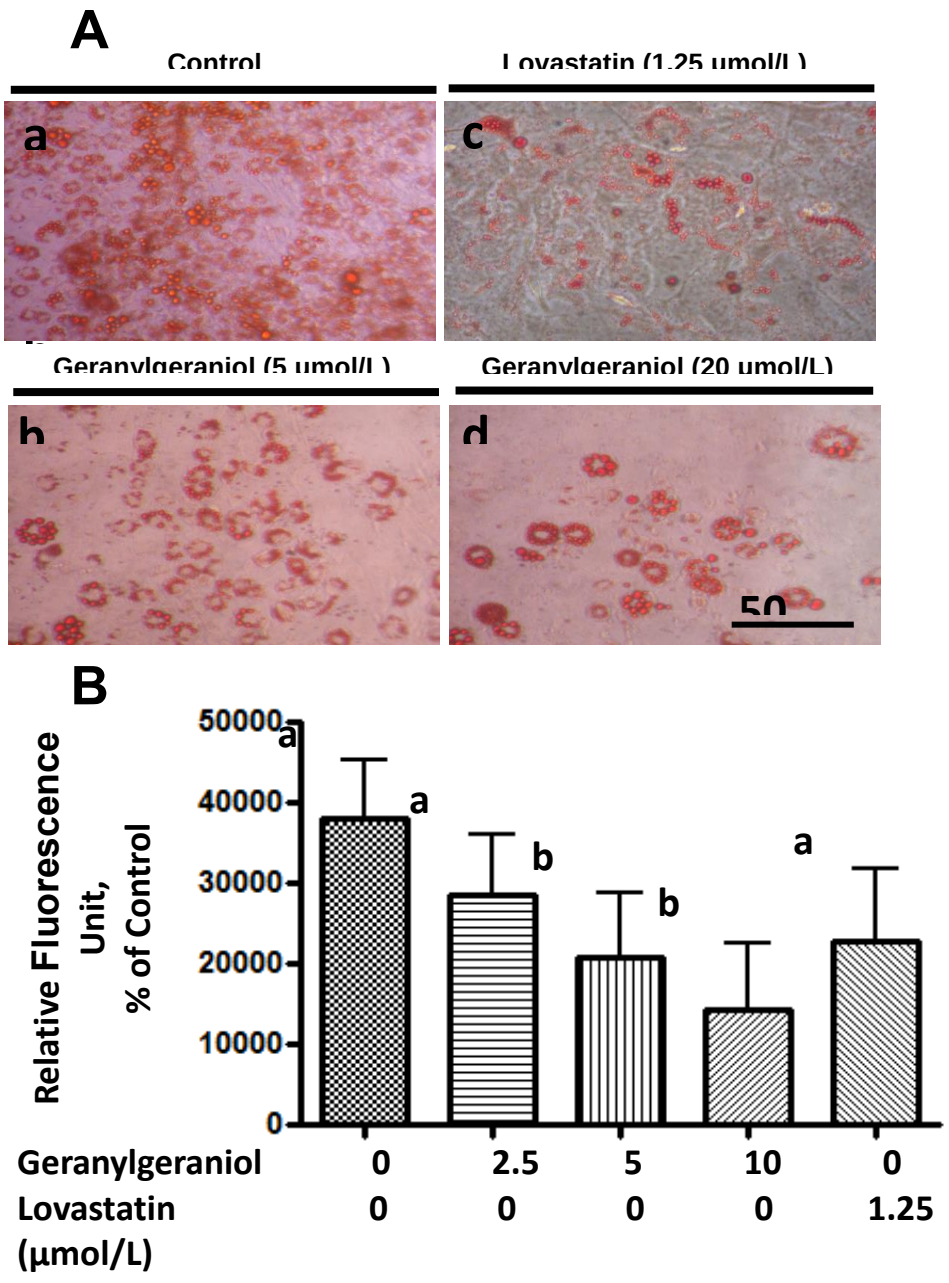

Figure 1. Geranylgeraniol suppresses the differentiation of murine 3T3-F442A preadipocytes. (A) Phase-contrast microscopy of Oil Red O-stained 3T3-F442A preadipocytes subsequent to 8-d differentiation. Cells were incubated with 0 (a), 5 (b) or 20 (c) μmol/L geranylgeraniol or 1.25μmol/L lovastatin during differentiation. (B) Intracellular triglyceride content of 3T3-F442A cells determined by AdipoRed™ Assay subsequent to 8-d differentiation. Cells were incubated with 0, 2.5, 5 or 10 μmol/L geranylgeraniol or 1.25μmol/L lovastatin during differentiation.

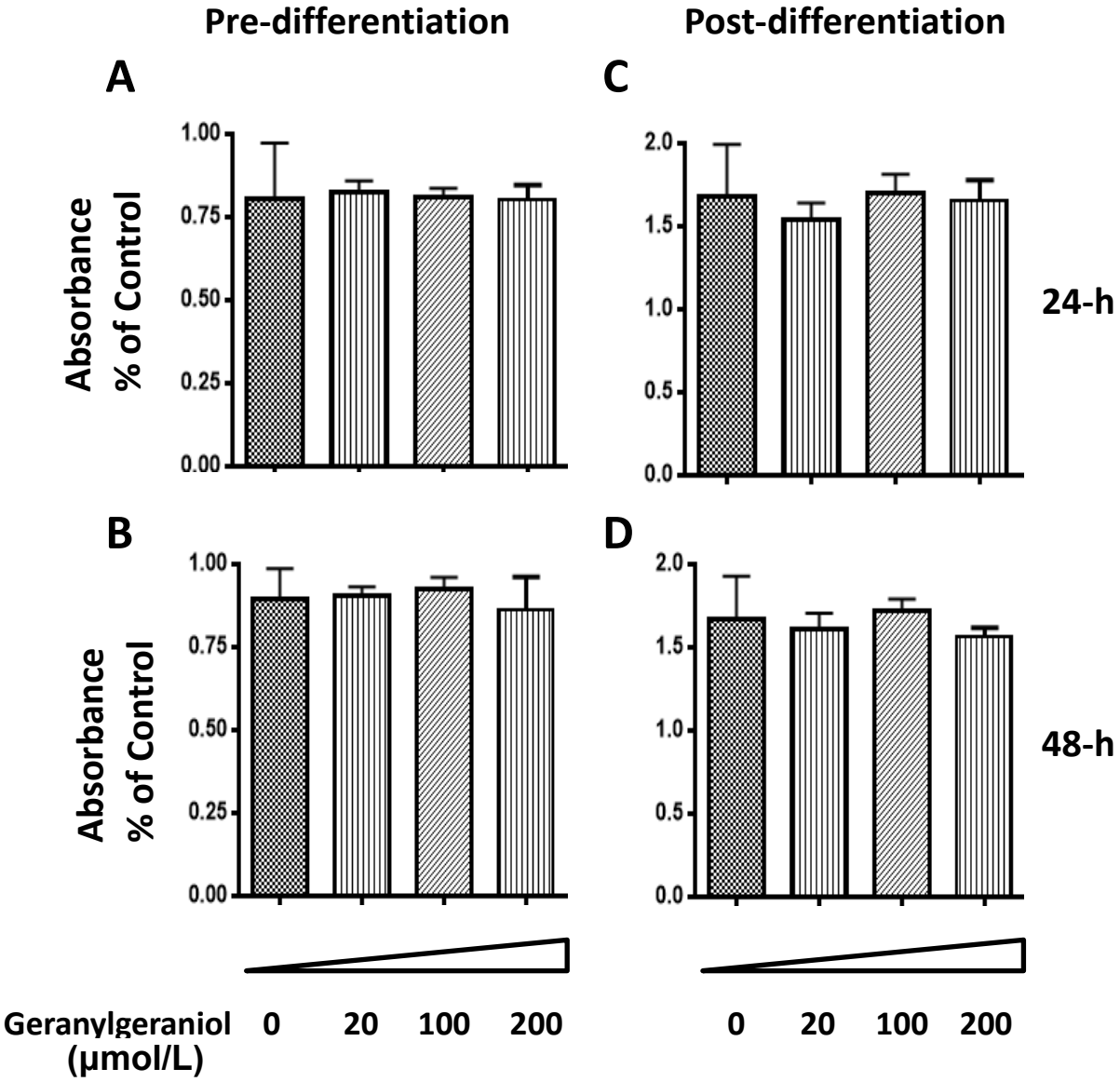

Figure 2. The concentration- and time- dependent impact of geranylgeraniol on the cell viability of murine 3T3-F442A preadipocytes prior to (A & B) and subsequent to (C & D) 8-d differentiation. The pre-differentiation and differentiated 3T3-F442A cells were incubated with geranylgeraniol (0-200 μmol/L) for 24- (A & C) or 48- (B & D) hours before cell viability was determined by CellTiter 96® Aqueous One Assay.

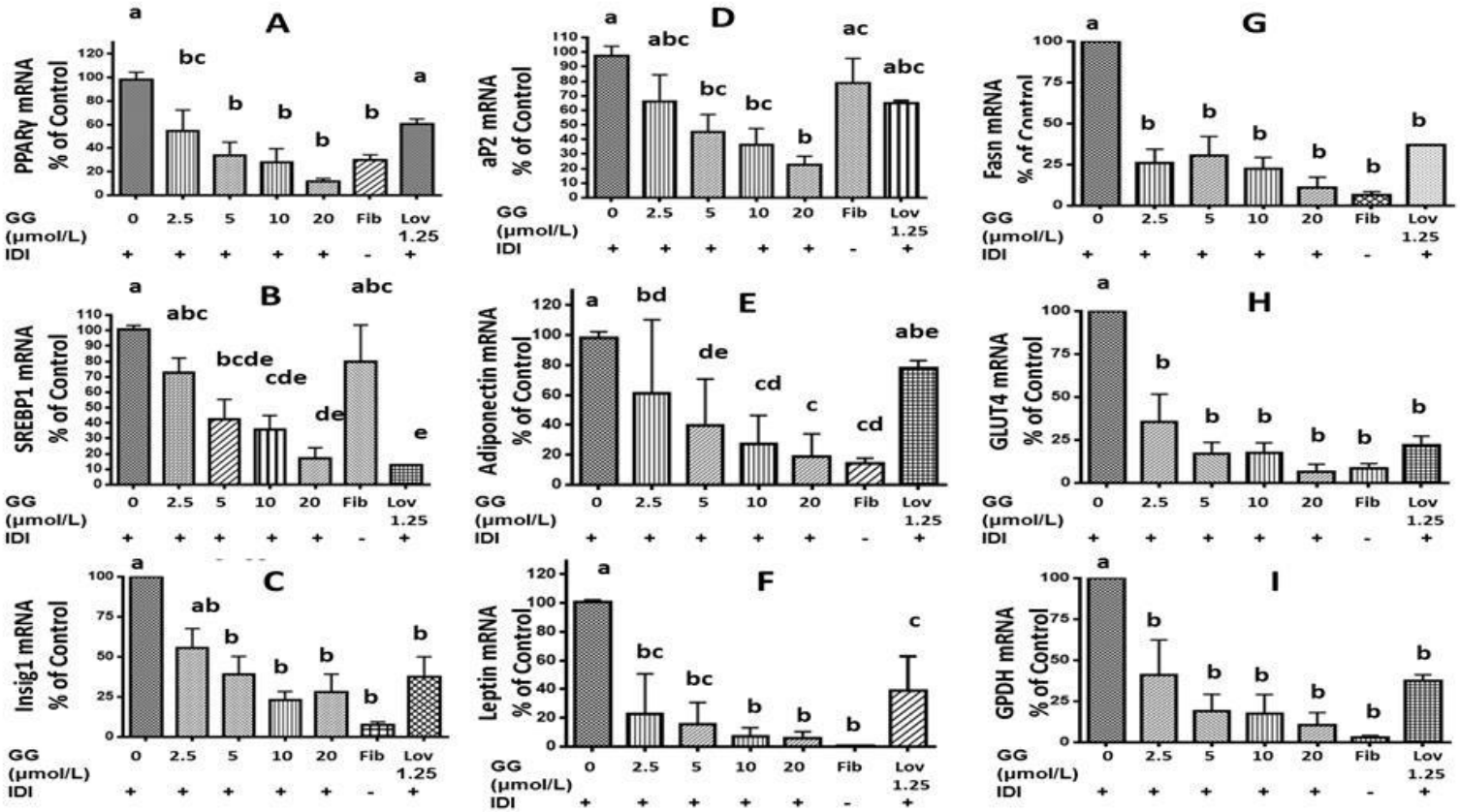

Figure 3. The impact of geranylgeraniol on the expression of adipogenic marker genes. 3T3-F442A preadipocytes were incubated in the absence (-) or presence (+) of IDI and geranylgeraniol as indicated for 8 days. The differentiated cells were lysed and total RNA was extracted. Cellular mRNA levels of PPARγ (A), SREBP-1c (B), INSIG1 (C), aP2 (D), leptin (E), adiponectin (F), Fasn (G), GLUT4 (H) and GPDH (I) were measured by RT-PCR.

Discussion

Little research has been done on the mevalonate suppressive activity of geranylgeraniol and its effect on human health. No research has explored the potential role of geranylgeraniol in inhibiting the insulin signaling pathway and consequently preadipocyte differentiation by way of down regulation of the mevalonate pathway. Some research has explored naturally occurring mevalonate suppressors such as vitamin E tocotrienols [32], terpenoids [33], genistein [34], and berberine [35] and has determined suppression in adipocyte differentiation with down regulation of *Pparγ*, *C/EBPa*, and *Fabp4* expression. However, much of our knowledge of the role mevalonate suppressors in modulating adipocyte differentiation comes from research done on statins. A large amount of evidence exhibits that statins have a strong inhibitory impact on the adipogenesis process [36-40] by suppressing lipid accumulation, down-regulating the expression of adipogenic transcriptional factors including *Pparγ*2, *Fabp4* and *GLUT4* [41], inhibiting adipocyte maturation, suppressing *C/EBPα* expression and disrupting insulin signaling [39, 42].

In this study, we found that geranylgeraniol down regulates the expression of various genes which are crucial at different stages in the adipogenesis process, as measured by real-time qPCR. *Pparγ* and *SREBP-1c* are both involved in the early phase of adipocyte differentiation [43] and their presence is critical in the initiation of adipogenesis. There are several adipogenic genes which are stimulated by these earlier processes such as *INSIG1, Lep*, *Fabp4*, adiponectin and *GPDH*, which are important in

the progression of adipocyte differentiation. Mature, fully differentiated adipocytes are characterized by *GLUT4* and *Fasn*, important biomarkers of terminal differentiation. Since we observed markedly lower mRNAs levels among all of these adipogenic genes, the geranylgeraniol mediated suppression of adipocyte differentiation may have probably impacted the earlier stages of the process which influenced the progression of adipogenesis. Our findings are consistent with previous studies which have examined mevalonate suppressors, mainly statins, and their inhibition of 3T3-L1 preadipocyte differentiation by down regulation of *Pparγ* [37, 39, 41], *C/EBPα* [39], *Fabp4* [40, 44], *AdipoQ* [40, 45], *GLUT4* [37] and *Lep* [41].

The differentiation of fibroblasts to adipocytes is complex process which involves the occurrence of several crucial events that require the activation of signaling pathways including those mediated by insulin, insulin like growth factor (IGF)-1, Ras protein and *Pparγ*2 [13, 46]. SREBP-1c is also an important component of the development of adipogenesis and is known to stimulate fat specific genes such as *Fasn*, glycerol-3-phosphate acyltransferase, and stearoyl CoA desaturase 2 [47] that are important in adipocyte differentiation. ADD1/SREBP-1c is thought to intervene with the insulin-induced changes in adipogenic gene expression in adipose tissue [22] and its up regulation provides *Pparγ* agonists that further fuel the differentiation process [48]. INSIG1 is believed to act as a "check" on the highly integrated network of transcription factors (*C/EBP*s, *Ppar*s, and SREBPs) and provides a key link between insulin sensitization, glucose homeostasis and lipid homeostasis [22]. *INSIG1*, a *Pparγ* target

gene, is an important regulator in the processing of the SREBPs and is in turn regulated by *Pparγ* [21]. *Lep* expression is stimulated by insulin, *C/EBPα* and *Pparγ* [49, 50] and is involved in the expression of SREBP-1c. Given that mRNA levels of *Pparγ*, *SREBP-1c*, *INSIG1*, *Lep* and *Fasn* levels were all found to be suppressed highlights their mutual interaction.

Another SREBP responsive enzyme is 3-hydroxy-3-methylglutaryl coenzyme A (HMG-CoA) reductase, a vital component of the mevalonate pathway. Through the mevalonate pathway, HMG-CoA reductase provides mevalonate-derived sterol (cholesterol) and non-sterol products (isoprenoids) [23] crucial to insulin signaling. There are two specific enzymes in the mevalonate pathway that are implicated in the function of the insulin signaling pathway consequently leading to adipocyte differentiation. HMG-CoA reductase and GGPP synthetase activity provide prenyl pyrophosphates in the form of GGPP and FPP that are required for the modification and biological activity of the IGF-1 receptor and Ras, respectively, [23] ultimately leading to the activation of *Pparγ*2 and the adipogenesis process (Figure 2). Insulin stimulates the mevalonate pathway activity necessary for the modification of p21 Ras in fibroblasts [24].

When fibroblasts undergo differentiation into mature adipocytes, the expression of GGPP synthetase increases by more than 20-fold. To explore the effect of insulin on the regulation of GGPP synthetase expression, 3T3-L1 adipocytes were cultured with or without insulin for 24 hours followed by the measurement of mRNA expression. Insulin

did not induce GGPP synthetase mRNA expression, however, *Fasn* expression increased by 80% [51]. During the differentiation of the 3T3-L1 cells, there were large increases in the mRNA levels of low density lipoprotein (LDL) receptor and HMG-CoA synthetase and smaller increases in the levels of lipoprotein lipase (*LPL*). HMG-CoA reductase is markedly increased at day 3 of differentiation [52] and in differentiated 3T3-L1 cells [35] and adipose tissues from obese rodents [53] and humans [54].

The inhibition of HMG-CoA reductase by mevalonate suppressors limits its activity, thus suppressing isoprenoid synthesis. Geranylgeraniol has been shown to down-regulate HMG-CoA reductase activity [27]. It is believed that by down regulating HMG-CoA reductase activity, pools of FPP and GGPP will be limited, thereby attenuating preadipocyte differentiation into adipocytes. Inhibition of HMG-CoA reductase is associated with a reduced expression of *GLUT4* [36] which explains the decreased *GLUT4* mRNA levels that were observed in the geranylgeraniol treated cells.

Statins have been shown to play an important role in preadipocyte differentiation, unfortunately, the potential for the long-term application of statins in obesity prevention and treatment is unknown by their dose-limiting toxicities [55]. Emerging evidence suggests that statins may have adverse side effects such as elevated liver enzymes, muscle problems, cognitive loss, pancreatic dysfunction, hepatic dysfunction and neuropathy [25]. Dietary mevalonate suppressors such as geranylgeraniol may have anti-adipogenic benefits without the potential complications associated with statins.

Insulin resistance [39, 56-58] and reduction of insulin-induced glucose uptake [59] may be stimulated by statins but the effect of geranylgeraniol is unclear. In this study, both geranylgeraniol and lovastatin significantly decreased the expression of *GLUT4*, similar to the findings of another study [60], which supports the observation that statins induce insulin resistance. Knockout mice that are heterogeneous for *GLUT4* were shown to develop insulin resistance and diabetes [61]. Adiponectin, a known biomarker for insulin sensitivity, [62] was not down regulated by lovastatin in this study. However, geranylgeraniol did suppress the expression of adiponectin. Nevertheless, both geranylgeraniol and lovastatin exhibited decreases in *Pparγ* and *Fabp4* mRNA expression. Reduction in *Pparγ* activity has been shown to prevent insulin resistance [63-66]. Additionally, down regulation of *Fabp4* may play an important function in controlling metabolic syndrome and diabetes since it has a central role in linking obesity and insulin resistance. Mice deficient in *Fabp4* did not develop insulin resistance or diabetes [67]. The impact of geranylgeraniol on insulin resistance may necessitate further study.

In conclusion, geranylgeraniol may potential as an anti-adipogenesis compound by way of suppression of the preadipocyte differentiation into mature adipocytes. To our knowledge, the effects of geranylgeraniol on modulating the differentiation of 3T3-F442A preadipocytes had not yet been explored. Further examination of specific mechanisms of action involved in the impact of geranylgeraniol on suppressing differentiation in murine 3T3-F442A preadipocytes would be necessary. Assessment of

the potential reversal of the effect of geranylgeraniol by the Ppar agonist mevalonate warrants additional investigation.

Acknowledgement

We thank Dr. Parakat Vijayagopal for technical assistance in the culture of 3T3 cells.

References

1. Caballero, B., The global epidemic of obesity: an overview. Epidemiol Rev, 2007. 29: p. 1-5.
2. Romero-Corral, A., et al., Association of bodyweight with total mortality and with cardiovascular events in coronary artery disease: a systematic review of cohort studies. Lancet, 2006. 368(9536): p. 666-78.
3. Kissebah, A.H. and G.R. Krakower, Regional adiposity and morbidity. Physiol Rev, 1994. 74(4): p. 761-811.
4. Badman, M.K. and J.S. Flier, The adipocyte as an active participant in energy balance and metabolism. Gastroenterology, 2007. 132(6): p. 2103-15.
5. NIH, Clinical Guidelines on the Identification, Evaluation, and Treatment of Overweight and Obesity in Adults. , N.O.E. Initiative, Editor 1998.
6. Gesta, S., Y.H. Tseng, and C.R. Kahn, Developmental origin of fat: tracking obesity to its source. Cell, 2007. 131(2): p. 242-56.
7. Flier, J.S., Obesity wars: molecular progress confronts an expanding epidemic. Cell, 2004. 116(2): p. 337-50.
8. Wood, R.J., Vitamin D and adipogenesis: new molecular insights. Nutr Rev, 2008. 66(1): p. 40-6.
9. Green, H. and M. Meuth, Sublines of mouse 3T3 cells that accumulate lipid. Cell, 1974. 1(3): p. 113-6.
10. Cowherd, R.M., R.E. Lyle, and R.E. McGehee, Jr., Molecular regulation of adipocyte differentiation. Semin Cell Dev Biol, 1999. 10(1): p. 3-10.
11. Green, H. and O. Kehinde, Formation of normally differentiated subcutaneous fat pads by an established preadipose cell line. J Cell Physiol, 1979. 101(1): p. 169-71.
12. Morrison, R.F. and S.R. Farmer, Insights into the transcriptional control of adipocyte differentiation. J Cell Biochem, 1999. Suppl 32-33: p. 59-67.
13. Fernyhough, M.E., et al., Pparγ and GLUT-4 expression as developmental regulators/markers for preadipocyte differentiation into an adipocyte. Domest Anim Endocrinol, 2007. 33(4): p. 367-78.
14. Castrillo, A. and P. Tontonoz, Nuclear receptors in macrophage biology: at the crossroads of lipid metabolism and inflammation. Annual Review of Cell and Developmental Biology, 2004. 20: p. 455-80.

15. Tontonoz, P., et al., mPpar gamma 2: tissue-specific regulator of an adipocyte enhancer. Genes Dev, 1994. 8(10): p. 1224-34.
16. Krapivner, S., et al., Insulin-induced gene 2 involvement in human adipocyte metabolism and body weight regulation. J Clin Endocrinol Metab, 2008. 93(5): p. 1995-2001.
17. Rosen, E.D. and B.M. Spiegelman, Molecular regulation of adipogenesis. Annual Review of Cell and Developmental Biology, 2000. 16: p. 145-71.
18. Kim, J.B. and B.M. Spiegelman, ADD1/SREBP1 promotes adipocyte differentiation and gene expression linked to fatty acid metabolism. Genes Dev, 1996. 10(9): p. 1096-107.
19. Kim, J.B., et al., ADD1/SREBP1 activates Ppargamma through the production of endogenous ligand. Proceedings of the National Academy of Sciences of the United States of America, 1998. 95(8): p. 4333-7.
20. Brown, M.S. and J.L. Goldstein, The SREBP pathway: regulation of cholesterol metabolism by proteolysis of a membrane-bound transcription factor. Cell, 1997. 89(3): p. 331-40.
21. Doran, A.C., et al., The helix-loop-helix factors Id3 and E47 are novel regulators of adiponectin. Circulation Research, 2008. 103(6): p. 624-34.
22. Kast-Woelbern, H.R., et al., Rosiglitazone induction of INSIG1 in white adipose tissue reveals a novel interplay of peroxisome proliferator-activated receptor gamma and sterol regulatory element-binding protein in the regulation of adipogenesis. J Biol Chem, 2004. 279(23): p. 23908-15.
23. Goldstein, J.L. and M.S. Brown, Regulation of the mevalonate pathway. Nature, 1990. 343(6257): p. 425-30.
24. Goalstone, M.L. and B. Draznin, Effect of insulin on farnesyltransferase activity in 3T3-L1 adipocytes. J Biol Chem, 1996. 271(44): p. 27585-9.
25. Golomb, B.A. and M.A. Evans, Statin adverse effects : a review of the literature and evidence for a mitochondrial mechanism. Am J Cardiovasc Drugs, 2008. 8(6): p. 373-418.
26. Fedeli, E., et al., Isolation of geranyl geraniol from the unsaponifiable fraction of linseed oil. J Lipid Res, 1966. 7(3): p. 437-41.
27. Katuru, R., et al., Mevalonate depletion mediates the suppressive impact of geranylgeraniol on murine B16 melanoma cells. Exp Biol Med (Maywood), 2011. 236(5): p. 604-13.
28. Ramirez-Zacarias, J.L., F. Castro-Munozledo, and W. Kuri-Harcuch, Quantitation of adipose conversion and triglycerides by staining intracytoplasmic lipids with Oil red O. Histochemistry, 1992. 97(6): p. 493-7.
29. Greenspan, P., E.P. Mayer, and S.D. Fowler, Nile red: a selective fluorescent stain for intracellular lipid droplets. Journal of Cell Biology, 1985. 100(3): p. 965-73.
30. de Jonge, H.J., et al., Evidence based selection of housekeeping genes. PLoS One, 2007. 2(9): p. e898.

31. Rozen, H.J.S.a.S., Primer3 on the WWW for general users and for biologist programmers, in Bioinformatics Methods and Protocols: Methods in Molecular Biology, M.S.e. Krawetz S, Editor. 2000, Humana Press
Totowa, NJ. p. 365-386.
32. Uto-Kondo, H., et al., Tocotrienol suppresses adipocyte differentiation and Akt phosphorylation in 3T3-L1 preadipocytes. Journal of Nutrition, 2009. 139(1): p. 51-7.
33. Gong, Z., et al., The role of tanshinone IIA in the treatment of obesity through peroxisome proliferator-activated receptor gamma antagonism. Endocrinology, 2009. 150(1): p. 104-13.
34. Kim, M.H., et al., Genistein and daidzein repress adipogenic differentiation of human adipose tissue-derived mesenchymal stem cells via Wnt/beta-catenin signalling or lipolysis. Cell Prolif, 2010. 43(6): p. 594-605.
35. Huang, C., et al., Berberine inhibits 3T3-L1 adipocyte differentiation through the Pparγ pathway. Biochem Biophys Res Commun, 2006. 348(2): p. 571-8.
36. Nishio, E., et al., 3-Hydroxy-3-methylglutaryl coenzyme A reductase inhibitor impairs cell differentiation in cultured adipogenic cells (3T3-L1). Eur J Pharmacol, 1996. 301(1-3): p. 203-6.
37. Nicholson, A.C., et al., Anti-adipogenic action of pitavastatin occurs through the coordinate regulation of Ppargamma and Pref-1 expression. Br J Pharmacol, 2007. 151(6): p. 807-15.
38. Tomiyama, K., E. Nishio, and Y. Watanabe, Both wortmannin and simvastatin inhibit the adipogenesis in 3T3-L1 cells during the late phase of differentiation. Jpn J Pharmacol, 1999. 80(4): p. 375-8.
39. Nakata, M., et al., Effects of statins on the adipocyte maturation and expression of glucose transporter 4 (SLC2A4): implications in glycaemic control. Diabetologia, 2006. 49(8): p. 1881-92.
40. Goto, T., et al., Farnesyl pyrophosphate regulates adipocyte functions as an endogenous Ppargamma agonist. Biochemical Journal, 2011. 438(1): p. 111-9.
41. Jeon, T., et al., Red yeast rice extracts suppress adipogenesis by down-regulating adipogenic transcription factors and gene expression in 3T3-L1 cells. Life Sci, 2004. 75(26): p. 3195-203.
42. Siddals, K.W., et al., Abrogation of insulin-like growth factor-I (IGF-I) and insulin action by mevalonic acid depletion: synergy between protein prenylation and receptor glycosylation pathways. J Biol Chem, 2004. 279(37): p. 38353-9.
43. Gregoire, F.M., C.M. Smas, and H.S. Sul, Understanding adipocyte differentiation. Physiological Reviews, 1998. 78(3): p. 783-809.
44. Nicholson, A.C., et al., Anti-adipogenic action of pitavastatin occurs through the coordinate regulation of Ppargamma and Pref-1 expression. British Journal of Pharmacology, 2007. 151(6): p. 807-15.
45. Furuhashi, M., et al., Treatment of diabetes and atherosclerosis by inhibiting fatty-acid-binding protein *Fabp4*. Nature, 2007. 447(7147): p. 959-65.

46. Ntambi, J.M. and K. Young-Cheul, Adipocyte differentiation and gene expression. J Nutr, 2000. 130(12): p. 3122S-3126S.
47. Konig, B., et al., Activation of Pparα and Pparγ reduces triacylglycerol synthesis in rat hepatoma cells by reduction of nuclear SREBP-1. European Journal of Pharmacology, 2009. 605(1-3): p. 23-30.
48. Fajas, L., J.C. Fruchart, and J. Auwerx, Transcriptional control of adipogenesis. Current Opinion in Cell Biology, 1998. 10(2): p. 165-73.
49. Yang, R. and L.A. Barouch, Leptin signaling and obesity: cardiovascular consequences. Circ Res, 2007. 101(6): p. 545-59.
50. Margetic, S., et al., Leptin: a review of its peripheral actions and interactions. Int J Obes Relat Metab Disord, 2002. 26(11): p. 1407-33.
51. Vicent, D., E. Maratos-Flier, and C.R. Kahn, The branch point enzyme of the mevalonate pathway for protein prenylation is overexpressed in the ob/ob mouse and induced by adipogenesis. Mol Cell Biol, 2000. 20(6): p. 2158-66.
52. Shimomura, I., et al., Differential expression of exons 1a and 1c in mRNAs for sterol regulatory element binding protein-1 in human and mouse organs and cultured cells. J Clin Invest, 1997. 99(5): p. 838-45.
53. Le Lay, S., et al., Cholesterol : A cell size dependent signal which regulates glucose metabolism and gene expression in adipocytes. J Biol Chem, 2001. 27: p. 27.
54. Le Lay, S., P. Ferre, and I. Dugail, Adipocyte cholesterol balance in obesity. Biochemical Society Transactions, 2004. 32(Pt 1): p. 103-6.
55. Thibault, A., et al., Phase I study of lovastatin, an inhibitor of the mevalonate pathway, in patients with cancer. Clin Cancer Res, 1996. 2(3): p. 483-91.
56. Freeman, D.J., et al., Pravastatin and the development of diabetes mellitus: evidence for a protective treatment effect in the West of Scotland Coronary Prevention Study. Circulation, 2001. 103(3): p. 357-62.
57. Sever, P.S., et al., Prevention of coronary and stroke events with atorvastatin in hypertensive patients who have average or lower-than-average cholesterol concentrations, in the Anglo-Scandinavian Cardiac Outcomes Trial--Lipid Lowering Arm (ASCOT-LLA): a multicentre randomised controlled trial. Lancet, 2003. 361(9364): p. 1149-58.
58. Group, T.D.A.L.I.D.S., The effect of aggressive versus standard lipid lowering by atorvastatin on diabetic dyslipidemia: the DALI study: a double-blind, randomized, placebo-controlled trial in patients with type 2 diabetes and diabetic dyslipidemia. Diabetes Care, 2001. 24(8): p. 1335-41.
59. Mauser, W., et al., Direct adipotropic actions of atorvastatin: differentiation state-dependent induction of apoptosis, modulation of endocrine function, and inhibition of glucose uptake. Eur J Pharmacol, 2007. 564(1-3): p. 37-46.
60. Chamberlain, L.H., Inhibition of isoprenoid biosynthesis causes insulin resistance in 3T3-L1 adipocytes. FEBS Lett, 2001. 507(3): p. 357-61.
61. Stenbit, A.E., et al., *GLUT4* heterozygous knockout mice develop muscle insulin resistance and diabetes. Nat Med, 1997. 3(10): p. 1096-101.

62. Asterholm, I.W. and P.E. Scherer, Enhanced metabolic flexibility associated with elevated adiponectin levels. American Journal of Pathology, 2010. 176(3): p. 1364-76.
63. Altshuler, D., et al., The common Ppargamma Pro12Ala polymorphism is associated with decreased risk of type 2 diabetes. Nature Genetics, 2000. 26(1): p. 76-80.
64. Yamauchi, T., et al., Inhibition of RXR and Ppargamma ameliorates diet-induced obesity and type 2 diabetes. Journal of Clinical Investigation, 2001. 108(7): p. 1001-13.
65. Kubota, N., et al., Ppar gamma mediates high-fat diet-induced adipocyte hypertrophy and insulin resistance. Molecular Cell, 1999. 4(4): p. 597-609.
66. Miles, P.D., et al., Improved insulin-sensitivity in mice heterozygous for Ppar-gamma deficiency. Journal of Clinical Investigation, 2000. 105(3): p. 287-92.
67. Hotamisligil, G.S., et al., Uncoupling of obesity from insulin resistance through a targeted mutation in *Fabp4*, the adipocyte fatty acid binding protein. Science, 1996. 274(5291): p. 1377-9.

CHAPTER V

MEVALONATE DEPRIVATION MEDIATES THE IMPACT OF LOVASTATIN ON THE DIFFERENTIATION OF MURINE 3T3-F442A PREADIPOCYTES

A Paper to Be Submitted For Publication

In The Journal of Expermential Biology and Medicine

Manal Elfakhani, Sheida Torabi, Deema Hussein, Nathaniel Mills, Guido F. Verbeck, Huanbiao Mo

Abbreviations: ***AdipoQ***: Adiponectin; **ADD1:** adipocyte determination- and differentiation-dependent factor 1; ***Fabp4***: fatty acid-binding protein 4; **HMG-CoA**: 3-hydroxy-3-methylglutaryl coenzyme A; **IDI**: adipogenic inducers (isobutylmethylxanthine, dexamethasone, and insulin); ***Lep***: Leptin; ***Pparγ***: peroxisome proliferator-activated receptor γ; **SREBP**: sterol regulatory element binding protein

Supported by Texas Department of Agriculture Food and Fiber Research Program and Texas Woman's University Research Enhancement Program.

Abstract

The use of statins, competitive inhibitors of 3-hydroxy-3-methylglutaryl coenzyme A (HMG-CoA) reductase, is associated with insulin resistance, presumably due to the impaired differentiation and diminished glucose utilization of adipocytes. We hypothesize that mevalonate, the product of HMG-CoA reductase, is essential to adipocyte differentiation and adipogenic gene expression. Adipo-Red assay and oil Red

O staining showed that 7-d incubation with 1.25-5 μmol/L lovastatin dose-dependently reduced the intracellular triglyceride content of murine 3T3-F442A adipocytes. Concomitantly, lovastatin down-regulated the expression of peroxisome proliferator-activated receptor γ (*Pparγ*), leptin, fatty acid binding protein 4, and adiponectin as measured by real-time qPCR. The expression of sterol regulatory element binding protein 1, a transcriptional regulator of *Pparγ* and leptin genes, was also suppressed by lovastatin. The impact of lovastatin on intracellular triglyceride content and expression of the adipogenic genes was reversed by supplemental mevalonate. Mevalonate-derived metabolites have essential roles in promoting adipocyte differentiation and adipogenic gene expression.

Key words

lovastatin, adipocyte, differentiation, mevalonate, Pparγ, SREBP-1c, leptin, adiponectin, Fabp4

Introduction

Obesity is characterized by, among many other physiological changes, over-accumulation of differentiated adipocytes, and is a risk factor for chronic diseases such as type 2 diabetes, hypertension, coronary heart disease and cancer. At the cellular level, obesity is characterized by hyperplasia and hypertrophy of adipocytes differentiated from fibroblastic preadipocytes. Suppressing adipocyte differentiation or adipogenesis is one of the potential approaches in obesity prevention.

Adipocyte differentiation is a well-orchestrated multi-step process involving several genes [1]. Peroxisome proliferator-activated receptor γ (*Pparγ*) is one of the central regulators of adipocyte differentiation and is essential to adipose tissue formation *in vivo* [2]. *Pparγ* regulates the expression of adipogenic genes including leptin (*Lep*) [3], adipocyte fatty acid-binding protein 4 (*Fabp4*) [4], and Adiponectin (*AdipoQ*), all playing important roles in fatty acid metabolism and adipocyte functions. *Pparγ* activity is enhanced by adipocyte determination- and differentiation-dependent factor 1/sterol regulatory element (SRE) binding protein 1 (ADD1/SREBP1) [5], a promoter of adipocyte differentiation that increases the availability of ligands for *Pparγ* [6]. SREBP-1c binds to the SRE of adiponectin promoter and stimulates adiponectin expression [7]. Both *Pparγ* and SREBP-1c are involved in early stages of adipocyte differentiation [8].

The 3T3 preadipocyte cells are a well-established *in vitro* model [9] for studying adipocyte differentiation because their morphology resembles that of fibroblastic preadipocytes from animal fat tissues. Mature 3T3-L1 cells share virtually all characteristics with adipocytes in the adipose tissues [10]. In this study we used 3T3-F442A preadipocytes, a subclone [11] of 3T3-L1 cells with greater frequency of adipose conversion and increased rate of lipid accumulation than the original 3T3-L1 cell line. The 3T3-F442A preadipocytes are able to form fat pads similar to normal adipose tissues when injected into mice [12]. The formation and appearance of fat droplets in these differentiated cells mimic adipose tissue *in vivo*.

It has been suggested that the signaling of insulin, a promoter of preadipocyte differentiation [13], requires mevalonate-derived metabolites [14]. Statins are competitive inhibitors of 3-hydroxy-3-methylglutaryl coenzyme A (HMG-CoA) reductase, the rate-limiting enzyme in the mevalonate pathway to provide mevalonate-derived sterol and non-sterol products [15]. Statins have been shown to inhibit 3T3-L1 preadipocyte differentiation. Nevertheless, their effect on the genes involved in adipocyte differentiation is poorly understood and whether their impact on preadipocyte differentiation is mediated by mevalonate deprivation in uncertain; the latter is shown in the contradictory evidence for the ability of supplemental mevalonate to reverse the effect of statins [16, 17]. The effect of statins has also never been studied with 3T3-F442A cells.

In this study we evaluated the impact of lovastatin on 3T3-F442A preadipocyte differentiation and the expression of adipogenic genes including *Pparγ*, *SREBP-1c*, *Fabp4*, *AdipoQ* and *Lep*. We further determined whether the impact of lovastatin is mediated by mevalonate deprivation.

Materials and Methods

Culture and Oil Red O staining of 3T3-F442A cells

Murine 3T3-F442A cells purchased from Dr. Howard Green (Harvard Medical School) were cultured in 24 well (1 x 104 cells/0.3 mL medium/well) and 6-well (4 x 104 cells/3 mL medium/well) plates in Dulbecco's modified Eagle's medium (DMEM) adjusted by American Type Culture Collection (ATCC, Manassas, VA) to contain 4

mmol/L L-glutamine, 1.5 g/L sodium bicarbonate and 4.5 g/L glucose, supplemented with 10% bovine calf serum (BCS, Fisher Scientific Company LLC, Houston, TX) and 1% penicillin/streptomycin (GIBCO, Grand Island, NY) at 37^{o}C in a humidified atmosphere of 10% CO2. Upon reaching ~70% confluency the 3T3-F442A cells were switched from the maintenance medium above to DMEM supplemented with 10% fetal bovine serum (FBS, Fisher Scientific Company), 5 μg/mL insulin (Sigma Aldrich, St. Louis, MO), and 1% penicillin/streptomycin (GIBCO). Lovastatin (gift from Merck Research Laboratories, Rahway, NJ; 1.25 and 2.5 μmol/L) was added to the experimental groups and control cells were incubated in medium containing dimethyl sulfoxide (DMSO, ATCC) (0.1%, v/v); both were kept until the end of the study. Following a 2-day incubation the cells were then cultured in DMEM supplemented with 10% FBS and 5 μg/mL insulin for additional 2 days. Cells were continued in medium without insulin for additional 5-7 days until the differentiation of adipocytes. Cells were rinsed with phosphate buffer solution (PBS) twice and fixed in 1mL of 10% formalin per well at room temperature for 1 h. Cells were then rinsed with deionized water and stained with 0.5 mL of 0.3% freshly filtered Oil red O working solution per well at room temperature for 30 min [18] to visualize cellular neutral lipids. The cells were then washed with 1 mL deionized water per well for three times before photomicrographs of representative fields of monolayer cells were taken with a Nikon Eclipse TS 100 microscope (Nikon Corporation, Tokyo, Japan) equipped with a Nikon Coolpix 995 digital camera (Nikon Corporation).

AdipoRed™ Assay for measuring intracellular triglyceride content

Eight days after the induction of differentiation, lipid content was quantified using an AdipoRed™ Assay kit (Lonza, Walkersville, MD) according to manufacturer's instructions. AdipoRed is a reagent that contains the hydrophilic Nile Red stain and allows the quantification of intracellular lipid droplets [19]. Differentiated cells were rinsed with 2 mL Hank's Balanced Salt Solution (HBSS) and to each well, 5 mL HBSS and 140 µL of AdipoRed reagent were added. After 10-15 min. of incubation, the plates were positioned in a Tecan Infinite M200 micro plate reader (Tecan Systems Inc., Salzburg, Austria) and fluorescence was measured with an excitation wavelength of 485 nm and an emission wavelength of 572 nm.

Cell viability assay

To measure the viability of preadipocytes, cultures of 3T3-F442A preadipocytes were seeded (2500 cells/well) in 100µL maintenance medium in 96-well plates and incubated for 48 hours at 37°C in a humidified atmosphere of 10% CO2. The medium was then aspirated from each well and replaced with 100µL of fresh medium containing DMSO or increasing concentrations of lovastatin (1.25 – 10µmol/L). The cells continued to incubate for an additional 24 or 48 hours. Cell viability following a quick rinse with 0.1 mL HBSS was determined by adding 100µL of serum free medium and 20µL of CellTiter 96® Aqueous One Solution (Promega, Madison, WI); plates were held in the dark at 37°C for two hours and then read at 490 nm with a Tecan infiniteM200 plate reader with Magellan™ software version 6.3 (Tecan Systems Inc., Salzburg, Austria).

Absorbances from wells containing cell-free medium were used as baselines and were deducted from absorbances of other cell-containing wells. Cell viability was also measured in mature adipocytes. Cultures of 3T3-F442A preadipocytes were seeded (5000 cells/well) and incubated as described above. Cells were then induced to differentiate as described above and grown to maturation. On day 8 – 10 of differentiation, the medium was aspirated from each well and replaced with 100µL of fresh medium containing DMSO or increasing concentrations of lovastatin (1.25 - 10µmol/L). The cells continued to incubate for an additional 24 or 48 hours. Cell viability following a quick rinse with 0.1 mL HBSS was determined with CellTiter 96® Aqueous One Solution as described above.

Quantitative real-time polymerase chain reaction

Murine 3T3-F442A cells cultured in tissue culture dishes (100 mm x 20 mm, Corning Life Sciences, Wilkes Barre, PA) at 2x105 cells per dish were incubated in the presence or absence of lovastatin for 8-10 days. Once the cells became mature adipocytes, total cellular RNA was extracted using TRIZOL reagent (Invitrogen, Carlsbad, CA) according to the manufacturer's protocols. The concentration and purity of the isolated total RNA were determined spectrophotometrically using OD260:280 ratios. The integrity of the purified total RNA was verified by detecting a 2:1 ratio for the 28S:18S ribosomal RNA (rRNA) using gel electrophoresis. Samples were run on a 1.5% agarose gel (Tris-acetate (TAE) buffer) at 80 volts for 90 min. and visualized by Chemi Doc XRS imaging system (Bio-Rad, Hercules, CA) following the addition of 0.5 µg/ml

ethidium bromide. The mRNA expression levels of *Pparγ*, SREBP-1c, *Fabp4*, leptin and adiponectin were analyzed by reverse transcription (RT) followed by quantitative real-time polymerase chain reaction (qPCR). 2 μg of total RNA in a 20 μl reaction buffer was reverse transcribed into cDNA using an Oligo (dT)20 primer and SuperScript® III First-Strand kit (Invitrogen, Grand Island, NY) following the manufacturer's instructions. cDNA was diluted by 25-fold with 25μg/mL acetylated bovine serum albumin (BSA) and 6 μl of diluted cDNA was amplified in a 25 μl PCR solution containing 250 nM of both forward and reverse primers of the gene and iQTM SYBR® Green Supermix (Bio-Rad). The cDNA was denatured at 95oC for 3 minutes followed by 40 cycles of PCR (94oC for 30 s, 60oC for 25 s, 72oC for 25 s, and 78oC for 9 s) by means of an iQTM5 multi-color Real-Time PCR Detection System (Bio-Rad) with Bio-Rad iQ5 Optical System Software (version 2.1). The mRNA levels of all the genes were normalized using ribosomal protein L22 (*RPL22*) as internal control [20] by using the ΔCT method. Fold changes of gene expression were calculated by the 2-ΔΔCT method.

DNA Sequencing

Primers were designed using Vector NTI Advance version 11 software (Invitrogen). The sequences for the primers are listed in Table 1. To ensure that a single gene was amplified, the melting profile of double stranded DNA product of PCR generated from each primer was analyzed. The specific PCR products were purified with HT ExoSAP-IT® High Throughput PCR Product Clean-Up (USB® Products, Affymetrix Inc., Cleveland, Ohio, USA) and incubated at 37oC for 30 minutes to degrade remaining

primers and nucleotides (dNTPs).). The purified double-stranded DNA was kept at 80°C for 30 minutes to inactivate the ExoSAP-IT and was then quickly chilled on ice. To confirm specificity, PCR primers were used to sequence both strands of DNA.

Statistics

One-way analysis of variance (ANOVA) and Tukey's post hoc tests were performed to assess the differences between groups using Prism® 4.0 software (GraphPad Software Inc., San Diego, CA). Levels of significance were designated as $P < 0.05$.

Results

We first determined the impact of lovastatin on the differentiation of murine 3T3-F442A cells. Figure 1A (a-c) shows that lovastatin (0-2.5 μmol/L) induced a concentration-dependent reduction in the number of lipid droplets stained by Oil Red O in each cell and the total amount of visible lipids. Supplemental mevalonate (500 μmol/L) reversed the effect of lovastatin by enhancing the lipid content of 3T3-F442A cells (Figure 1A, d-f). Cellular triglyceride content measured by AdipoRed™ Assay was also reduced by lovastatin in a dose-dependent manner (Figure 1B). Consistent with the results of oil Red O staining, supplemental mevalonate reversed the lovastatin-mediated reduction of triglyceride content.

To evaluate whether the decreased cellular triglyceride was caused by cytotoxicity, cell viability was measured with 3T3-F442A preadipocytes prior to (Figure 2, A & B) and following (Figure 2, C & D) differentiation process. When 3T3-F442A

preadipocytes were incubated with 1.25 – 10 μmol/L of lovastatin for 24 (Figure 2A) or 48 h (Figure 2B) prior to differentiation, only 10 μmol/L of lovastatin reduced cell viability following a 48-h incubation. The same concentration of lovastatin (10 μmol/L) was required to decrease the viability of mature, fully-differentiated 3T3-F442A cells (Figure 2, C & D), suggesting that the lower lipid content shown in Figure 1A was not due to lovastatin-induced cytotoxicity.

We then examined the effect of lovastatin on the expression of two genes, *Pparγ* and *SREBP-1c* that are critical in adipocyte differentiation. The *Pparγ* mRNA level in differentiated 3T3-F442A adipocytes had a near-significance (P = 0.11) increase over that in preadipocytes without adipogenic inducers (IDI-) (Figure 3A), an observation in accordance with the role of *Pparγ* in adipocyte differentiation. Consistent with lovastatin-mediated reduction in lipid content (Figure 1), lovastatin at 2.5 μmol/L suppressed the *Pparγ* mRNA level by >95%. Supplemental mevalonate restored *Pparγ* mRNA to the control level, suggesting that mevalonate or mevalonate-derived metabolite(s) are required for *Pparγ* expression and potentially adipocyte differentiation. The expression pattern of *SREBP-1c* in preadipocytes prior to and following differentiation follows that of *Pparγ*, and the impact of lovastatin and supplemental mevalonate on the expression of *SREBP-1c* (Figure 3B) mimics that on *Pparγ*.

Next we evaluated the genes under the regulation of *Pparγ* and *SREBP-1c*. Differentiated 3T3-F442A cells had much higher *Lep* mRNA level than preadipocytes (IDI-) (Figure 3C), an observation consistent with the role of leptin as a marker of

adipocyte differentiation and the expression pattern of *Pparγ* and *SREBP-1c*. In accordance with lovastatin-mediated reduction in lipid content (Figure 1), *Pparγ* and *SREBP-1c*, lovastatin at 2.5 μmol/L suppressed the *Lep* mRNA level by >95%. Supplemental mevalonate restored leptin mRNA to the control level, confirming the requirement of mevalonate-derived metabolites in adipocyte differentiation. The expression of *Fabp4* (Figure 3D) and *AdipoQ* (Figure 3E) in adipocytes and preadipocytes and the impact of lovastatin and supplemental mevalonate follow the same pattern as those of *Lep*.

Table 1.

Primer sequences (forward and reverse) and GenBank accession numbers used in the Real-Time qPCR

Gene	Accession#	Primer Sequence
Pparγ	NM_001127330	5'-AGAGGGCCAAGGATTCATGACCAGG-3'
	& NM_011146	5'-TTCAGCTTGAGCTGCAGTTCCAGGG-3'
SREBP-1	NM_011480	5'-TGGCACCCTCTTGCTCTGTAGGCAC-3
		5'-GCTGAGGCAGACATCTGCCTACCCA-3'
Lep	NM_008493	5'-TGGAGGTGAGCGGGATCAGGTTTTG-3
		5'-TGGCACGTGGGATCTTTCAGAAGCC-3'
Fabp4	NM_024406	5'-GTGTGATGCCTTTGTGGGAACCTGG-3'
		5'-TGCGGTGATTTCATCGAATTCCACG-3'
AdipoQ	NM_009605	5'-CGGCAGCACTGGCAAGTTCTACTGC-3'
		5'-TTGTGGTCCCCATCCCCATACACCT-3'

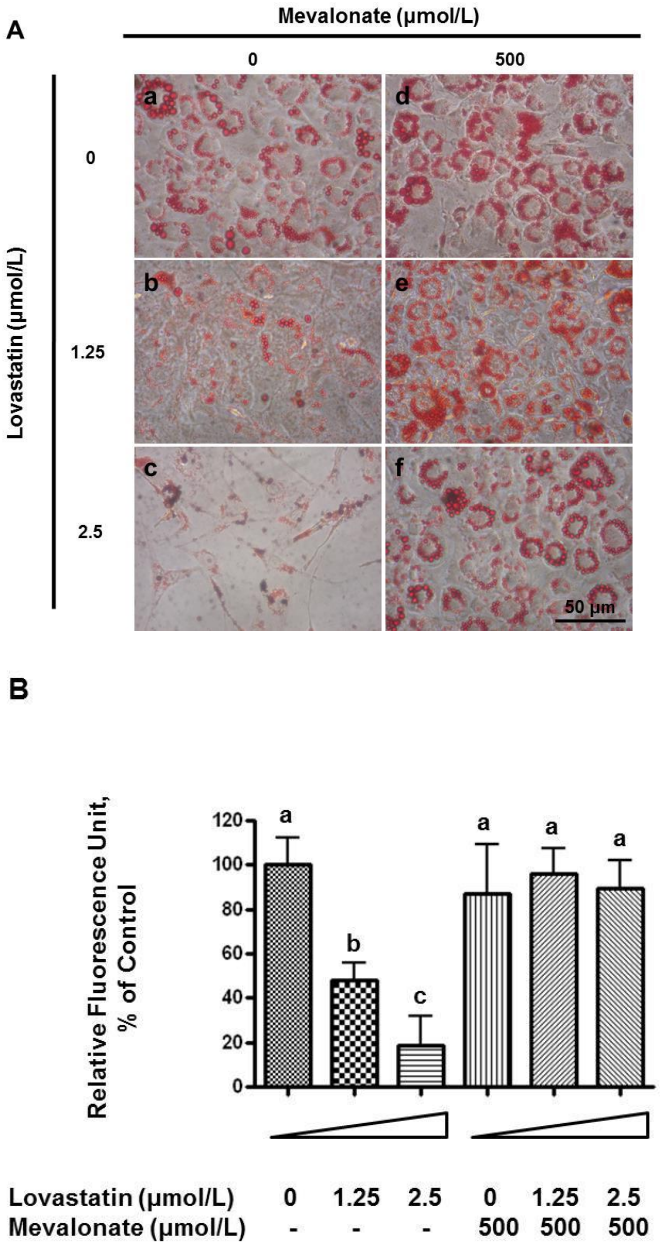

Figure 1. Lovastatin-mediated mevalonate deprivation suppresses the differentiation of murine 3T3-F442A preadipocytes. (A) Phase-contrast microscopy of Oil Red O-stained 3T3-F442A preadipocytes following 8-d differentiation. 3T3-F442A cells were incubated with 0 (a & d), 1.25 (b & e) and 2.5 (c & f) μmol/L lovastatin and 0 (a-c) and 500 (d-f) μmol/L mevalonolactone during differentiation. (B) Triglyceride content of 3T3-F442A cells at the end of 8-d differentiation determined by AdipoRed™ Assay.

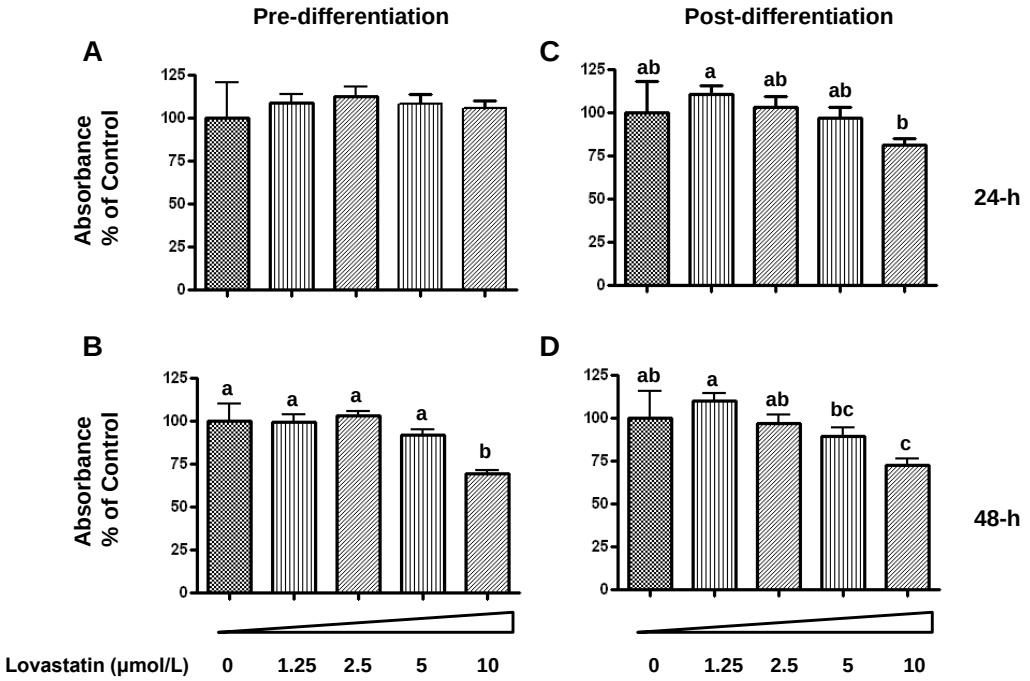

Figure 2. The concentration- and time- dependent impact of lovastatin on viability of murine 3T3-F442A preadipocytes prior to (A & B) and following (C & D) 8-d differentiation. The pre-differentiation (A & B) and differentiated 3T3-F442A cells were incubated with lovastatin (0-10 µmol/L) for 24- (A & C) and 48- (B & D) hours before cell viability was determined by CellTiter 96® Aqueous One Assay.

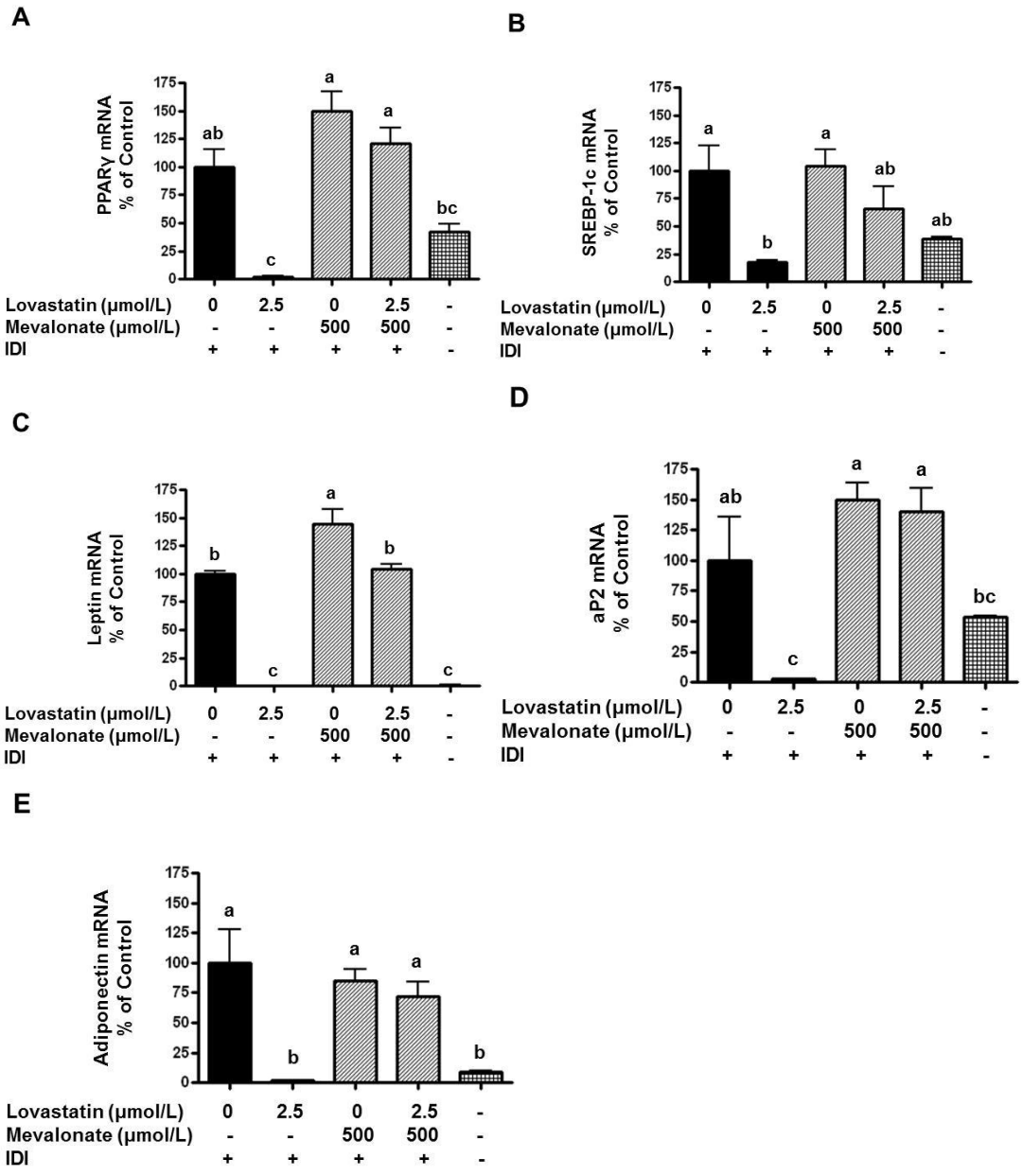

Figure 3. Mevalonate attenuates the impact of lovastatin on the expression of adipogenic genes. 3T3-F442A preadipocytes were incubated in the absence (-) or presence (+) of IDI, lovastatin and mevalonate as indicated for 8 days. At the end of incubation cells were lysed and total RNA extracted. Cellular mRNA levels of *Pparγ* (A), *SREBP-1c* (B), *Fabp4* (C), *Lep* (D), and *AdipoQ* (E) were measured by RT-PCR.

Discussion

Previous studies have shown that lovastatin [16, 21], atorvastatin [22], simvastatin [17, 23], rosuvastatin [17] and pitavastatin [17] inhibit 3T3-L1 preadipocyte differentiation. Simvastatin also inhibited adipogenesis of bone marrow stromal cells [24]. The anti-adipogenic effect of statins was also shown in animal studies. Lovastatin inhibited adipogenesis in rabbits [25]. When administered to high-fat fed pregnant animals, there were decreases in obesity, hypertension, and inflammation in offspring [26].

Our present study shows that 3T3-F442A cells are more sensitive than 3T3-L1 cells (IC50 = 10 μmol/L) [16] to lovastatin-mediated suppression of differentiation, suggesting that 3T3-F442A cells are a more suitable model to study the impact of mevalonate suppressors on adipogenesis. Interestingly, while lovastatin-containing red yeast rice [27] reduced triglyceride content of 3T3-L1 cells, the authors indicated that monocolin K, or lovastatin, did not have such an effect [28]. The level of lovastatin evaluated was not clear.

Our finding that lovastatin down regulates genes critical in adipocyte differentiation, *Pparγ* and *SREBP-1c*, and biomarkers of mature adipocytes, *Lep*, *Fabp4* and *AdipoQ*, is consistent with previous observations that statins inhibited 3T3-L1 preadipocyte differentiation by down regulating adiponectin [21, 29], *Pparγ* [22] and *Fabp4* [17, 21]. Chinese red yeast rice also reduced the levels of *Pparγ*, *Fabp4* and leptin in 3T3-L1 cells [28]. Down regulating *Fabp4* may have particular application in

controlling metabolic syndrome and diabetes because *Fabp4* gene plays a central role in linking obesity and insulin resistance [30].

SREBP-1c regulates genes such as fatty acid synthase, glycerol-3-phosphate acyltransferase, and stearoyl CoA desaturase 2 [31] that are important in adipocyte differentiation. Up regulation of ADD1/SREBP provides Pparγ agonists that further stimulate the differentiation process [32]. SREBP-1a and -1c differ in 5' exon. In mouse adipose tissues SREBP-1c mRNA dominates, with a 1c:1a ratio of 3:1. However, in cultured 3T3-L1 cells, SREBP-1c mRNA was virtually undetectable. Since our primer matches the sequence of exon 19 of SREBP-1, it does not differentiate 1a and 1c.

Our observation that supplemental mevalonate reversed the impact of lovastatin on cellular lipid content (Figure 1) and gene expression (Figure 3) in 3T3-F442A cells are consistent with previous reports that mevalonate (50-500 μmol/L) reversed statin-mediated inhibition of 3T3-L1 preadipocyte differentiation [16, 22]. At a much lower concentration (10 μmol/L), mevalonate was shown to be ineffective in reversing the effect of pitavastatin [17], consistent with our observation that 5 μmol/L mevalonate did not reverse the effect of lovastatin on intracellular triglyceride content (data not shown).

Similar to mevalonate-mediated reversal of the statin effect, mevalonate-derived non-sterol isoprenoids including farnesol, geraniol [16] and geranylgeranyl pyrophosphate [22], but not cholesterol [16, 17] or squalene [16], attenuated statin-mediated inhibition of 3T3-L1 preadipocyte differentiation, suggesting that mevalonate-derived non-sterols rather than sterols are required for adipocyte differentiation. Farnesyl

pyrophosphate (FPP), a downstream metabolite of mevalonate, may mediate the reversal effect of mevalonate because FPP is an endogenous Pparγ agonist; this is further supported by the observation that FPP could not reverse the inhibitory effect of Pparγ antagonist on 3T3-L1 differentiation [21].

The dependency of 3T3-F442A preadipocyte differentiation on mevalonate may also be mediated by protein prenylation. Small GTPases including Ras [33] and Rho [34] are involved in 3T3-L1 differentiation. Farnesylated Ras mediates insulin-induced adipocyte differentiation [13]. Insulin stimulated the activities of farnesyl transferase [35, 36] and geranylgeranyl transferase II [37] and the prenylation of Ras [35, 36], Rho [36], Rab-3 and Rab-4 [37] in 3T3-L1 adipocytes. Inhibitors of farnesyl- and geranylgeranyl-transferases block 3T3-L1 differentiation [13]. Insulin also unregulated the activity of HMG-CoA reductase in keratinocytes [38] and rat hepatoma cells [39]. It is not clear whether insulin stimulates HMG-CoA reductase in adipocytes.

The clonal expansion and subsequent differentiation of preadipocytes are also mediated by insulin-like growth factor 1 (IGF-1) receptor [40] that requires mevalonate-derived dolichol for its N-linked glycosylation and membrane attachment [41, 42]. The dual impact of statins on the N-linked glycosylation and mitogenic activity of IGF-1 receptor and the prenylation of GTPases [43] may explain the higher sensitivity of proliferating and differentiating preadipocytes than that of differentiated adipocytes to statin-mediated impact on cell viability and apoptosis [44]. In this study we found that the viability of undifferentiating preadipocytes and mature adipocytes was unaffected by

lovastatin at up to 10 μmol/L, a concentration 4-folder higher than that required to inhibit differentiation (Figure 2).

We examined whether the inhibitory effect of lovastatin on 3T3-F442A preadipocyte differentiation could be related to apoptosis. Prior to differentiation, 3T3-F442A preadipocytes incubated with 1.25-10μmol/L Lovastatin for 24- and 48-h exhibited no signs of apoptosis as determined by acridine orange and ethidium bromide dual staining and fluorescence microscopy (data not shown). Fully differentiated adipocytes, however, showed some indications of apoptosis following 24- and 48-h incubation with 5 and 10μmol/L Lovastatin. These observations warrant further studies. Alternatively, statins block the synthesis of oxysterols that are ligands of LXR, which is a transcriptional activator of ADD-1/SREBP-1c gene [2], and reduce SREBP 1-c mRNA in rat hepatoma cells [45]; the effect was reversed by mevalonate. It is unknown whether statin-mediated down regulation of SREBP-1c in adipocytes is attributed to decreased oxysterol synthesis, or the failure of cholesterol to attenuate the statin effect is due to poor cellular uptake.

An observation relevant to the role of mevalonate in adipocyte differentiation is that HMG-CoA reductase expression is unregulated in differentiating [46] and differentiated [47] 3T3-L1 cells and adipose tissues from obese rodents [48] and humans [49]. In addition, the expression of geranylgeranyl pyrophosphate (GGPP) synthase is unregulated by 20 fold in differentiating 3T3-L1 adipocytes and by 5-20 fold in adipose

tissue from ob/ob mice [50]. Up regulation of HMG-CoA reductase and GGPP synthase may provide essential intermediates for adipocyte differentiation.

It is controversial whether statins induce insulin resistance [22, 51-53]. Statin also reduced insulin-induced glucose uptake [44]. Our observation that lovastatin down regulates adiponectin, an adipokine produced exclusively in the adipose tissues [54] and a biomarker for insulin sensitivity [55], may support this possibility. Insulin resistance may also result from deficiency of isoprenoids including the coenzyme Q10 with functions in electron transduction chain in mitochondria [56]; mitochondrial dysfunction has been implicated in insulin resistance [57]. On the other hand, reduction in *Pparγ* activity has been suggested to prevent insulin resistance [58-61]; pitavastatin induced *GLUT4* mRNA level in 3T3-L1 cells when used during lipid accumulation period (day 8-16) [62] while rosuvastatin also increased insulin sensitivity in an animal model [63]. While statins impair insulin secretion and response in non-obese patients, they may reduce lipotoxicity caused by obesity-associated triglyceride-rich lipoproteins and help maintain glycemic control in obese type 2 diabetes patients [22].

The essential role of mevalonate in adipocyte differentiation shown herein may provide a molecular target for obesity intervention. Naturally occurring mevalonate suppressors including the vitamin E tocotrienols [64], terpenoids [65], genistein [66], and berberine [47] suppress adipocyte differentiation with concomitant down regulation of *Pparγ*, *C/EBPα*, and *Fabp4* expression. Dietary tocotrienols have been shown to increase insulin sensitivity [67]. Dietary mevalonate suppressors may have anti-adipogenic

benefits without the potential complications such as insulin resistance associated with statins.

Acknowldegment

We thank Dr. Parakat Vijayagopal for technical assistance in the culture of 3T3 cells, Ms. Hoda Yeganehjoo and Ms. Anureet Shah in RNA extraction, and Dr. Brian W. Beck in BLAST search.

References

1. Tang, Q.Q. and M.D. Lane, Adipogenesis: from stem cell to adipocyte. Annual Review of Biochemistry, 2012. 81: p. 715-36.
2. Castrillo, A. and P. Tontonoz, Nuclear receptors in macrophage biology: at the crossroads of lipid metabolism and inflammation. Annual Review of Cell and Developmental Biology, 2004. 20: p. 455-80.
3. Kawada, T., N. Takahashi, and T. Fushiki, Biochemical and physiological characteristics of fat cell. J Nutr Sci Vitaminol (Tokyo), 2001. 47(1): p. 1-12.
4. Tontonoz, P., et al., mPpar gamma 2: tissue-specific regulator of an adipocyte enhancer. Genes and Development, 1994. 8(10): p. 1224-34.
5. Kim, J.B. and B.M. Spiegelman, ADD1/SREBP1 promotes adipocyte differentiation and gene expression linked to fatty acid metabolism. Genes and Development, 1996. 10(9): p. 1096-107.
6. Kim, J.B., et al., ADD1/SREBP1 activates Ppargamma through the production of endogenous ligand. Proceedings of the National Academy of Sciences of the United States of America, 1998. 95(8): p. 4333-7.
7. Doran, A.C., et al., The helix-loop-helix factors Id3 and E47 are novel regulators of adiponectin. Circulation Research, 2008. 103(6): p. 624-34.
8. Gregoire, F.M., C.M. Smas, and H.S. Sul, Understanding adipocyte differentiation. Physiological Reviews, 1998. 78(3): p. 783-809.
9. Green, H. and M. Meuth, Sublines of mouse 3T3 cells that accumulate lipid. Cell, 1974. 1(3): p. 113-6.
10. Cowherd, R.M., R.E. Lyle, and R.E. McGehee, Jr., Molecular regulation of adipocyte differentiation. Semin Cell Dev Biol, 1999. 10(1): p. 3-10.
11. Green, H. and O. Kehinde, Spontaneous heritable changes leading to increased adipose conversion in 3T3 cells. Cell, 1976. 7(1): p. 105-13.
12. Green, H. and O. Kehinde, Formation of normally differentiated subcutaneous fat pads by an established preadipose cell line. Journal of Cellular Physiology, 1979. 101(1): p. 169-71.

13. Klemm, D.J., et al., Insulin-induced adipocyte differentiation. Activation of CREB rescues adipogenesis from the arrest caused by inhibition of prenylation. J Biol Chem, 2001. 276(30): p. 28430-5.
14. Chamberlain, L.H., Inhibition of isoprenoid biosynthesis causes insulin resistance in 3T3-L1 adipocytes. FEBS Lett, 2001. 507(3): p. 357-61.
15. Goldstein, J.L. and M.S. Brown, Regulation of the mevalonate pathway. Nature, 1990. 343(6257): p. 425-30.
16. Nishio, E., et al., 3-Hydroxy-3-methylglutaryl coenzyme A reductase inhibitor impairs cell differentiation in cultured adipogenic cells (3T3-L1). Eur J Pharmacol, 1996. 301(1-3): p. 203-6.
17. Nicholson, A.C., et al., Anti-adipogenic action of pitavastatin occurs through the coordinate regulation of Ppargamma and Pref-1 expression. British Journal of Pharmacology, 2007. 151(6): p. 807-15.
18. Ramirez-Zacarias, J.L., F. Castro-Munozledo, and W. Kuri-Harcuch, Quantitation of adipose conversion and triglycerides by staining intracytoplasmic lipids with Oil red O. Histochemistry, 1992. 97(6): p. 493-7.
19. Greenspan, P., E.P. Mayer, and S.D. Fowler, Nile red: a selective fluorescent stain for intracellular lipid droplets. Journal of Cell Biology, 1985. 100(3): p. 965-73.
20. de Jonge, H.J., et al., Evidence based selection of housekeeping genes. PLoS One, 2007. 2(9): p. e898.
21. Goto, T., et al., Farnesyl pyrophosphate regulates adipocyte functions as an endogenous Ppargamma agonist. Biochemical Journal, 2011. 438(1): p. 111-9.
22. Nakata, M., et al., Effects of statins on the adipocyte maturation and expression of glucose transporter 4 (SLC2A4): implications in glycaemic control. Diabetologia, 2006. 49(8): p. 1881-92.
23. Tomiyama, K., E. Nishio, and Y. Watanabe, Both wortmannin and simvastatin inhibit the adipogenesis in 3T3-L1 cells during the late phase of differentiation. Jpn J Pharmacol, 1999. 80(4): p. 375-8.
24. Song, C., et al., Simvastatin induces osteoblastic differentiation and inhibits adipocytic differentiation in mouse bone marrow stromal cells. Biochem Biophys Res Commun, 2003. 308(3): p. 458-62.
25. Pengde, K., et al., Lovastatin inhibits adipogenesis and prevents osteonecrosis in steroid-treated rabbits. Joint Bone Spine, 2008. 75(6): p. 696-701.
26. Elahi, M.M., et al., Statin treatment in hypercholesterolemic pregnant mice reduces cardiovascular risk factors in their offspring. Hypertension, 2008. 51(4): p. 939-44.
27. Endo, A., K. Hasumi, and S. Negishi, Monacolins J and L, new inhibitors of cholesterol biosynthesis produced by Monascus ruber. Journal of Antibiotics, 1985. 38(3): p. 420-2.
28. Jeon, T., et al., Red yeast rice extracts suppress adipogenesis by down-regulating adipogenic transcription factors and gene expression in 3T3-L1 cells. Life Sci, 2004. 75(26): p. 3195-203.

29. Furuhashi, M., et al., Treatment of diabetes and atherosclerosis by inhibiting fatty-acid-binding protein aP2. Nature, 2007. 447(7147): p. 959-65.
30. Hotamisligil, G.S., et al., Uncoupling of obesity from insulin resistance through a targeted mutation in aP2, the adipocyte fatty acid binding protein. Science, 1996. 274(5291): p. 1377-9.
31. Konig, B., et al., Activation of Pparα and Pparγ reduces triacylglycerol synthesis in rat hepatoma cells by reduction of nuclear SREBP-1. European Journal of Pharmacology, 2009. 605(1-3): p. 23-30.
32. Fajas, L., J.C. Fruchart, and J. Auwerx, Transcriptional control of adipogenesis. Current Opinion in Cell Biology, 1998. 10(2): p. 165-73.
33. Benito, M., et al., Differentiation of 3T3-L1 fibroblasts to adipocytes induced by transfection of ras oncogenes. Science, 1991. 253(5019): p. 565-8.
34. Hara, Y., et al., Rho and rho-kinase activity in adipocytes contributes to a vicious cycle in obesity that may involve mechanical stretch. Sci Signal, 2011. 4(157): p. ra3.
35. Goalstone, M.L. and B. Draznin, Effect of insulin on farnesyltransferase activity in 3T3-L1 adipocytes. J Biol Chem, 1996. 271(44): p. 27585-9.
36. Goalstone, M.L., et al., Insulin signals to prenyltransferases via the Shc branch of intracellular signaling. J Biol Chem, 2001. 276(16): p. 12805-12.
37. Goalstone, M.L., et al., Insulin promotes phosphorylation and activation of geranylgeranyltransferase II. Studies with geranylgeranylation of rab-3 and rab-4. J Biol Chem, 1999. 274(5): p. 2880-4.
38. Harris, I.R., et al., Regulation of HMG-CoA synthase and HMG-CoA reductase by insulin and epidermal growth factor in HaCaT keratinocytes. J Invest Dermatol, 2000. 114(1): p. 83-7.
39. Osborne, A.R., et al., Identification of insulin-responsive regions in the HMG-CoA reductase promoter. Biochem Biophys Res Commun, 2004. 318(4): p. 814-8.
40. Smith, P.J., et al., Insulin-like growth factor-I is an essential regulator of the differentiation of 3T3-L1 adipocytes. Journal of Biological Chemistry, 1988. 263(19): p. 9402-8.
41. Hjertman, M., et al., Evidence for protein dolichylation. FEBS Lett, 1997. 416(3): p. 235-8.
42. Dricu, A., et al., Mevalonate-regulated mechanisms in cell growth control: role of dolichyl phosphate in expression of the insulin-like growth factor-1 receptor (IGF-1R) in comparison to Ras prenylation and expression of c-myc. Glycobiology, 1997. 7(5): p. 625-33.
43. Siddals, K.W., et al., Abrogation of insulin-like growth factor-I (IGF-I) and insulin action by mevalonic acid depletion: synergy between protein prenylation and receptor glycosylation pathways. J Biol Chem, 2004. 279(37): p. 38353-9.
44. Mauser, W., et al., Direct adipotropic actions of atorvastatin: differentiation state-dependent induction of apoptosis, modulation of endocrine function, and inhibition of glucose uptake. Eur J Pharmacol, 2007. 564(1-3): p. 37-46.

45. DeBose-Boyd, R.A., et al., Expression of sterol regulatory element-binding protein 1c (SREBP-1c) mRNA in rat hepatoma cells requires endogenous LXR ligands. Proc Natl Acad Sci U S A, 2001. 98(4): p. 1477-82.
46. Shimomura, I., et al., Differential expression of exons 1a and 1c in mRNAs for sterol regulatory element binding protein-1 in human and mouse organs and cultured cells. Journal of Clinical Investigation, 1997. 99(5): p. 838-45.
47. Huang, C., et al., Berberine inhibits 3T3-L1 adipocyte differentiation through the Pparγ pathway. Biochem Biophys Res Commun, 2006. 348(2): p. 571-8.
48. Le Lay, S., et al., Cholesterol : A cell size dependent signal which regulates glucose metabolism and gene expression in adipocytes. J Biol Chem, 2001. 27: p. 27.
49. Le Lay, S., P. Ferre, and I. Dugail, Adipocyte cholesterol balance in obesity. Biochemical Society Transactions, 2004. 32(Pt 1): p. 103-6.
50. Vicent, D., E. Maratos-Flier, and C.R. Kahn, The branch point enzyme of the mevalonate pathway for protein prenylation is overexpressed in the ob/ob mouse and induced by adipogenesis. Mol Cell Biol, 2000. 20(6): p. 2158-66.
51. Freeman, D.J., et al., Pravastatin and the development of diabetes mellitus: evidence for a protective treatment effect in the West of Scotland Coronary Prevention Study. Circulation, 2001. 103(3): p. 357-62.
52. Sever, P.S., et al., Prevention of coronary and stroke events with atorvastatin in hypertensive patients who have average or lower-than-average cholesterol concentrations, in the Anglo-Scandinavian Cardiac Outcomes Trial--Lipid Lowering Arm (ASCOT-LLA): a multicentre randomised controlled trial. Lancet, 2003. 361(9364): p. 1149-58.
53. Group, T.D.A.L.I.D.S., The effect of aggressive versus standard lipid lowering by atorvastatin on diabetic dyslipidemia: the DALI study: a double-blind, randomized, placebo-controlled trial in patients with type 2 diabetes and diabetic dyslipidemia. Diabetes Care, 2001. 24(8): p. 1335-41.
54. Scherer, P.E., et al., A novel serum protein similar to C1q, produced exclusively in adipocytes. Journal of Biological Chemistry, 1995. 270(45): p. 26746-9.
55. Asterholm, I.W. and P.E. Scherer, Enhanced metabolic flexibility associated with elevated adiponectin levels. American Journal of Pathology, 2010. 176(3): p. 1364-76.
56. Bliznakov, E.G., Diabetes and the role of isoprenoid biosynthesis. FEBS Letters, 2002. 525: p. 169-70.
57. Lowell, B.B. and G.I. Shulman, Mitochondrial dysfunction and type 2 diabetes. Science, 2005. 307(5708): p. 384-7.
58. Altshuler, D., et al., The common Ppargamma Pro12Ala polymorphism is associated with decreased risk of type 2 diabetes. Nature Genetics, 2000. 26(1): p. 76-80.
59. Yamauchi, T., et al., Inhibition of RXR and Ppargamma ameliorates diet-induced obesity and type 2 diabetes. Journal of Clinical Investigation, 2001. 108(7): p. 1001-13.
60. Kubota, N., et al., Ppar gamma mediates high-fat diet-induced adipocyte hypertrophy and insulin resistance. Molecular Cell, 1999. 4(4): p. 597-609.

61. Miles, P.D., et al., Improved insulin-sensitivity in mice heterozygous for Ppar-gamma deficiency. Journal of Clinical Investigation, 2000. 105(3): p. 287-92.
62. Ishihara, Y., et al., Beneficial direct adipotropic actions of pitavastatin *in vitro* and their manifestations in obese mice. Atherosclerosis, 2010. 212(1): p. 131-8.
63. Naples, M., et al., Effect of rosuvastatin on insulin sensitivity in an animal model of insulin resistance: evidence for statin-induced hepatic insulin sensitization. Atherosclerosis, 2008. 198(1): p. 94-103.
64. Uto-Kondo, H., et al., Tocotrienol suppresses adipocyte differentiation and Akt phosphorylation in 3T3-L1 preadipocytes. Journal of Nutrition, 2009. 139(1): p. 51-7.
65. Gong, Z., et al., The role of tanshinone IIA in the treatment of obesity through peroxisome proliferator-activated receptor gamma antagonism. Endocrinology, 2009. 150(1): p. 104-13.
66. Kim, M.H., et al., Genistein and daidzein repress adipogenic differentiation of human adipose tissue-derived mesenchymal stem cells via Wnt/beta-catenin signalling or lipolysis. Cell Prolif, 2010. 43(6): p. 594-605.
67. Chen, C.W. and H.H. Cheng, A rice bran oil diet increases LDL-receptor and HMG-CoA reductase mRNA expressions and insulin sensitivity in rats with streptozotocin/nicotinamide-induced Type 2 diabetes. J Nutr, 2006. 136(6): p. 1472-6.

CHAPTER VI

SUMMARY AND CONCLUSION

This dissertation contributes valuable information in relation to the effect of geranylgeraniol on the suppression of adipocyte differentiation of murine 3T3-F442A preadipocytes. In this study we have shown that 3T3-F442A preadipocytes incubated with geranylgeraniol for 8 days exhibited a dose-dependent decrease in the intracellular triglyceride content, as determined by AdipoRed Assay and Oil Red O staining. Similar findings were demonstrated with lovastatin, a known competitive inhibitor of HMG-CoA reductase, a key enzyme necessary for mevalonate synthesis.

Our hypothesis proposed that geranylgeraniol suppresses the differentiation of murine 3T3-F442A preadipocytes by decreasing intracellular triglyceride accumulation and down regulating the expression of adipogenic transcriptional factors associated with the mevalonate pathway and the insulin signaling pathway, pathways that promote adipogenesis. Our study demonstrated that geranylgeraniol suppressed lipid accumulation in 3T3-F442A preadipocytes. Furthermore, geranylgeraniol down regulated the expression of various genes which are crucial at different stages in the adipogenesis process, as measured by real-time qPCR. *Pparγ* and SREBP-1c are both involved in the early phase of adipocyte differentiation (Gregoire et al., 1998) and their presence is critical in the initiation of adipogenesis. There are several adipogenic genes which are stimulated by these earlier processes such as *INSIG1, Lep, Fabp4, AdipoQ*

and *GPDH*, which are important in the progression of adipocyte differentiation. Mature, fully differentiated adipocytes are characterized by *GLUT4* and *Fasn*, important biomarkers of terminal differentiation. Since we observed markedly lower mRNAs levels among all of these adipogenic genes, the geranylgeraniol mediated suppression of adipocyte differentiation may have probably impacted the earlier stages of the process which influenced the progression of adipogenesis. It can be established that the mevalonate pathway plays a key role in preadipocyte differentiation through mediation of *Pparγ*.

The dose-dependent inhibition of intracellular triglyceride accumulation by both geranylgeraniol and lovastatin was not reversed by the addition of 5µM mevalonate as seen in Oil Red O staining and AdipoRed assay. The impact of geranylgeraniol and lovastatin on the expression of the adipogenic genes was also not reversed by supplemental mevalonate at this concentration. Nonetheless, reversal of the lovastatin effect was evident at higher concentrations of mevalonate (500µM), but this level is at the upper range of physiologically attainable concentrations.

The inhibitory effect of geranylgeraniol and lovastatin on 3T3-F442A preadipocyte differentiation is apparently not associated with cytotoxicity. Geranylgeraniol did not decrease cell viability in the preadipocytes prior to and following differentiation at any of the tested concentrations (20 - 200µmol/L) when incubated for 24 or 48 hours. Only 10 µmol/L of lovastatin reduced cell viability following 48 hour incubation in preadipocytes treated prior to differentiation. The same concentration of

lovastatin was required to decrease the viability of mature, fully-differentiated 3T3-F442A cells. Representative images of AO/EB and fluorescence microscopy demonstrated that when 3T3-F442A preadipocytes were incubated with 20 – 200 μmol/L geranylgeraniol or 1.25-10μmol/L Lovastatin for 24 or 48 hours prior to differentiation, only cells incubated with 200 μmol/L geranylgeraniol had signs of apoptosis. Mature adipocytes, however, may be more sensitive following 24 and 48 hour incubation with both treatments. With geranylgeraniol, all groups had some indications of apoptosis. There were also some signs of apoptosis with 5 and 10μmol/L Lovastatin. These observations, however, need further confirmation.

In conclusion, geranylgeraniol suppressed the differentiation of murine 3T3-F442A preadipocytes by down regulating several transcriptional factors and genes characteristic to the mature adipocyte which are essential in the adipogenesis process. This in turn resulted in decreased intracellular triglyceride accumulation. Mevalonate-derived metabolites have essential roles in promoting adipocyte differentiation and adipogenic gene expression. Dietary mevalonate suppressors such as geranylgeraniol may have potential as anti-adipogenesis compounds.

Recommendations on Future Directions

Further examination of specific mechanisms of action involved in the impact of geranylgeraniol on suppressing differentiation in murine 3T3-F442A preadipocytes would be beneficial. Western Blot analysis of the geranylgeraniol treated preadipocytes would provide useful insight into the detection of specific proteins involved in the

adipogenesis process. Assessment of the potential reversal of the effect of geranylgeraniol by the Ppar agonist mevalonate, at higher concentrations but physiologically acceptable levels, warrants additional investigation.

To our knowledge, the effects of geranylgeraniol on modulating the differentiation of preadipocytes in human or murine adipose tissue, had not been explored. The *in vitro* investigations in this dissertation could possibly lay the foundation for future studies examining the impact of geranylgeraniol on animal adipose tissue regulation *in vivo*.

REFERENCES

Adjei, A. A. (2001). Blocking oncogenic Ras signaling for cancer therapy. *J Natl Cancer Inst, 93*(14), 1062-1074.

Ahima, R. S., & Flier, J. S. (2000). Leptin. *Annu Rev Physiol, 62*, 413-437.

Ailhaud, G. (1996). Early adipocyte differentiation. *Biochem Soc Trans, 24*(2), 400-402.

Allison, D. B., Fontaine, K. R., Manson, J. E., Stevens, J., & VanItallie, T. B. (1999). Annual deaths attributable to obesity in the United States. *JAMA, 282*(16), 1530-1538.

Badman, M. K., & Flier, J. S. (2007). The adipocyte as an active participant in energy balance and metabolism. *Gastroenterology, 132*(6), 2103-2115.

Baxa, C. A., Sha, R. S., Buelt, M. K., Smith, A. J., Matarese, V., Chinander, L. L., . . . Bernlohr, D. A. (1989). Human adipocyte lipid-binding protein: purification of the protein and cloning of its complementary DNA. *Biochemistry, 28*(22), 8683-8690.

Berger, J., & Moller, D. E. (2002). The mechanisms of action of PPARs. *Annu Rev Med, 53*, 409-435.

Boucher, J., Masri, B., Daviaud, D., Gesta, S., Guigne, C., Mazzucotelli, A., . . . Valet, P. (2005). Apelin, a newly identified adipokine up-regulated by insulin and obesity. *Endocrinology, 146*(4), 1764-1771. doi: 10.1210/en.2004-1427

Boyartchuk, V. L., Ashby, M. N., & Rine, J. (1997). Modulation of Ras and a-factor function by carboxyl-terminal proteolysis. *Science, 275*(5307), 1796-1800.

Bozaoglu, K., Bolton, K., McMillan, J., Zimmet, P., Jowett, J., Collier, G., . . . Segal, D. (2007). Chemerin is a novel adipokine associated with obesity and metabolic syndrome. *Endocrinology, 148*(10), 4687-4694. doi: 10.1210/en.2007-0175

Briggs, M. R., Yokoyama, C., Wang, X., Brown, M. S., & Goldstein, J. L. (1993). Nuclear protein that binds sterol regulatory element of low density lipoprotein receptor promoter. I. Identification of the protein and delineation of its target nucleotide sequence. *J Biol Chem, 268*(19), 14490-14496.

Brown, M. S., & Goldstein, J. L. (1997). The SREBP pathway: regulation of cholesterol metabolism by proteolysis of a membrane-bound transcription factor. *Cell, 89*(3), 331-340.

Brun, R. P., & Spiegelman, B. M. (1997). PPAR gamma and the molecular control of adipogenesis. *J Endocrinol, 155*(2), 217-218.

Brun, R. P., Tontonoz, P., Forman, B. M., Ellis, R., Chen, J., Evans, R. M., & Spiegelman, B. M. (1996). Differential activation of adipogenesis by multiple PPAR isoforms. *Genes Dev, 10*(8), 974-984.

Caballero, B. (2007). The global epidemic of obesity: an overview. *Epidemiol Rev, 29*, 1-5. doi: 10.1093/epirev/mxm012

Campbell, S. L., Khosravi-Far, R., Rossman, K. L., Clark, G. J., & Der, C. J. (1998). Increasing complexity of Ras signaling. *Oncogene, 17*(11 Reviews), 1395-1413. doi: 10.1038/sj.onc.1202174

Cao, Z., Umek, R. M., & McKnight, S. L. (1991). Regulated expression of three C/EBP isoforms during adipose conversion of 3T3-L1 cells. *Genes Dev, 5*(9), 1538-1552.
Considine, R. V., Sinha, M. K., Heiman, M. L., Kriauciunas, A., Stephens, T. W., Nyce, M. R., . . . et al. (1996). Serum immunoreactive-leptin concentrations in normal-weight and obese humans. *N Engl J Med, 334*(5), 292-295. doi: 10.1056/NEJM199602013340503
Correll, C. C., Ng, L., & Edwards, P. A. (1994). Identification of farnesol as the non-sterol derivative of mevalonic acid required for the accelerated degradation of 3-hydroxy-3-methylglutaryl-coenzyme A reductase. *J Biol Chem, 269*(26), 17390-17393.
Cypess, A. M., Lehman, S., Williams, G., Tal, I., Rodman, D., Goldfine, A. B., . . . Kahn, C. R. (2009). Identification and importance of brown adipose tissue in adult humans. *N Engl J Med, 360*(15), 1509-1517. doi: 10.1056/NEJMoa0810780
Dani, C., Doglio, A., Amri, E. Z., Bardon, S., Fort, P., Bertrand, B., . . . Ailhaud, G. (1989). Cloning and regulation of a mRNA specifically expressed in the preadipose state. *J Biol Chem, 264*(17), 10119-10125.
de Jonge, H. J., Fehrmann, R. S., de Bont, E. S., Hofstra, R. M., Gerbens, F., Kamps, W. A., . . . ter Elst, A. (2007). Evidence based selection of housekeeping genes. [$]. *PLoS One, 2*(9), e898. doi: 10.1371/journal.pone.0000898
Eglit, Triin, Lember, Margus, Ringmets, Inge, & Rajasalu, Tarvo. (2012). Gender Differences in Serum High-Molecular-Weight (HMW) Adiponectin Levels in Metabolic Syndrome. *European Journal of Endocrinology*. doi: 10.1530/eje-12-0688
Elson, C. E., Peffley, D. M., Hentosh, P., & Mo, H. (1999). Isoprenoid-mediated inhibition of mevalonate synthesis: potential application to cancer. *Proc Soc Exp Biol Med, 221*(4), 294-311.
Fajas, L., Schoonjans, K., Gelman, L., Kim, J. B., Najib, J., Martin, G., . . . Auwerx, J. (1999). Regulation of peroxisome proliferator-activated receptor gamma expression by adipocyte differentiation and determination factor 1/sterol regulatory element binding protein 1: implications for adipocyte differentiation and metabolism. *Mol Cell Biol, 19*(8), 5495-5503.
Farmer, S. R. (2006). Transcriptional control of adipocyte formation. *Cell Metab, 4*(4), 263-273. doi: 10.1016/j.cmet.2006.07.001
Fedeli, E., Capella, P., Cirimele, M., & Jacini, G. (1966). Isolation of geranyl geraniol from the unsaponifiable fraction of linseed oil. *J Lipid Res, 7*(3), 437-441.
Fernyhough, M. E., Okine, E., Hausman, G., Vierck, J. L., & Dodson, M. V. (2007). PPARgamma and GLUT-4 expression as developmental regulators/markers for preadipocyte differentiation into an adipocyte. *Domest Anim Endocrinol, 33*(4), 367-378. doi: 10.1016/j.domaniend.2007.05.001
Finkelstein, E. A., Trogdon, J. G., Cohen, J. W., & Dietz, W. (2009). Annual medical spending attributable to obesity: payer-and service-specific estimates. *Health Affairs, 28*(5), w822-831. doi: hlthaff.28.5.w822 [pii]

10.1377/hlthaff.28.5.w822
Flegal, K. M., Carroll, M. D., Kit, B. K., & Ogden, C. L. (2012). Prevalence of obesity and trends in the distribution of body mass index among US adults, 1999-2010. *JAMA, 307*(5), 491-497. doi: 10.1001/jama.2012.39
Flier, J. S. (2004). Obesity wars: molecular progress confronts an expanding epidemic. *Cell, 116*(2), 337-350.
Fonseca-Alaniz, M. H., Takada, J., Alonso-Vale, M. I., & Lima, F. B. (2007). Adipose tissue as an endocrine organ: from theory to practice. *J Pediatr (Rio J), 83*(5 Suppl), S192-203. doi: doi:10.2223/JPED.1709
Forman, B. M., Tontonoz, P., Chen, J., Brun, R. P., Spiegelman, B. M., & Evans, R. M. (1995). 15-Deoxy-delta 12, 14-prostaglandin J2 is a ligand for the adipocyte determination factor PPAR gamma. *Cell, 83*(5), 803-812.
Freytag, S. O., Paielli, D. L., & Gilbert, J. D. (1994). Ectopic expression of the CCAAT/enhancer-binding protein alpha promotes the adipogenic program in a variety of mouse fibroblastic cells. *Genes Dev, 8*(14), 1654-1663.
Fried, S. K., Ricci, M. R., Russell, C. D., & Laferrere, B. (2000). Regulation of leptin production in humans. *J Nutr, 130*(12), 3127S-3131S.
Fukuhara, A., Matsuda, M., Nishizawa, M., Segawa, K., Tanaka, M., Kishimoto, K., . . . Shimomura, I. (2005). Visfatin: a protein secreted by visceral fat that mimics the effects of insulin. *Science, 307*(5708), 426-430. doi: 10.1126/science.1097243
Geloen, A., Collet, A. J., Guay, G., & Bukowiecki, L. J. (1989). Insulin stimulates *in vivo* cell proliferation in white adipose tissue. *Am J Physiol, 256*(1 Pt 1), C190-196.
Gesta, S., Tseng, Y. H., & Kahn, C. R. (2007). Developmental origin of fat: tracking obesity to its source. *Cell, 131*(2), 242-256. doi: S0092-8674(07)01272-X [pii]
10.1016/j.cell.2007.10.004
Goalstone, M. L., & Draznin, B. (1996). Effect of insulin on farnesyltransferase activity in 3T3-L1 adipocytes. *J Biol Chem, 271*(44), 27585-27589.
Goalstone, M. L., Leitner, J. W., Berhanu, P., Sharma, P. M., Olefsky, J. M., & Draznin, B. (2001). Insulin signals to prenyltransferases via the Shc branch of intracellular signaling. *J Biol Chem, 276*(16), 12805-12812.
Goldberg, I. J. (1996). Lipoprotein lipase and lipolysis: central roles in lipoprotein metabolism and atherogenesis. *J Lipid Res, 37*(4), 693-707.
Goldstein, J. L., & Brown, M. S. (1990). Regulation of the mevalonate pathway. *Nature, 343*(6257), 425-430. doi: 10.1038/343425a0
Golomb, B. A., & Evans, M. A. (2008). Statin adverse effects : a review of the literature and evidence for a mitochondrial mechanism. *Am J Cardiovasc Drugs, 8*(6), 373-418. doi: 10.2165/0129784-200808060-00004
Green, H., & Kehinde, O. (1976). Spontaneous heritable changes leading to increased adipose conversion in 3T3 cells. *Cell, 7*(1), 105-113.
Green, H., & Kehinde, O. (1979). Formation of normally differentiated subcutaneous fat pads by an established preadipose cell line. *J Cell Physiol, 101*(1), 169-171. doi: 10.1002/jcp.1041010119

Greenberg, A. S., Egan, J. J., Wek, S. A., Garty, N. B., Blanchette-Mackie, E. J., & Londos, C. (1991). Perilipin, a major hormonally regulated adipocyte-specific phosphoprotein associated with the periphery of lipid storage droplets. *J Biol Chem, 266*(17), 11341-11346.

Greenspan, P., Mayer, E. P., & Fowler, S. D. (1985). Nile red: a selective fluorescent stain for intracellular lipid droplets. *Journal of Cell Biology, 100*(3), 965-973.

Gregoire, F. M., Smas, C. M., & Sul, H. S. (1998). Understanding adipocyte differentiation. *Physiological Reviews, 78*(3), 783-809.

Hamm, J. K., Park, B. H., & Farmer, S. R. (2001). A role for C/EBPbeta in regulating peroxisome proliferator-activated receptor gamma activity during adipogenesis in 3T3-L1 preadipocytes. *J Biol Chem, 276*(21), 18464-18471. doi: 10.1074/jbc.M100797200

Hampton, R. Y. (2002). Proteolysis and sterol regulation. *Annu Rev Cell Dev Biol, 18*, 345-378. doi: 10.1146/annurev.cellbio.18.032002.131219

Haslam, D. W., & James, W. P. (2005). Obesity. *Lancet, 366*(9492), 1197-1209. doi: 10.1016/S0140-6736(05)67483-1

Hua, X., Sakai, J., Brown, M. S., & Goldstein, J. L. (1996). Regulated cleavage of sterol regulatory element binding proteins requires sequences on both sides of the endoplasmic reticulum membrane. *J Biol Chem, 271*(17), 10379-10384.

Huang, H., Song, T. J., Li, X., Hu, L., He, Q., Liu, M., . . . Tang, Q. Q. (2009). BMP signaling pathway is required for commitment of C3H10T1/2 pluripotent stem cells to the adipocyte lineage. *Proc Natl Acad Sci U S A, 106*(31), 12670-12675. doi: 10.1073/pnas.0906266106

Hunter-Cevera, J. C., and A. Belt. (1996). *Preservation and Maintenance of Cultures Used in Biotechnology*. San Diego: Academic Press.

Jeon, T., Hwang, S. G., Hirai, S., Matsui, T., Yano, H., Kawada, T., . . . Park, D. K. (2004). Red yeast rice extracts suppress adipogenesis by down-regulating adipogenic transcription factors and gene expression in 3T3-L1 cells. [*]. *Life Sci, 75*(26), 3195-3203.

Ji, X., Chen, D., Xu, C., Harris, S. E., Mundy, G. R., & Yoneda, T. (2000). Patterns of gene expression associated with BMP-2-induced osteoblast and adipocyte differentiation of mesenchymal progenitor cell 3T3-F442A. *J Bone Miner Metab, 18*(3), 132-139.

Kast-Woelbern, H. R., Dana, S. L., Cesario, R. M., Sun, L., de Grandpre, L. Y., Brooks, M. E., . . . Leibowitz, M. D. (2004). Rosiglitazone induction of Insig-1 in white adipose tissue reveals a novel interplay of peroxisome proliferator-activated receptor gamma and sterol regulatory element-binding protein in the regulation of adipogenesis. *J Biol Chem, 279*(23), 23908-23915. doi: 10.1074/jbc.M403145200

Katuru, R., Fernandes, N. V., Elfakhani, M., Dutta, D., Mills, N., Hynds, D. L., . . . Mo, H. (2011). Mevalonate depletion mediates the suppressive impact of geranylgeraniol on murine B16 melanoma cells. *Exp Biol Med (Maywood), 236*(5), 604-613. doi: 10.1258/ebm.2011.010379

Kawada, T., Goto, T., Hirai, S., Kang, M. S., Uemura, T., Yu, R., & Takahashi, N. (2008). Dietary regulation of nuclear receptors in obesity-related metabolic syndrome. *Asia Pac J Clin Nutr, 17 Suppl 1*, 126-130.

Kawada, T., Takahashi, N., & Fushiki, T. (2001). Biochemical and physiological characteristics of fat cell. *J Nutr Sci Vitaminol (Tokyo), 47*(1), 1-12.

Kim, J. B., & Spiegelman, B. M. (1996). ADD1/SREBP1 promotes adipocyte differentiation and gene expression linked to fatty acid metabolism. *Genes Dev, 10*(9), 1096-1107.

Kim, J. B., Spotts, G. D., Halvorsen, Y. D., Shih, H. M., Ellenberger, T., Towle, H. C., & Spiegelman, B. M. (1995). Dual DNA binding specificity of ADD1/SREBP1 controlled by a single amino acid in the basic helix-loop-helix domain. *Mol Cell Biol, 15*(5), 2582-2588.

Kim, J. B., Wright, H. M., Wright, M., & Spiegelman, B. M. (1998). ADD1/SREBP1 activates PPARγ through the production of endogenous ligand. *Proceedings of the National Academy of Sciences of the United States of America, 95*(8), 4333-4337.

Kissebah, A. H., & Krakower, G. R. (1994). Regional adiposity and morbidity. *Physiol Rev, 74*(4), 761-811.

Krapivner, S., Popov, S., Chernogubova, E., Hellenius, M. L., Fisher, R. M., Hamsten, A., & van't Hooft, F. M. (2008). Insulin-induced gene 2 involvement in human adipocyte metabolism and body weight regulation. *J Clin Endocrinol Metab, 93*(5), 1995-2001. doi: 10.1210/jc.2007-1850

Latchman, D. S. (1997). Transcription factors: an overview. *Int J Biochem Cell Biol, 29*(12), 1305-1312.

Laufs, U., & Liao, J. K. (2000). Direct vascular effects of HMG-CoA reductase inhibitors. *Trends Cardiovasc Med, 10*(4), 143-148.

Linhart, H. G., Ishimura-Oka, K., DeMayo, F., Kibe, T., Repka, D., Poindexter, B., . . . Darlington, G. J. (2001). C/EBPalpha is required for differentiation of white, but not brown, adipose tissue. *Proc Natl Acad Sci U S A, 98*(22), 12532-12537. doi: 10.1073/pnas.211416898

Lonnqvist, F., Nordfors, L., Jansson, M., Thorne, A., Schalling, M., & Arner, P. (1997). Leptin secretion from adipose tissue in women. Relationship to plasma levels and gene expression. *J Clin Invest, 99*(10), 2398-2404. doi: 10.1172/JCI119422

Macdonald, S. G., Crews, C. M., Wu, L., Driller, J., Clark, R., Erikson, R. L., & McCormick, F. (1993). Reconstitution of the Raf-1-MEK-ERK signal transduction pathway *in vitro*. *Mol Cell Biol, 13*(11), 6615-6620.

Maeda, K., Cao, H., Kono, K., Gorgun, C. Z., Furuhashi, M., Uysal, K. T., . . . Hotamisligil, G. S. (2005). Adipocyte/macrophage fatty acid binding proteins control integrated metabolic responses in obesity and diabetes. *Cell Metab, 1*(2), 107-119. doi: 10.1016/j.cmet.2004.12.008

Margetic, S., Gazzola, C., Pegg, G. G., & Hill, R. A. (2002). Leptin: a review of its peripheral actions and interactions. *Int J Obes Relat Metab Disord, 26*(11), 1407-1433. doi: 10.1038/sj.ijo.0802142

Marlow, L. A., Reynolds, L. A., Cleland, A. S., Cooper, S. J., Gumz, M. L., Kurakata, S., . . . Copland, J. A. (2009). Reactivation of suppressed RhoB is a critical step for the inhibition of anaplastic thyroid cancer growth. *Cancer Res, 69*(4), 1536-1544. doi: 10.1158/0008-5472.CAN-08-3718

Marshall, C. J. (1995). Specificity of receptor tyrosine kinase signaling: transient versus sustained extracellular signal-regulated kinase activation. *Cell, 80*(2), 179-185.

Mauser, W., Perwitz, N., Meier, B., Fasshauer, M., & Klein, J. (2007). Direct adipotropic actions of atorvastatin: differentiation state-dependent induction of apoptosis, modulation of endocrine function, and inhibition of glucose uptake. *Eur J Pharmacol, 564*(1-3), 37-46.

Mo, H., & Elson, C. E. (1999). Apoptosis and cell-cycle arrest in human and murine tumor cells are initiated by isoprenoids. *J Nutr, 129*(4), 804-813.

Mo, H., & Elson, C. E. (2004). Studies of the isoprenoid-mediated inhibition of mevalonate synthesis applied to cancer chemotherapy and chemoprevention. *Exp Biol Med (Maywood), 229*(7), 567-585.

Mo, H., & Elson, C. E. (2006). Isoprenoids and novel inhibitors of mevalonate pathway activities. In D. Heber, G. L. Blackburn, V. L. W. Go & J. Milner (Eds.), *Nutritional Oncology* (pp. 629-644). Burlington: Academic Press.

Morrison, R. F., & Farmer, S. R. (1999). Insights into the transcriptional control of adipocyte differentiation. *J Cell Biochem, Suppl 32-33*, 59-67. doi: 10.1002/(SICI)1097-4644(1999)75:32+<59::AID-JCB8>3.0.CO;2-1 [pii]

Nakanishi, M., Goldstein, J. L., & Brown, M. S. (1988). Multivalent control of 3-hydroxy-3-methylglutaryl coenzyme A reductase. Mevalonate-derived product inhibits translation of mRNA and accelerates degradation of enzyme. *J Biol Chem, 263*(18), 8929-8937.

Nakata, M., Nagasaka, S., Kusaka, I., Matsuoka, H., Ishibashi, S., & Yada, T. (2006). Effects of statins on the adipocyte maturation and expression of glucose transporter 4 (SLC2A4): implications in glycaemic control. *Diabetologia, 49*(8), 1881-1892.

Nicholson, A. C., Hajjar, D. P., Zhou, X., He, W., Gotto, A. M., Jr., & Han, J. (2007). Anti-adipogenic action of pitavastatin occurs through the coordinate regulation of PPARgamma and Pref-1 expression. *Br J Pharmacol, 151*(6), 807-815. doi: 10.1038/sj.bjp.0707250

NIH. (1998). *Clinical Guidelines on the Identification, Evaluation, and Treatment of Overweight and Obesity in Adults. .*

Nishio, E., Tomiyama, K., Nakata, H., & Watanabe, Y. (1996). 3-Hydroxy-3-methylglutaryl coenzyme A reductase inhibitor impairs cell differentiation in cultured adipogenic cells (3T3-L1). [$]. *Eur J Pharmacol, 301*(1-3), 203-206.

Ntambi, J. M., & Young-Cheul, K. (2000). Adipocyte differentiation and gene expression. *J Nutr, 130*(12), 3122S-3126S.
Ogden, C. L., Carroll, M. D., Kit, B. K., & Flegal, K. M. (2012). Prevalence of obesity and trends in body mass index among US children and adolescents, 1999-2010. *JAMA, 307*(5), 483-490. doi: 10.1001/jama.2012.40
Olefsky, J. M. (1990). The insulin receptor. A multifunctional protein. *Diabetes, 39*(9), 1009-1016.
Otto, T. C., & Lane, M. D. (2005). Adipose development: from stem cell to adipocyte. *Crit Rev Biochem Mol Biol, 40*(4), 229-242. doi: 10.1080/10409230591008189
Park, K. G., Park, K. S., Kim, M. J., Kim, H. S., Suh, Y. S., Ahn, J. D., . . . Lee, I. K. (2004). Relationship between serum adiponectin and leptin concentrations and body fat distribution. *Diabetes Res Clin Pract, 63*(2), 135-142.
Park, K. W., Halperin, D. S., & Tontonoz, P. (2008). Before they were fat: adipocyte progenitors. *Cell Metab, 8*(6), 454-457. doi: S1550-4131(08)00353-7 [pii]
10.1016/j.cmet.2008.11.001
Petras, S. F., Lindsey, S., & Harwood, H. J., Jr. (1999). HMG-CoA reductase regulation: use of structurally diverse first half-reaction squalene synthetase inhibitors to characterize the site of mevalonate-derived nonsterol regulator production in cultured IM-9 cells. *J Lipid Res, 40*(1), 24-38.
Pond, C. (2001). Ecology of storage and allocation of resources: animals *Encyclopedia of Life Sciences* (pp. 1-5). Chichester, UK
John Wiley & Sons.
Rajala, M. W., & Scherer, P. E. (2003). Minireview: The adipocyte--at the crossroads of energy homeostasis, inflammation, and atherosclerosis. *Endocrinology, 144*(9), 3765-3773.
Rajalingam, K., Schreck, R., Rapp, U. R., & Albert, S. (2007). Ras oncogenes and their downstream targets. *Biochim Biophys Acta, 1773*(8), 1177-1195. doi: 10.1016/j.bbamcr.2007.01.012
Ramirez-Zacarias, J. L., Castro-Munozledo, F., & Kuri-Harcuch, W. (1992). Quantitation of adipose conversion and triglycerides by staining intracytoplasmic lipids with Oil red O. *Histochemistry, 97*(6), 493-497.
Repko, E. M., & Maltese, W. A. (1989). Post-translational isoprenylation of cellular proteins is altered in response to mevalonate availability. *J Biol Chem, 264*(17), 9945-9952.
Rhodes, C. J., & White, M. F. (2002). Molecular insights into insulin action and secretion. *Eur J Clin Invest, 32 Suppl 3*, 3-13.
Romero-Corral, A., Montori, V. M., Somers, V. K., Korinek, J., Thomas, R. J., Allison, T. G., . . . Lopez-Jimenez, F. (2006). Association of bodyweight with total mortality and with cardiovascular events in coronary artery disease: a systematic review of cohort studies. *Lancet, 368*(9536), 666-678. doi: 10.1016/S0140-6736(06)69251-9

Rosen, E. D., & MacDougald, O. A. (2006). Adipocyte differentiation from the inside out. *Nat Rev Mol Cell Biol, 7*(12), 885-896. doi: 10.1038/nrm2066

Rosen, E. D., & Spiegelman, B. M. (2000). Molecular regulation of adipogenesis. *Annual Review of Cell and Developmental Biology, 16*, 145-171. doi: 10.1146/annurev.cellbio.16.1.145

16/1/145 [pii]

Rosen, E. D., & Spiegelman, B. M. (2006). Adipocytes as regulators of energy balance and glucose homeostasis. *Nature, 444*(7121), 847-853. doi: nature05483 [pii]

10.1038/nature05483

Rosen, E. D., Walkey, C. J., Puigserver, P., & Spiegelman, B. M. (2000). Transcriptional regulation of adipogenesis. *Genes Dev, 14*(11), 1293-1307.

Rothman, S. S. (2002). *Lessons from the living cell: the culture of science and the limits of reductionism*. New York: McGraw-Hill.

Rozen, Helen J. Skaletsky and Steve. (2000). Primer3 on the WWW for general users and for biologist programmers. In M. S. e. Krawetz S (Ed.), *Bioinformatics Methods and Protocols: Methods in Molecular Biology* (pp. 365-386). Totowa, NJ: Humana Press

Sacchettini, J. C., & Poulter, C. D. (1997). Creating isoprenoid diversity. *Science, 277*(5333), 1788-1789.

Sakai, J., Duncan, E. A., Rawson, R. B., Hua, X., Brown, M. S., & Goldstein, J. L. (1996). Sterol-regulated release of SREBP-2 from cell membranes requires two sequential cleavages, one within a transmembrane segment. *Cell, 85*(7), 1037-1046.

Sarruf, D. A., Iankova, I., Abella, A., Assou, S., Miard, S., & Fajas, L. (2005). Cyclin D3 promotes adipogenesis through activation of peroxisome proliferator-activated receptor gamma. *Mol Cell Biol, 25*(22), 9985-9995. doi: 10.1128/MCB.25.22.9985-9995.2005

Sasaoka, T., Draznin, B., Leitner, J. W., Langlois, W. J., & Olefsky, J. M. (1994). Shc is the predominant signaling molecule coupling insulin receptors to activation of guanine nucleotide releasing factor and p21ras-GTP formation. *J Biol Chem, 269*(14), 10734-10738.

Sato, R., Inoue, J., Kawabe, Y., Kodama, T., Takano, T., & Maeda, M. (1996). Sterol-dependent transcriptional regulation of sterol regulatory element-binding protein-2. *J Biol Chem, 271*(43), 26461-26464.

Sato, R., Yang, J., Wang, X., Evans, M. J., Ho, Y. K., Goldstein, J. L., & Brown, M. S. (1994). Assignment of the membrane attachment, DNA binding, and transcriptional activation domains of sterol regulatory element-binding protein-1 (SREBP-1). *J Biol Chem, 269*(25), 17267-17273.

Sattar, N., Preiss, D., Murray, H. M., Welsh, P., Buckley, B. M., de Craen, A. J., . . . Ford, I. (2010). Statins and risk of incident diabetes: a collaborative meta-analysis

of randomised statin trials. *Lancet, 375*(9716), 735-742. doi: 10.1016/S0140-6736(09)61965-6

Schwartz, M. W., Woods, S. C., Porte, D., Jr., Seeley, R. J., & Baskin, D. G. (2000). Central nervous system control of food intake. *Nature, 404*(6778), 661-671. doi: 10.1038/35007534

Sharma, P. M., Egawa, K., Gustafson, T. A., Martin, J. L., & Olefsky, J. M. (1997). Adenovirus-mediated overexpression of IRS-1 interacting domains abolishes insulin-stimulated mitogenesis without affecting glucose transport in 3T3-L1 adipocytes. *Mol Cell Biol, 17*(12), 7386-7397.

Shimomura, I., Shimano, H., Horton, J. D., Goldstein, J. L., & Brown, M. S. (1997). Differential expression of exons 1a and 1c in mRNAs for sterol regulatory element binding protein-1 in human and mouse organs and cultured cells. [a]. *J Clin Invest, 99*(5), 838-845.

Siddals, K. W., Marshman, E., Westwood, M., & Gibson, J. M. (2004). Abrogation of insulin-like growth factor-I (IGF-I) and insulin action by mevalonic acid depletion: synergy between protein prenylation and receptor glycosylation pathways. *J Biol Chem, 279*(37), 38353-38359.

Small, D. M., & Shipley, G. G. (1974). Physical-chemical basis of lipid deposition in atherosclerosis. *Science, 185*(4147), 222-229.

Snijder, M. B., Heine, R. J., Seidell, J. C., Bouter, L. M., Stehouwer, C. D., Nijpels, G., . . . Dekker, J. M. (2006). Associations of adiponectin levels with incident impaired glucose metabolism and type 2 diabetes in older men and women: the hoorn study. *Diabetes Care, 29*(11), 2498-2503. doi: 10.2337/dc06-0952

Straka, M. S., & Panini, S. R. (1995). Post-transcriptional regulation of 3-hydroxy-3-methylglutaryl coenzyme A reductase by mevalonate. *Arch Biochem Biophys, 317*(1), 235-243. doi: 10.1006/abbi.1995.1158

Sutherland, C., Waltner-Law, M., Gnudi, L., Kahn, B. B., & Granner, D. K. (1998). Activation of the ras mitogen-activated protein kinase-ribosomal protein kinase pathway is not required for the repression of phosphoenolpyruvate carboxykinase gene transcription by insulin. *J Biol Chem, 273*(6), 3198-3204.

Takai, Y., Sasaki, T., & Matozaki, T. (2001). Small GTP-binding proteins. *Physiol Rev, 81*(1), 153-208.

Tanaka, T., Yoshida, N., Kishimoto, T., & Akira, S. (1997). Defective adipocyte differentiation in mice lacking the C/EBPbeta and/or C/EBPdelta gene. *EMBO J, 16*(24), 7432-7443. doi: 10.1093/emboj/16.24.7432

Tang, Q. Q., Otto, T. C., & Lane, M. D. (2003). Mitotic clonal expansion: a synchronous process required for adipogenesis. *Proceedings of the National Academy of Sciences of the United States of America, 100*(1), 44-49. doi: 10.1073/pnas.0137044100

0137044100 [pii]

Theisen, M. J., Misra, I., Saadat, D., Campobasso, N., Miziorko, H. M., & Harrison, D. H. (2004). 3-hydroxy-3-methylglutaryl-CoA synthase intermediate complex

observed in "real-time". *Proc Natl Acad Sci U S A, 101*(47), 16442-16447. doi: 10.1073/pnas.0405809101

Thibault, A., Samid, D., Tompkins, A. C., Figg, W. D., Cooper, M. R., Hohl, R. J., . . . Myers, C. E. (1996). Phase I study of lovastatin, an inhibitor of the mevalonate pathway, in patients with cancer. *Clin Cancer Res, 2*(3), 483-491.

Tontonoz, P., Hu, E., Graves, R. A., Budavari, A. I., & Spiegelman, B. M. (1994a). mPPAR gamma 2: tissue-specific regulator of an adipocyte enhancer. *Genes Dev, 8*(10), 1224-1234.

Tontonoz, P., Hu, E., Graves, R. A., Budavari, A. I., & Spiegelman, B. M. (1994b). mPPARγ2: tissue-specific regulator of an adipocyte enhancer. *Genes Dev, 8*(10), 1224-1234.

Tontonoz, P., Hu, E., & Spiegelman, B. M. (1994c). Stimulation of adipogenesis in fibroblasts by PPARγ2, a lipid-activated transcription factor. *Cell, 79*(7), 1147-1156.

Trayhurn, P. (2007). Adipocyte biology. *Obes Rev, 8 Suppl 1*, 41-44. doi: 10.1111/j.1467-789X.2007.00316.x

USDHHS. (2001). *The Surgeon General's call to action to prevent and decrease overweight and obesity.* . Rockville, MD: US GPO, Washington.

Vicent, D., Maratos-Flier, E., & Kahn, C. R. (2000). The branch point enzyme of the mevalonate pathway for protein prenylation is overexpressed in the ob/ob mouse and induced by adipogenesis. *Mol Cell Biol, 20*(6), 2158-2166.

Villena, J. A., Kim, K. H., & Sul, H. S. (2002). Pref-1 and ADSF/resistin: two secreted factors inhibiting adipose tissue development. *Horm Metab Res, 34*(11-12), 664-670. doi: 10.1055/s-2002-38244

Waki, H., & Tontonoz, P. (2007). Endocrine functions of adipose tissue. *Annu Rev Pathol, 2*, 31-56. doi: 10.1146/annurev.pathol.2.010506.091859

Walkey, C. J., & Spiegelman, B. M. (2008). A functional peroxisome proliferator-activated receptor-gamma ligand-binding domain is not required for adipogenesis. *J Biol Chem, 283*(36), 24290-24294. doi: 10.1074/jbc.C800139200

Wang, X., Sato, R., Brown, M. S., Hua, X., & Goldstein, J. L. (1994). SREBP-1, a membrane-bound transcription factor released by sterol-regulated proteolysis. *Cell, 77*(1), 53-62.

Wang, Y., & Beydoun, M. A. (2007). The obesity epidemic in the United States--gender, age, socioeconomic, racial/ethnic, and geographic characteristics: a systematic review and meta-regression analysis. *Epidemiol Rev, 29*, 6-28. doi: mxm007 [pii]
10.1093/epirev/mxm007

WHO.). "Obesity and overweight". Retrieved March 1, 2013, from http://www.who.int/mediacentre/factsheets/fs311/en/index.html

Wood, R. J. (2008). Vitamin D and adipogenesis: new molecular insights. *Nutr Rev, 66*(1), 40-46. doi: 10.1111/j.1753-4887.2007.00004.x

Yang, R., & Barouch, L. A. (2007). Leptin signaling and obesity: cardiovascular consequences. *Circ Res, 101*(6), 545-559. doi: 10.1161/CIRCRESAHA.107.156596

Yang, T., Espenshade, P. J., Wright, M. E., Yabe, D., Gong, Y., Aebersold, R., . . . Brown, M. S. (2002). Crucial step in cholesterol homeostasis: sterols promote binding of SCAP to INSIG-1, a membrane protein that facilitates retention of SREBPs in ER. *Cell, 110*(4), 489-500.

Zuo, Y., Qiang, L., & Farmer, S. R. (2006). Activation of CCAAT/enhancer-binding protein (C/EBP) alpha expression by C/EBP beta during adipogenesis requires a peroxisome proliferator-activated receptor-gamma-associated repression of HDAC1 at the C/ebp alpha gene promoter. *J Biol Chem, 281*(12), 7960-7967. doi: 10.1074/jbc.M510682200

APPENDIX A

Additional Results and Discussion

ADDITIONAL RESULTS AND DISCUSSION

Apoptosis

We examined whether the decreased cellular triglyceride could be related to programmed cell death (PCD) by measuring apoptosis in 3T3-F442A preadipocytes prior to (Figures 5,6 and 9,10) and following (Figure 7,8 and 11,12) the differentiation process with the acridine orange ethidium bromide dual staining assay.

Representative images of AO/EB and fluorescence microscopy demonstrated that when 3T3-F442A preadipocytes were incubated with 20 – 200 μmol/L geranylgeraniol for 24 (Figure 5) or 48 hours (Figure 6) prior to differentiation, only cells incubated with 200 μmol/L geranylgeraniol had signs of apoptosis. Mature adipocytes, however, may be more sensitive to the apoptotic effect of geranylgeraniol in that all groups had some indications of apoptosis (Figures 7, 8). These observations, however, need further confirmation.

Prior to differentiation, 3T3-F442A preadipocytes incubated with 1.25-10μmol/L Lovastatin for 24 (Figure 9) or 48 hours (Figure 10) exhibited no signs of apoptosis as determined by representative images of AO/EB and fluorescence microscopy. Fully differentiated adipocytes, however, showed some indications of apoptosis following 24 (Figure 11) and 48 hour (Figure 12) incubation with 5 and 10μmol/L Lovastatin. These observations warrant further studies.

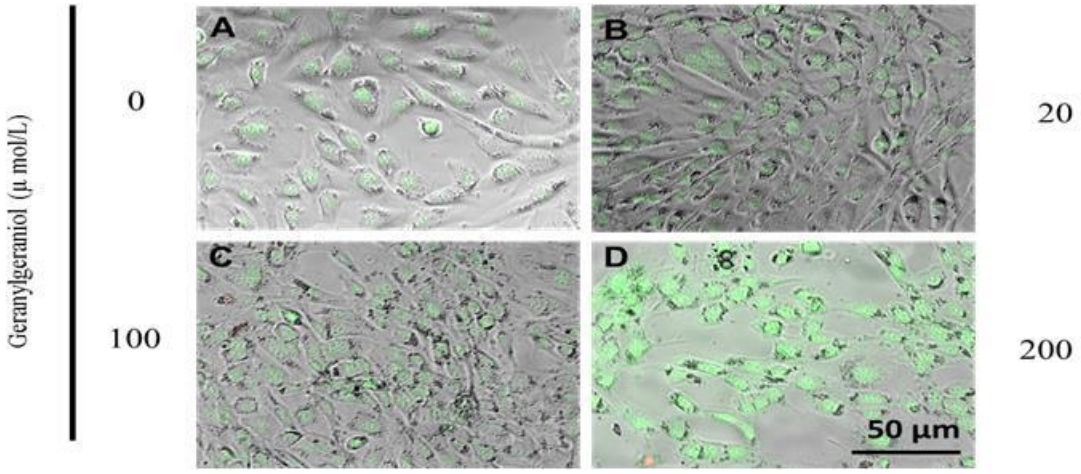

Figure 5. The effect of geranylgeraniol on apoptosis in murine 3T3-F442A preadipocytes prior to 8-d differentiation. The pre-differentiation 3T3-F442A cells were incubated with 0 (A), 20 (B), 100 (C) and 200 (D) μmol/L geranylgeraniol for 24 hours before apoptosis was determined by Acridine Orange and Ethidium Bromide Dual Staining Assay.

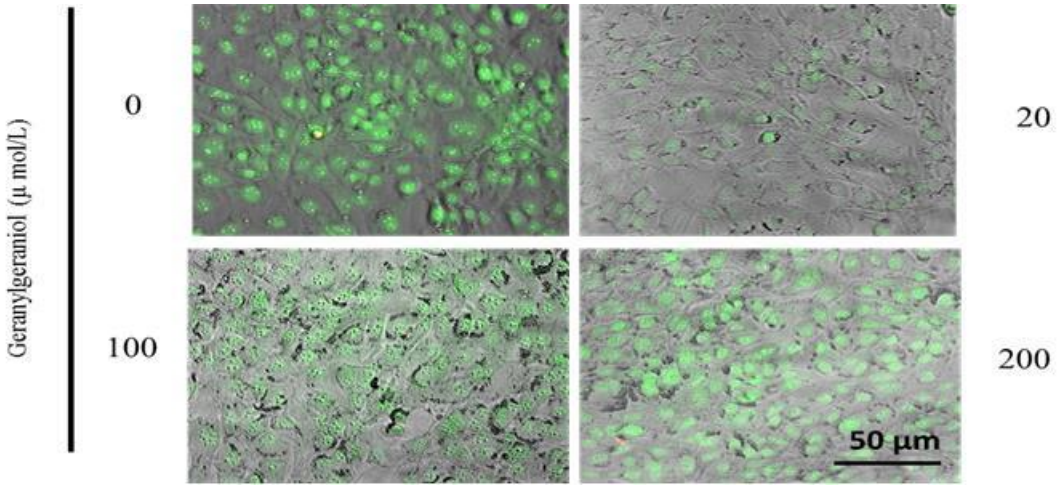

Figure 6. The effect of geranylgeraniol on apoptosis in murine 3T3-F442A preadipocytes prior to 8-d differentiation. The pre-differentiation 3T3-F442A cells were incubated with 0 (A), 20 (B), 100 (C) and 200 (D) μmol/L geranylgeraniol for 48 hours before apoptosis was determined by Acridine Orange and Ethidium Bromide Dual Staining Assay.

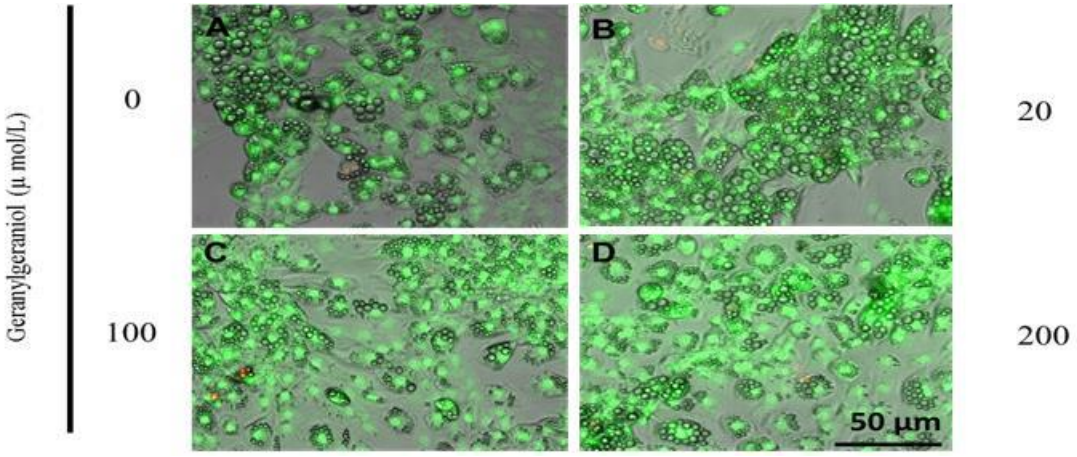

Figure 7. The effect of geranylgeraniol on apoptosis in murine 3T3-F442A preadipocytes following 8-d differentiation. The differentiated 3T3-F442A cells were incubated with 0 (A), 20 (B), 100 (C) and 200 (D) μmol/L geranylgeraniol for 24 hours before apoptosis was determined by Acridine Orange and Ethidium Bromide Dual Staining Assay.

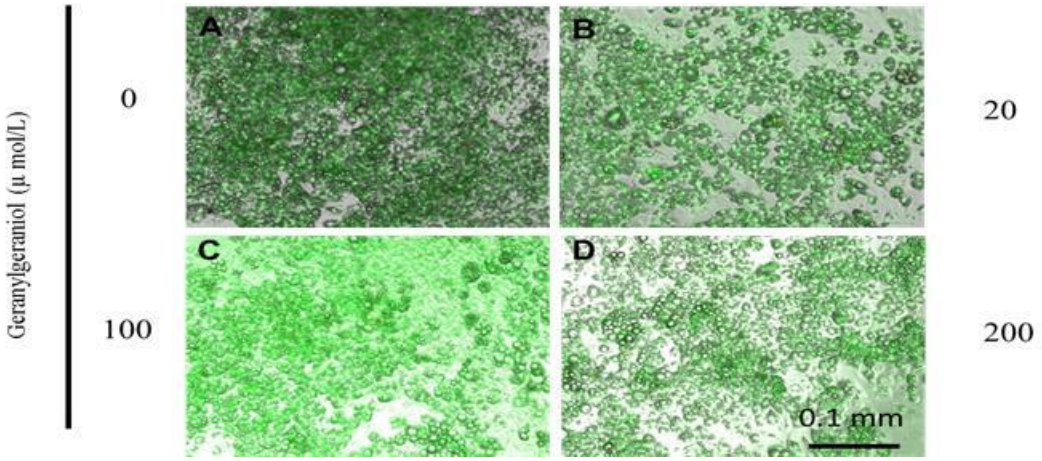

Figure 8. The effect of geranylgeraniol on apoptosis in murine 3T3-F442A preadipocytes following 8-d differentiation. The differentiated 3T3-F442A cells were incubated with 0 (A), 20 (B), 100 (C) and 200 (D) μmol/L geranylgeraniol for 48 hours before apoptosis was determined by Acridine Orange and Ethidium Bromide Dual Staining Assay.

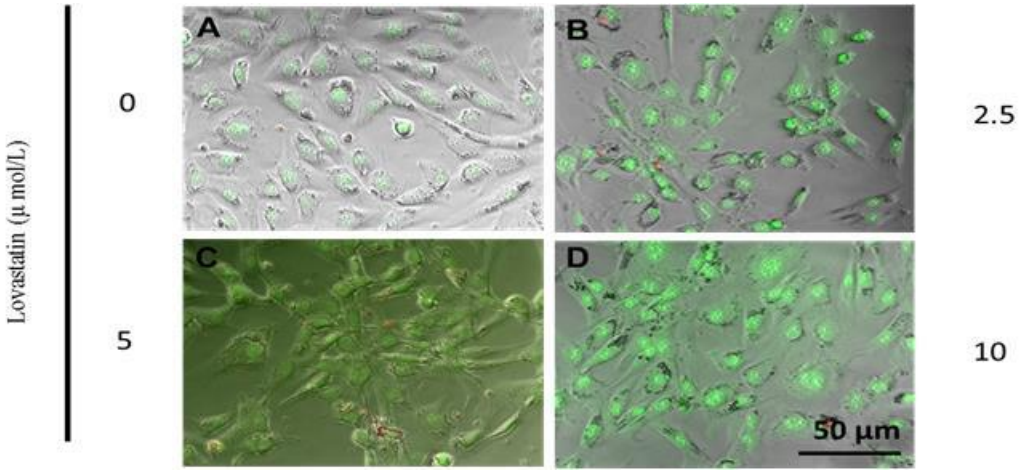

Figure 9. The effect of lovastatin on apoptosis in murine 3T3-F442A preadipocytes prior to 8-d differentiation. The pre-differentiation 3T3-F442A cells were incubated with 0 (A), 2. 5 (B), 5 (C) and 10 (D) μmol/L lovastatin for 24 hours before apoptosis was determined by Acridine Orange and Ethidium Bromide Dual Staining Assay.

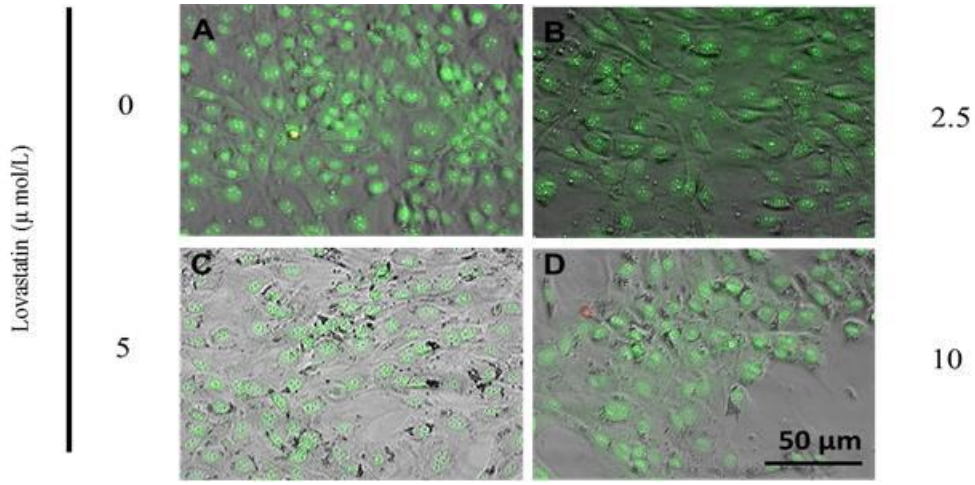

Figure 10. The effect of lovastatin on apoptosis in murine 3T3-F442A preadipocytes prior to 8-d differentiation. The pre-differentiation 3T3-F442A cells were incubated with 0 (A), 2. 5 (B), 5 (C) and 10 (D) μmol/L lovastatin for 48 hours before apoptosis was determined by Acridine Orange and Ethidium Bromide Dual Staining Assay.

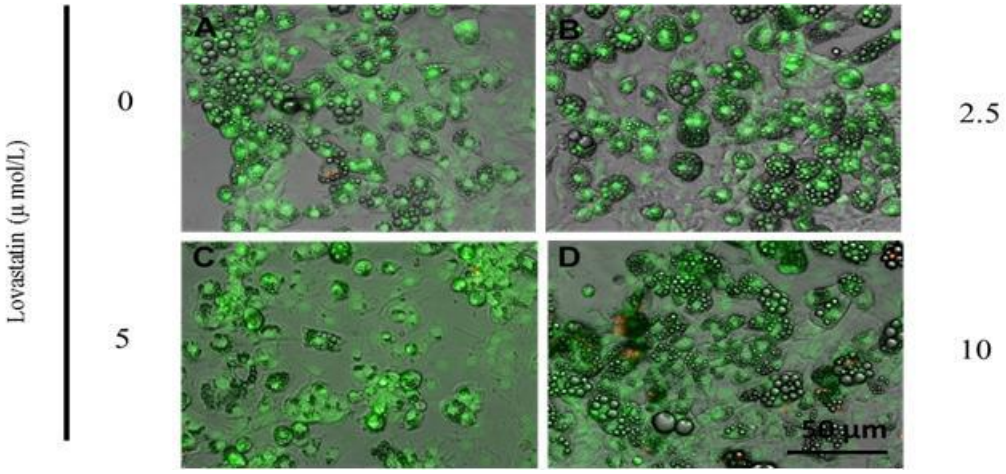

Figure 11. The effect of lovastatin on apoptosis in murine 3T3-F442A preadipocytes following 8-d differentiation. The differentiated 3T3-F442A cells were incubated with 0 (A), 2. 5 (B), 5 (C) and 10 (D) μmol/L lovastatin for 24 hours before apoptosis was determined by Acridine Orange and Ethidium Bromide Dual Staining Assay.

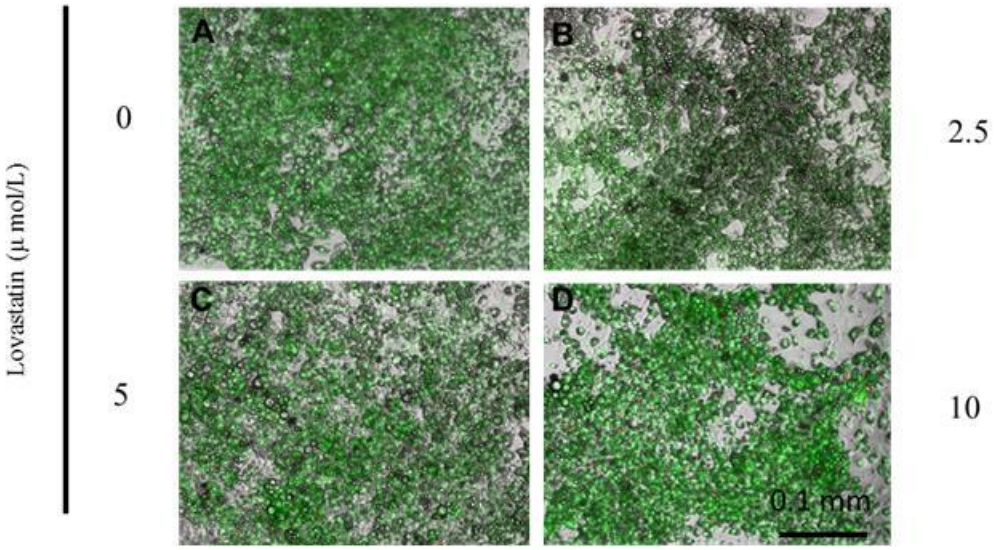

Figure 12. The effect of lovastatin on apoptosis in murine 3T3-F442A preadipocytes following 8-d differentiation. The differentiated 3T3-F442A cells were incubated with 0 (A), 2. 5 (B), 5 (C) and 10 (D) μmol/L lovastatin for 48 hours before apoptosis was determined by Acridine Orange and Ethidium Bromide Dual Staining Assay.

Primer Verification

Melting Profile

Purity of the double stranded DNA (dsDNA) was determined by analyzing the melting profile of the PCR products generated from each primer. Melt peak charts were obtained from DNA sequences of the genes of interest and amplified by real-time qPCR using iQ^{TM} SYBR® Green Supermix (Figure 13 A, B, C, D). The melting curve analysis showed one peak corresponding to a specific PCR product for the following genes: *AdipoQ, ADD1, Fabp4, Fasn, GLUT4, GPDH, HMG-CoA reductase, Lep, LPL, Pref1, RPL22, SCD1* and *SREBP1*.

The melt peak chart attained from the DNA sequence of *C/EBPα* did not show a distinct peak but rather multiple ones at varying temperatures denoting non-specificity of the primer (Figure 13 A). As for *INSIG1*, the melt peak chart obtained from its DNA sequence shows two different peaks, one large peak at ~84^{o}C and a small one at ~80^{o}C (Figure 13 C). This implies that there may have been more than one product generated during the amplification. The sequence was then blasted and it was established that the sequence matched one other gene, serine palmitoyltransferase, in small quantity, so there was slight contamination of the primer. However, sequencing the purified DNA of the product showed a high quality primer meaning that *INSIG1* was dominant.

The melt peak chart produced from the DNA sequences of *Pparγ* showed two peaks, one at ~84.5^{o}C and the other at ~85.5^{o}C (Figure 13 C). The primer designed for the PCR reactions is a combination of *Pparγ*1 and *Pparγ*2 which may explain why this

was observed. The sequencing results for *Pparγ* showed a high quality primer, but non-specificity was detected due to two isoforms present. After the sequence was blasted, it was confirmed that the sequence did not match any other genes. It appears as though *Pparγ*1 and *Pparγ*2 were amplified simultaneously since the two peaks were very close to each other, with slight preference towards one isoform, as depicted by its higher peak.

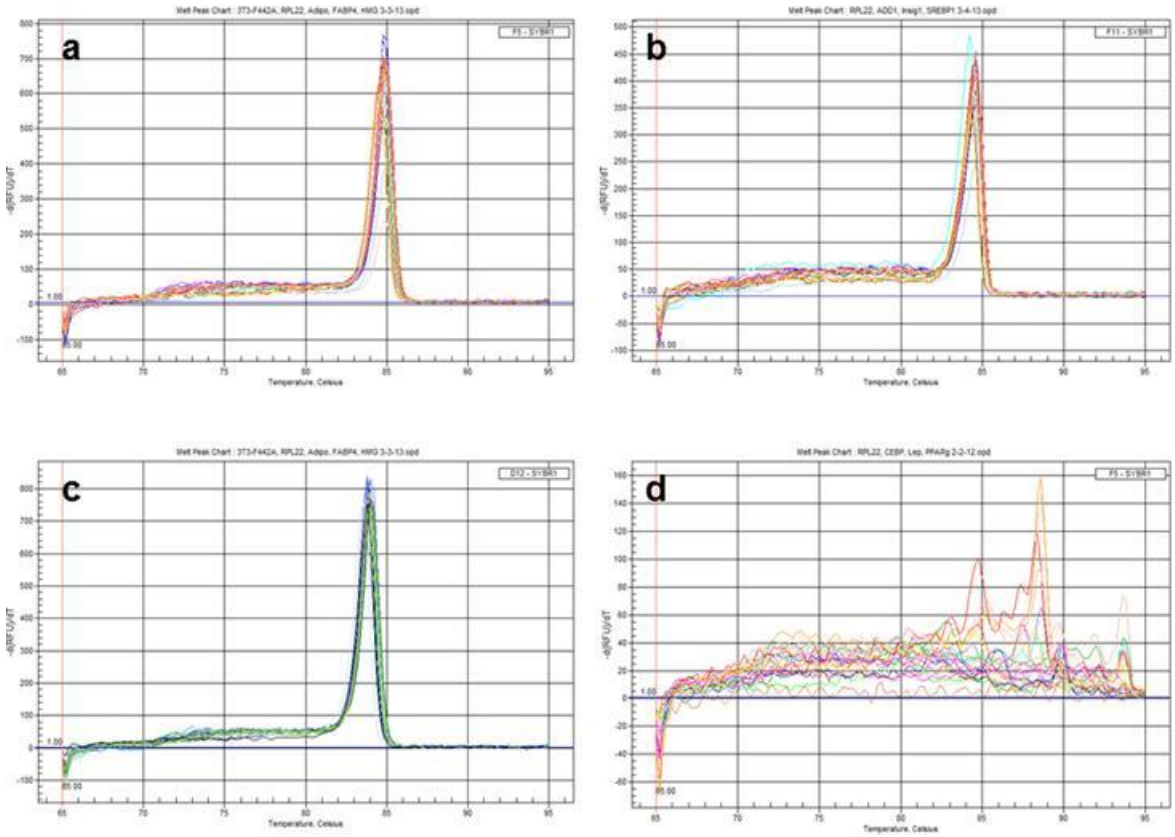

Figure 13A. Melting peaks charts obtained from a) adiponectin b) *ADD1* c) *Fabp4* and d) *C/EBPα* DNA sequences amplified by real-time qPCR using iQ™ SYBR® Green Supermix. The melting curve analysis showed one peak corresponding to the specific PCR product, with the exception of *C/EBPα*.

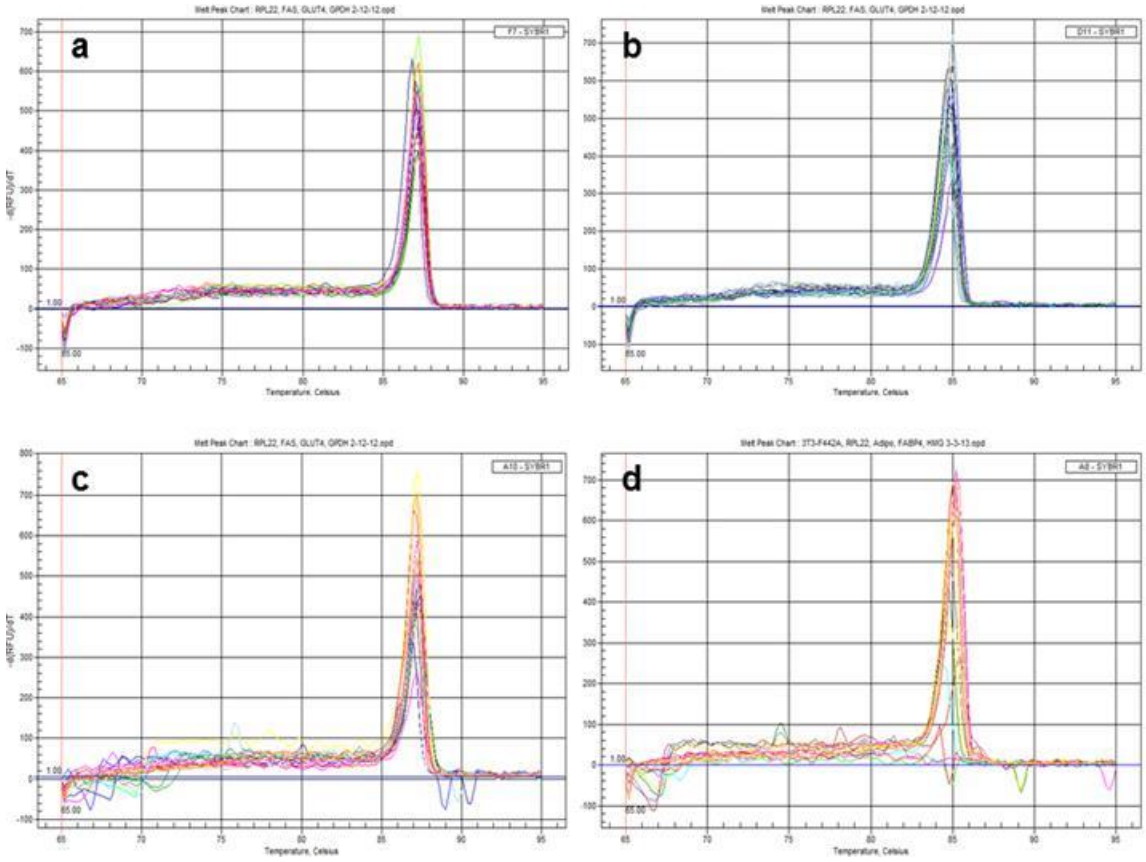

Figure 13B. Melting peaks charts obtained from a) *Fasn* b) *GLUT4* c) *GPDH* and d) HMG-CoA R DNA sequences amplified by real-time qPCR using iQ™ SYBR® Green Supermix. The melting curve analysis showed one peak corresponding to the specific PCR product.

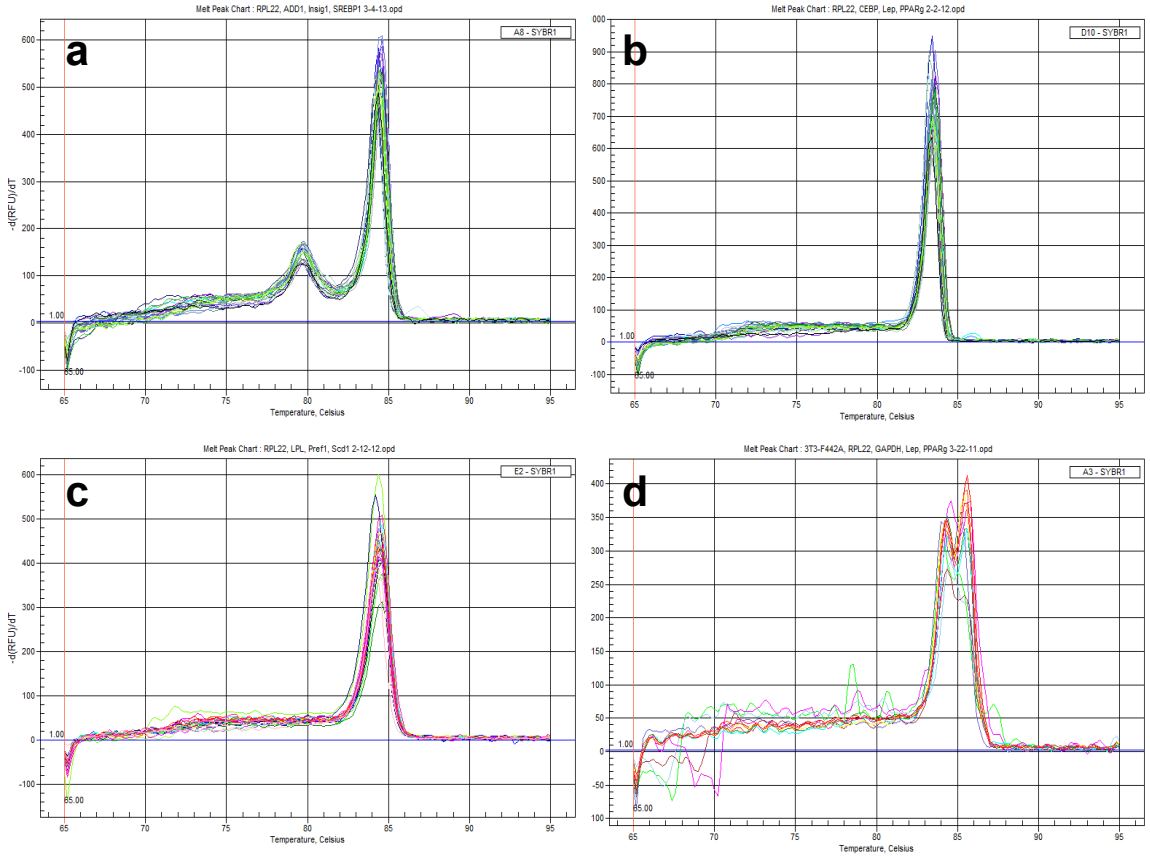

Figure 13C. Melting peaks charts obtained from a) *INSIG1* b) *Lep* c) *LPL* and d) *Pparγ* DNA sequences amplified by real-time qPCR using iQ™ SYBR® Green Supermix. The melting curve analysis showed one peak corresponding to the specific PCR product, with the exception of *INSIG1* and *Pparγ*.

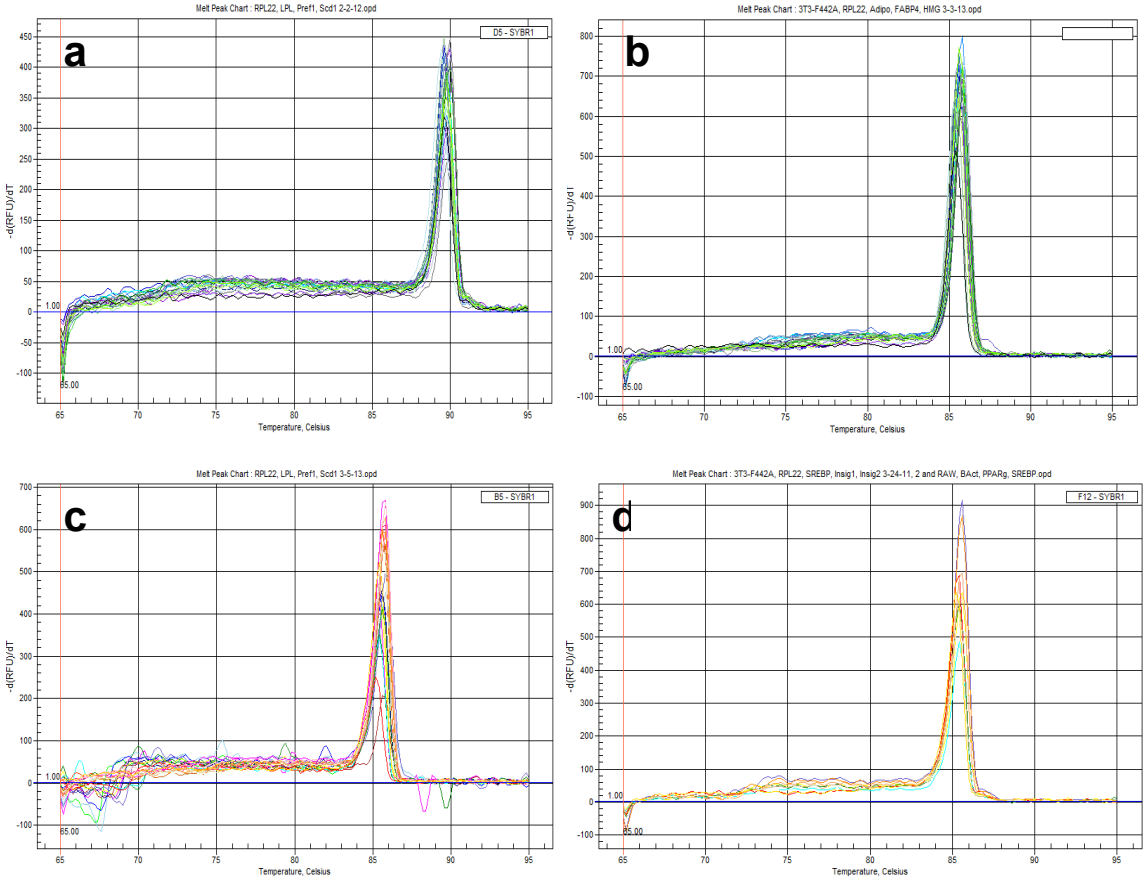

Figure 13D. Melting peaks charts obtained from a) *Pref1* b) *RPL22* c) *SCD1* and d) SREBP1 DNA sequences amplified by real-time qPCR using iQ™ SYBR® Green Supermix. The melting curve analysis showed one peak corresponding to the specific PCR product.

DNA Sequencing

To confirm specificity and rule out the possibility of two products being generated by RT-PCR, primers used to generate the PCR products were used as sequencing primers to sequence both strands of the dsDNA. The quality scores obtained from the DNA sequencing for each gene analyzed are summarized in Table 3. When analyzing the final

PCR data for each gene, we took into consideration both the melt peak chart analysis and the quality scores of the gene from DNA sequencing.

Table 3.
DNA Sequencing results: Quality scores of the individual primer sequences

Gene	Direction	Quality Score (QS)**	Gene	Direction	Quality Score (QS)**
AdipoQ*	Up+	43	***INSIG1****	Up+	48
	Dn-	44		Dn-	44
ADD1	Up+	30	***Lep****	Up+	45
	Dn-	32		Dn-	46
C/EBPα	Up+	19	***LPL***	Up+	21
	Dn-	15		Dn-	21
Fabp4*	Up+	41	***Pparγ****	Up+	43
	Dn-	42		Dn-	34
Fasn*	Up+	29	***Pref1***	Up+	25
	Dn-	27		Dn-	28
GLUT4*	Up+	32	***RPL22****	Up+	36
	Dn-	23		Dn-	42
GPDH*	Up+	24	***SCD1***	Up+	32
	Dn-	29		Dn-	33
HMGCoAR	Up+	13	***SREBP-1****	Up+	43
	Dn-	34		Dn-	47

* Genes were included in the final data analysis of Real Time RT-qPCR
** QS of ≥ 40: Automatic pass, good trace results
QS of 25 – 39: Manual review, acceptable traces results
QS of 15 – 24: May indicate problems, examine trace data

APPENDIX B

Publication in Experimental Biology and Medicine Journal

Mevalonate Depletion Mediates the Suppressive Impact of Geranylgeraniol on Murine B16 Melanoma Cells

Katuru R., Fernandes N., Elfakhani M., Dutta D., Mills N., Hynds D., King C. and Mo H. 2011. Mevalonate Depletion Mediates the Suppressive Impact of Geranylgeraniol on Murine B16 Melanoma Cells. *Experimental Biology and Medicine,* 236(5): 604 - 13

Key words: geranylgeraniol, B16 melanoma, HMG-CoA reductase, mevalonate, cell cycle, apoptosis, differentiation

ABSTRACT

The diterpene geranylgeraniol suppresses the growth of human liver, lung, ovary, pancreas, colon, stomach, and blood tumors with undefined mechanisms. We evaluated the growth-suppressive activity of geranylgeraniol in murine B16 melanoma cells. Geranylgeraniol induced dose-dependent suppression of B16 cell growth (IC50=55±13 μmol/L) following a 48-h incubation in 96-well plates. Cell cycle arrest at the G1 phase, manifested by a geranylgeraniol-induced increase in G1/S ratio and decreased expression of cyclin D1 and cyclin-dependent kinase 4, apoptosis detected by Guava Nexin™ assay and fluorescence microscopy following acridine orange and ethidium bromide dual staining, and cell differentiation shown by increased alkaline phosphatase activity, contributed to the growth suppression. Murine 3T3-L1 fibroblasts were 10-fold more resistant than B16 cells to geranylgeraniol-mediated growth suppression. Geranylgeraniol at near IC50 concentration (60 μmol/L) suppressed the mRNA level of 3-hydroxy-3-methylglutaryl coenzyme A (HMG-CoA) reductase by 50%. The impact of geranylgeraniol on B16 cell growth, cell cycle arrest and apoptosis were attenuated by supplemental mevalonate, the product of HMG-CoA reductase that is essential for cell growth. Geranylgeraniol and *d*-δ-tocotrienol, a down-regulator of HMG-CoA reductase, additively suppressed the growth of B16 cells. These results support our hypothesis that mevalonate depletion mediates the tumor-specific growth-suppressive impact of geranylgeraniol. Geranylgeraniol may have potential in cancer chemoprevention and/or therapy.

INTRODUCTION

The mevalonate-derived intermediates, farnesyl pyrophosphate and geranylgeranyl pyrophosphate, are covalently attached to the carboxy-terminal cysteine residue of the nuclear lamins (1) and members of the small G proteins (2). This post-translational modification is essential to the membrane attachment and biological functions of these proteins that are vital to cell survival and growth.

3-Hydroxy-3-methylglutaryl coenzyme A (HMG-CoA) reductase, the rate-limiting activity in mevalonate synthesis (3), is differentially regulated in sterologenic

and tumor tissues (4). In sterologenic tissues HMG-CoA reductase is under a multivalent regulation consisting of sterol-mediated transcriptional feedback regulation and non-sterol-mediated post-transcriptional regulation. Tumor reductase activity, to the contrary, is resistant to the sterol-mediated transcriptional regulation and consequently elevated. Nevertheless, tumor reductase remains responsive to the isoprenoid-mediated down regulation.

The essential role of mevalonate in growth and the uniquely dysregulated tumor HMG-CoA reductase render the tumor reductase a viable target for intervention. The statins, competitive inhibitors of HMG-CoA reductase (3), and the isoprenoids, down-regulators of reductase (5), suppress the growth of melanoma cells. Geranylgeraniol (all trans-3,7,11,15-tetramethyl-2,6,10,14-hexadecatetraen-1-ol), a diterpene found in linseed oil (6), Cedrela toona wood oil (7), and sucupira branca fruit oil (8), suppresses HMG-CoA reductase activity in human fibroblasts (9, 10) and human A549 lung adenocarcinoma cells (11). Geranylgeraniol also suppresses the proliferation of tumor cells derived from human blood (12-15), lung (11, 16, 17), colon (13, 14), liver (14, 18), ovary (14, 19), pancreas (14, 20), and stomach (14). Nevertheless, the role of mevalonate in geranylgeraniol-mediated growth inhibition has not been delineated.

We hypothesize that mevalonate depletion mediates the growth-suppressive impact of geranylgeraniol in tumors. In the present study we tested this hypothesis in murine B16 melanoma cells. Geranylgeraniol-induced concentration-dependent suppression of the B16 cell growth was accompanied by cell cycle arrest at the G1 phase, initiation of apoptosis and increased alkaline phosphatase (ALP) activity suggesting cell differentiation. Supplemental mevalonolactone attenuated the impact of geranylgeraniol on cell growth, cell cycle arrest and apoptosis. Blends of geranylgeraniol and *d*-δ-tocotrienol, a down-regulator of HMG-CoA reductase activity, synergistically suppressed the growth of B16 cells.

MATERIALS AND METHODS

Chemicals:

Lovastatin and *d*-δ-tocotrienol were gifts from Merck Research Laboratories (Rahway, NJ) and American River Nutrition, Inc. (Hadley, MA), respectively. Geranylgeraniol was purchased from Sigma-Aldrich (St. Louis, MO).

Cell growth assay:

Murine B16 melanoma cell growth was measured by using CellTiter 96® Aqueous One Solution (Promega, Madison, WI) as previously described (21). Briefly, B16 melanoma cells, purchased from the American Type Culture Collection (ATCC, Manassas, VA) and cultured in RPMI 1640 medium (Sigma-Aldrich) supplemented with 10% fetal bovine serum (FBS, Hyclone Lab Inc., Logan, UT) and 1% penicillin-streptomycin (MP biomedicals, Solon, OH) at 37^{o}C in a humidified atmosphere of 5%

CO_2, were seeded at 1000 cells/0.1 mL medium/well in 96-well tissue culture plates (Fisher Scientific Company LLC, Houston, TX). At 24 h the medium was decanted from each well and replaced with 0.1 mL fresh medium containing geranylgeraniol that was pre-dissolved in ethyl alcohol. All cultures contained 1 mL/L of ethyl alcohol. Cells were further incubated for an additional 48 h. The 72-h cell populations following a quick rinse with 0.1 mL Hank's Balanced Salt Solution (HBSS) were determined by adding 20 µL of CellTiter 96® Aqueous One Solution to each well; plates were held in the dark at 37°C for 2 h and then read at 490 nm with a SPECTRAmax® 190 multi-plate reader with SOFTmax® PRO version 3.0 (Molecular Devices, Sunnyvale, CA). Absorbances from wells containing cell-free medium were used as baselines and were deducted from absorbances of other cell-containing wells. The IC50 value is the concentration of geranylgeraniol required to suppress the net increase in cell number by 50%.

Murine 3T3-L1 embryo fibroblasts (ATCC) were grown in Dulbecco's modified Eagle's medium (DMEM) with 4 mmol/L L-glutamine adjusted by ATCC to contain 1.5 g/L sodium bicarbonate and 4.5 g/L glucose, supplemented with 10% bovine calf serum and 1% penicillin/streptomycin (Invitrogen, Carlsbad, CA). Cultures, seeded in 0.1 mL medium with $2x10^3$ cells/well in a 96-well plate, were incubated for 24 h at 37°C in a humidified atmosphere of 5% CO_2. At 24 h the medium was decanted from each well and replaced with 0.1 mL fresh medium containing geranylgeraniol. Incubation continued for additional 48 h. Cell populations of all wells were determined using the CellTiter 96® Aqueous One Solution.

Microscopy:

Photomicrographs of representative fields of monolayers of B16 cells in the cell growth assay were made with a Nikon Eclipse TS 100 microscope (Nikon Corporation, Tokyo, Japan) equipped with a Nikon Coolpix 995 digital camera (Nikon Corporation).

Cell cycle distribution:

B16 cells were seeded in 25 cm^2 flasks (Becton Dickinson Labware, Franklin Lakes, NJ) at $1x10^6$ cells/flask with 5 mL medium/flask and incubated for 24 h. Medium was then decanted and cultures replenished with medium containing geranylgeraniol that had been dissolved in ethyl alcohol. Following additional 12- and 24-h incubations, adherent cells were harvested by trypsinization and pelleted by low speed centrifugation. Cell pellets were fixed in 1 mL 70% ethanol at -20°C overnight and washed in 1 mL phosphate-buffered saline (PBS). Cells (5×10^5) were re-suspended in 500 µL PBS containing 0.5 mg RNase A (Sigma-Aldrich) and incubated at 37ºC for 30 min. Following gentle mixing a 100 µL aliquot of propidium iodide (Sigma-Aldrich, 1 g/L in PBS containing 0.1% Triton X-100) was added. The cells were incubated in the dark at room temperature for 15 min and then held at 4°C in the dark for flow cytometric analysis (22). Aliquots of 1×10^4 cells were analyzed for DNA content using a BD FACSCaliber™ Flow Cytometer (BD Biosciences, San Jose, CA). The distribution of cells in the G1, S, and G2/M phases of the cell cycle was determined using MultiCycle AV software (Phoenix Flow Systems, San Diego, CA).

Annexin V assay for apoptosis

B16 cells were seeded in 25 cm^2 flasks (Becton Dickinson Labware) at $1x10^6$ cells/flask with 5 mL medium/flask and incubated for 24 h. Medium was then decanted and cultures replenished with medium containing geranylgeraniol. Following additional 12- and 24-h incubations, adherent cells were harvested by trypsinization and pelleted by refrigerated centrifugation at 300 g for 10 min. Resuspended cells in 150 µL medium containing $2x10^4$ cells were mixed with 50 µL of the Guava Nexin™ reagent containing Annexin V-PE and Nexin 7-amino-actinomycin D (7-AAD), loaded onto the 96 well plate, and incubated at room temperature in the dark for 20 min. Samples containing 5 x 10^3 cells were analyzed by using a Guava EasyCyte flow cytometer (Guava Technologies, Inc., Hayward, CA) with the Guava ExpressPlus program (22, 23). Annexin V is a phospholipid-binding protein that has high affinity for phosphatidylserine translocated from the internal surface to the outer surface of cell membrane at the early stage of apoptosis. 7-AAD selectively permeates late stage apoptotic and dead cells. Therefore cells that are viable (Annexin V- and 7-AAD-), early apoptotic (Annexin V+ and 7-AAD-), late apoptotic (Annexin V+ and 7-AAD+) and dead cells with nuclear debris (Annexin V- and 7-AAD+) can be separated and percentages of these cell populations quantified.

Acridine orange and ethidium bromide dual staining assay for apoptosis

B16 cells were seeded in 25 cm^2 flasks (Becton Dickinson Labware, Franklin Lakes, NJ) at $1.5x10^6$ cells/flask with 5 mL medium/flask and incubated for 24 h. Medium was then decanted and cultures replenished with medium containing geranylgeraniol. Following additional 24-h incubation the monolayer cells were harvested by trypsinization. Cells were resuspended in 100 µL cold PBS and a dye mixture (4 µL) containing 50 µg/mL acridine orange (Becton, Dickinson and Company, Sparks, MD) and 50 µg/mL ethidium bromide (Sigma-Aldrich) was added to each sample. The cells were then immediately observed under an Axiovert 200 M microscope (Carl Zeiss MicroImaging Inc., Thornwood, NY) equipped with a FluoArc lamp, an AxioCam MRm digital camera system (Carl Zeiss), and AxioVision Rel. 4.3 program (Carl Zeiss). The phase-contrast images of representative fields of each well and the green and red fluorescence emitted by acridine orange and ethidium bromide staining were captured by using bright field phase 2, fluorescein isothiocyanate (FITC) and tetramethylrhodamine isothiocyanate (TRITC) filters, respectively (23).

Alkaline phosphatase activity assay

B16 cells were inoculated in Petri-dishes (100 mm x 20 mm, Corning Life Sciences, Wilkes Barre, PA) at $5x10^6$ per dish. Following a 24-h incubation, medium was aspirated and replaced with fresh medium containing 0, 30, 60 and 90 µmol/L geranylgeraniol and the incubation continued for additional 48 h. Cells were washed with PBS twice and lysed with 0.5 mL of 0.5% Triton X-100 per dish. Cell lysates were

collected and shaken at room temperature for 20 min before being centrifuged at 14,000 rpm for 5 min. In a 96-well plate 150 µL supernatant was added to 50 µL of working solution from QuantiChrom™ Alkaline Phosphatase Assay Kit (BioAssay Systems, Hayward, CA) according to manufacturer's instruction and the absorbance was read at 405 nm with a Tecan Infinite M200 micro plate reader (Tecan, Salzburg, Austria). Protein concentration of each sample was determined with BCA™ Protein Assay Kit (Pierce, Rockford, IL) and alkaline phosphatase activity was normalized based on protein concentrations.

Western-blot:

Murine B16 melanoma cells cultured in 150 cm^2 flasks (Midwest Scientific, Valley Park, MO) at $5x10^6$ per flask were incubated with geranylgeraniol for 12 and 24 h. Following the incubation the growth medium was aspirated and cells washed with 10 mL ice cold PBS twice and then 150 µL of lysis buffer (50 mmol/L Tris-HCl, pH 8.8, 5 mmol/L EDTA, 1% SDS) containing freshly mixed 1% protease inhibitor cocktail (Sigma-Aldrich) was added to the flask. Cells were sonicated (Fisher Scientific) for 45 seconds and placed in a dry bath incubator (Boekel Scientific, Feasterville, PA) at 90°C for 20 minutes. Protein concentration of each sample was determined with BCA™ Protein Assay Kit (Pierce). Samples containing 60 µg proteins were mixed with lamelli buffer (Bio-Rad Laboratories, Hercules, CA) at 1:1 ratio (v/v) and boiled for 5 min before being loaded onto a Mini PROTEAN® 3 (Bio-Rad) electrophoresis unit with a 15% SDS-polyacrylamide gel and run at 150 V for 2-4 h. The proteins were then transferred to Immobilon-P transfer membrane (Millipore, Bedford, MA) with a Mini Trans-Blot® Cell (Bio-Rad) at 100 mA overnight. The immobilon-P transfer membranes were then incubated in blocking solution (5% non-fat dry milk in PBS) for 2 h at room temperature with shaking, rinsed with PBS, and then incubated with monoclonal antibodies to cyclin D1 and cyclin-dependent kinase (Cdk) 4 (Cell Signaling Technology, Beverly, MA) at 4ºC overnight. After rinsing with PBS containing 0.1% Tween-20 (PBST) for 10 min., the membrane was incubated with a secondary antibody (horseradish peroxidase linked, Cell Signaling Technology, 1:3,000 in PBST) for 45 min. at room temperature, washed with PBST for 15 min., and reacted with SuperSignal West Pico Chemiluminescence Kit (Pierce) before being photographed at Chemi Doc XRS imaging system (Bio-Rad). Precision Strep Tactin-HRP (Bio-Rad) protein standards were used to identify the molecular weight of protein bands. A non-specific IgG (Cell Signaling Technology) was used for background control.

Quantitative Real-Time Polymerase Chain Reaction (qPCR):

Murine B16 melanoma cells cultured in Petri-dishes (100 mm x 20 mm, Corning Life Sciences) at $5x10^6$ cells per dish were incubated with geranylgeraniol for 24 h. Total cellular RNA was extracted using TRIzol reagent (Invitrogen) according to the manufacturer's protocols. The concentration and purity of the isolated total RNA were determined spectrophotometrically using OD260:280 ratio. The integrity of the purified

total RNA was verified by detecting a 2:1 ratio for the 28S:18S ribosomal RNA (rRNA) using agarose gel electrophoresis. Samples were run on a 1.5% agarose gel (Tris-acetate (TAE) buffer) at 80 volts for 90 min. Gels were soaked in 0.5 µg/mL ethidium bromide for 1 h with shaking and then visualized by Chemi Doc XRS imaging system (Bio-Rad). The mRNA expression levels of HMG-CoA reductase gene (GenBank accession number NM_008255) were analyzed by reverse transcription followed by qPCR. Total RNA (2 µg) in a 20 µL reaction buffer was reverse transcribed into cDNA using an Oligo $(dT)_{20}$ primer and SuperScript® III First-Strand kit (Invitrogen) following the manufacturer's instructions. cDNA was diluted by 25-fold with 25 µg/mL of acetylated bovine serum albumin (Invitrogen) and 6 µL of diluted cDNA was amplified in a 25 µL PCR solution containing 250 nmol/L of both forward and reverse primers of the HMG-CoA reductase gene and iQ™ SYBR® Green Supermix (Bio-Rad). The following primer sequences were designed using Vector NTI Advance version 11 software (Invitrogen): forward, GCTTGGGCCAGAGAAGACAGTGCTC; Reverse, ACTCTGCTGACCCCCTGAGGAAGCT. The cDNA was denatured at 95°C for 3 minutes followed by 40 cycles of PCR (94°C for 30 s, 60°C for 25 s, 72°C for 25 s, and 78°C for 9 s) using DNA Engine Opticon® 2 System (Bio-Rad) with the Opticon Monitor program (version 3). The mRNA levels were normalized using ribosomal protein L22 (*RPL22*) as internal control (24) and quantified by using the δCt method. Fold changes of gene expression were calculated by the 2-δδCt method.

Statistics

One-way or two-way analysis of variance (ANOVA) was performed to assess the differences between groups using Prism® 4.0 software (GraphPad Software Inc., San Diego, CA). Differences in means were analyzed by Dunnett's multiple comparison test unless specified otherwise. Levels of significance were designated as $P < 0.05$.

RESULTS

Figure 1A shows the geranylgeraniol-mediated suppression of the growth of murine B16 melanoma cells and 3T3-L1 fibroblasts. The IC50 values, concentrations of geranylgeraniol required to suppress cell growth by 50%, for B16 cells (55±13 µmol/L, n=6) was lower than one-tenth of that for 3T3-L1 cells (>640 µmol/L, n=3), indicating the higher sensitivities of the tumorigenic B16 cells to geranylgeraniol-mediated growth suppression. The photomicrographs shown in Figure 1B reveal the impact of geranylgeraniol on the B16 cells following a 24-h incubation. The untreated cells (I) exhibited the characteristic contact inhibition-disabled growth of B16 cells. Increasing the concentration of geranylgeraniol from 0 to 30 (II) and 60 (III) µmol/L yielded dose-dependent decreases in cell density and marked cell elongation.

Since geranylgeraniol-mediated growth suppression may stem from the down-regulation of HMG-CoA reductase, we then evaluated the impact of supplemental mevalonate, the product of HMG-CoA reductase activity, on geranylgeraniol-induced

growth suppression (Figures 2). While geranylgeraniol (30-90 μmol/L) induced concentration-dependent growth suppression, supplemental mevalonate (500 μmol/L) significantly attenuated the effect of geranylgeraniol at all concentrations evaluated.

The effect of geranylgeraniol on HMG-CoA reductase was further demonstrated by real-time qPCR. Following a 24-h incubation with 60 μmol/L geranylgeraniol, B16 cells had a significantly lower level of HMG-CoA mRNA (Mann-Whitney post hoc analysis, n=4, $P<0.05$) with a medium value of 50% of that of control.

HMG-CoA reductase down-regulators have been shown to induce cell cycle arrest at the G1 phase (5). We then evaluated the impact of geranylgeraniol on the cell cycle distribution of the B16 cells (Figure 3). The percentages of cells at G1, S and G2 phases prior to incubation with geranylgeraniol were shown in Figure 3A. Following a 12-h incubation with geranylgeraniol the percentage of cells at the G1 phase increased from 42.2 ± 1.7% (control) to 59.1 ± 2.1% (30 μmol/L geranylgeraniol, $P<0.01$), 61.7 ± 0.3% (60 μmol/L geranylgeraniol, $P<0.01$), and 60.3 ± 0.4% (90 μmol/L geranylgeraniol, $P<0.01$), respectively. Co-incubation with 500 μmol/L mevalonolactone and 60 μmol/L geranylgeraniol reduced the percentage of cells at the G1 phase (42.2 ± 1.9%) to the control level (Figure 3B). Conversely, the percentage of cells at the S phase decreased from 45.6 ± 2.0% (control) to 25.5 ± 1.6% (30 μmol/L geranylgeraniol, $P<0.01$), 19.6 ± 3.3% (60 μmol/L geranylgeraniol, $P<0.01$), and 19.6 ± 1.3% (90 μmol/L geranylgeraniol, $P<0.01$), respectively. Co-incubation with 500 μmol/L mevalonolactone and 60 μmol/L geranylgeraniol increased the percentage of cells at the S phase (43.3 ± 0.9%, $P>0.05$) to the control level (Figure 3C). The G1/S ratio, an indicator of cell cycle arrest at the G1 phase, followed the pattern of G1 phase; that is, the ratio increased from 0.9 ± 0.1 (control) to 2.3 ± 0.2 (30 μmol/L geranylgeraniol, $P<0.01$), 3.2 ± 0.6 (60 μmol/L geranylgeraniol, $P<0.01$), and 3.1 ± 0.2 (90 μmol/L geranylgeraniol, $P<0.01$), respectively. Co-incubation with 500 μmol/L mevalonolactone and 60 μmol/L geranylgeraniol reduced the G1/S ratio (1.0 ± 0.1, $P>0.05$) to the control level (Figure 3E). The percentage of cells at the G2 phase also increased from 12.4 ± 0.9% (control) to 15.4 ± 1.2% (30 μmol/L geranylgeraniol, $P>0.05$), 18.7 ± 3.5% (60 μmol/L geranylgeraniol, $P<0.01$), and 20.1 ± 1.7% (90 μmol/L geranylgeraniol, $P<0.01$), respectively. Co-incubation with 500 μmol/L mevalonolactone and 60 μmol/L geranylgeraniol decreased the percentage of cells at the G2 phase (14.5 ± 1.0%, $P>0.05$) to the control level (Figure 3D).

Following a 24-h incubation with geranylgeraniol the percentage of cells at the G1 phase increased from 53.5 ± 6.5% (control) to 70.1 ± 0.5% (30 μmol/L geranylgeraniol, $P<0.01$) and 67.9 ± 0.7% (60 μmol/L geranylgeraniol, $P<0.01$), respectively (Figure 3F). Conversely, the percentage of cells at the S phase decreased from 33.3 ± 2.4% (control) to 16.5 ± 1.5% (30 μmol/L geranylgeraniol, $P<0.01$) and 11.4 ± 1.4% (60 μmol/L geranylgeraniol, $P<0.01$), respectively (Figure 3G). The G1/S ratio followed the pattern of G1 phase; that is, the ratio increased from 1.6 ± 0.3 (control) to 4.3 ± 0.4 (30 μmol/L geranylgeraniol, $P<0.01$) and 6.0 ± 0.8 (60 μmol/L geranylgeraniol, $P<0.01$), respectively (Figure 3I). Although supplemental mevalonolactone did not

significantly change the percentage of cells in either G1 or S phase, co-incubation with 500 µmol/L mevalonolactone and 60 µmol/L geranylgeraniol reduced the G1/S ratio to 4.5 ± 0.7, a value significantly different (P<0.05) from that for 60 µmol/L geranylgeraniol alone. The percentage of cells at the G2 phase also increased from 10.7 ± 0.9% (control) to 13.3 ± 1.0% (30 µmol/L geranylgeraniol, P>0.05) and 20.6 ± 0.9% (60 µmol/L geranylgeraniol, P<0.01), respectively. Co-incubation with 500 µmol/L mevalonolactone and 60 µmol/L geranylgeraniol decreased the percentage of cells at the G2 phase (13.3 ± 1.2%, P>0.05) to near the control level (Figure 3H).

The G1 arrest induced by geranylgeraniol was accompanied by a concentration-dependent suppression of the expression of cyclin D1 and Cdk4 (Figure 4), key regulators in the G1/S cell cycle progression (25). Cells incubated with 90 µmol/L of geranylgeraniol for 12 h had significantly lower expression of cyclin D1 and Cdk4 (P<0.01) than the control.

At 24-h, geranylgeraniol and lovastatin induced concentration-dependent decreases in the expression of cyclin D1.

HMG-CoA reductase suppressors also induce tumor cell apoptosis (5), an effect we examined next in B16 cells using the Guava Nexin™ assay with flow cytometry. The percentage of viable, early apoptotic and late apoptotic and necrotic cells in 12- (Figure 5A2-4) and 24-h (Figure 5A5-7) untreated groups were not different (P>0.05) from the 0-h values prior to incubation with geranylgeraniol (Figure 5A1). Following 12-h incubation with 90 µmol/L geranylgeraniol the percentage of viable cells (Figure 5A2) decreased significantly (P<0.05) whereas that of early apoptotic cells (Figure 5A3) increased (P<0.05). A greater impact of geranylgeraniol was observed when the incubation was extended to 24-h (Figure 5A5-7). The percentages of viable cells (Figure 5A5) following 24-h incubation with 60 and 90 µmol/L geranylgeraniol decreased significantly (P<0.01) whereas those of late apoptotic and necrotic cells (Figure 5A7) increased (P< 0.01). Worth noting is that supplemental mevalonate (500 µmol/L) attenuated the impact of 24-h incubation with 60 µmol/L geranylgeraniol by increasing the percentage of viable cells to the control level. Concurrently, the percentage of late apoptotic and necrotic cells also dropped to the control level when 60 µmol/L geranylgeraniol was blended with mevalonate (Figure 5A7). The high level of late apoptotic cells following the 24-h incubation with 90 µmol/L geranylgeraniol may have contributed to the lack of increase in the percentage of cells in the G1 phase (Figure 3F).

Photomicrographs of B16 cells (Figure 5B) obtained by acridine orange and ethidium bromide dual staining also confirmed geranylgeraniol-induced apoptosis. Viable cells have acridine orange staining with normal cell morphology. Acridine orange and ethidium bromide stained cells with condensed nucleus are in early and late apoptosis stages, respectively (23, 26). The number and percentage of ethidium bromide stained B16 cells following 24-h incubation with 75 µmol/L, or a mid-range value between 60 and 90 µmol/L, of geranylgeraniol (Figure 5B7) were higher than the control (Figure 5B3). Geranylgeraniol-treated cells showed nuclear condensation and membrane blebbing (Figure 5B6 & 7), morphological characteristics of apoptosis.

We then examined the impact of geranylgeraniol on ALP activity, a biomarker upregulated during differentiation (27). Geranylgeraniol induced ALP activity in B16 cells (Figure 6). The ALP activities for B16 cells incubated with 0, 30, 60 and 90 µmol/L geranylgeraniol for 48-h were 0.29 ± 0.02 (IU/L), 0.57 ± 0.00 (P<0.01), 0.55 ± 0.01 (P<0.05), and 0.77 ± 0.14 (P<0.001), with all geranylgeraniol-treated groups significantly different from the control.

Previously studies have shown that mevalonate suppressors have potentially synergistic impact on cell growth (28, 29). Next we evaluated the potential synergy attained with blends of geranylgeraniol and *d*-δ-tocotrienol, a vitamin E isomer with HMG-CoA reductase- (30, 31) and tumor- (32) suppressive activities, in suppressing the growth of B16 cells. Geranylgeraniol at 15 µmol/L and *d*-δ-tocotrienol at 10 µmol/L suppressed the growth of B16 cells by 11% and 24%, respectively; a blend of the agents suppressed cell growth by 39% (Table 1), approximating the sum of individual impacts and indicating an additive effect. The cumulative effect was also shown with the blend containing 15 µmol/L geranylgeraniol and 20 µmol/L *d*-δ-tocotrienol.

Table 1. Cumulative impact of geranylgeraniol and *d*-δ-tocotrienol on the proliferation of murine B16 melanoma cells

	Growth,	Suppression % of control
Control	100 ±6 [a*]	
Geranylgeraniol (15 µmol/L)	89 ±4 [ab]	11
d-δ-Tocotrienol (10 µmol/L)	76 ±13 [bc]	24
d-δ-Tocotrienol (20 µmol/L)	44 ±10 [de]	56
Geranylgeraniol (15 µmol/L)+*d*-δ-Tocotrienol (10 µmol/L)	61 ±4 [cd]	39(35)**
Geranylgeraniol (15 µmol/L)+*d*-δ-Tocotrienol (20 µmol/L)	29 ±4 [e]	71 (67)

*Values are mean ± SD, n = 3. Means that are not denoted with a common letter are different (P<0.05) based on one-way ANOVA with Tukey's Multiple Comparison Test.
**Numbers in the parentheses indicate expected percentage of growth suppression based on the sum of individual suppressions.

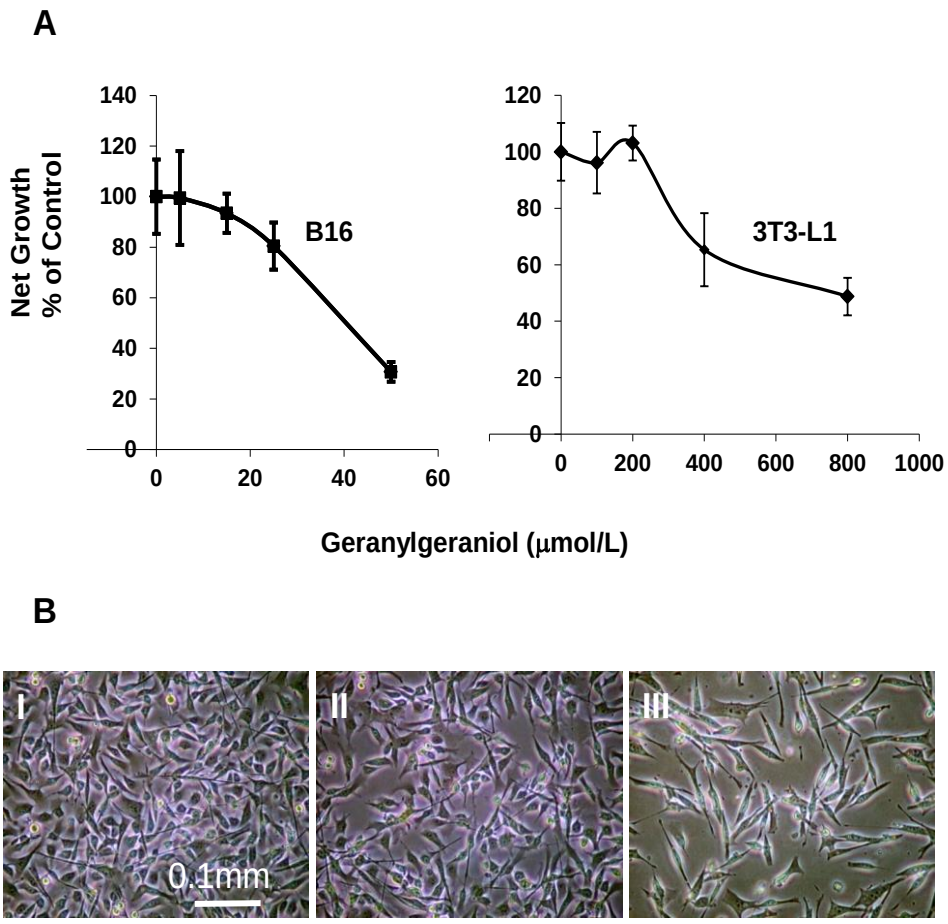

Figure 1.

Figure 1. The differential impacts of geranylgeraniol on the growth of murine B16 melanoma cells and murine 3T3-L1 embryo fibroblasts. (A) Representative growth curves showing the concentration-dependent impact of geranylgeraniol on the growth of murine B16 melanoma cells (■) and the impact of geranylgeraniol on 3T3-L1 embryo fibroblasts (♦). Cells were cultured and incubated with geranylgeraniol for 48 h before cell growth was measured by CellTiter 96® Aqueous One Solution. Values are mean ± SD, n = 4. (B) The concentration-dependent inhibition of murine B16 melanoma cell growth shown in photomicrographs of B16 cells following a 24-h incubation with 0 (I), 30 (II), and 60 (III) μmol/L geranylgeraniol. The contact inhibition-disabled growth of the B16 cells is shown in the Control culture (I). Concentration-dependent cell elongation and decrease in cell density occur progressively as the concentration of geranylgeraniol is increased (II & III).

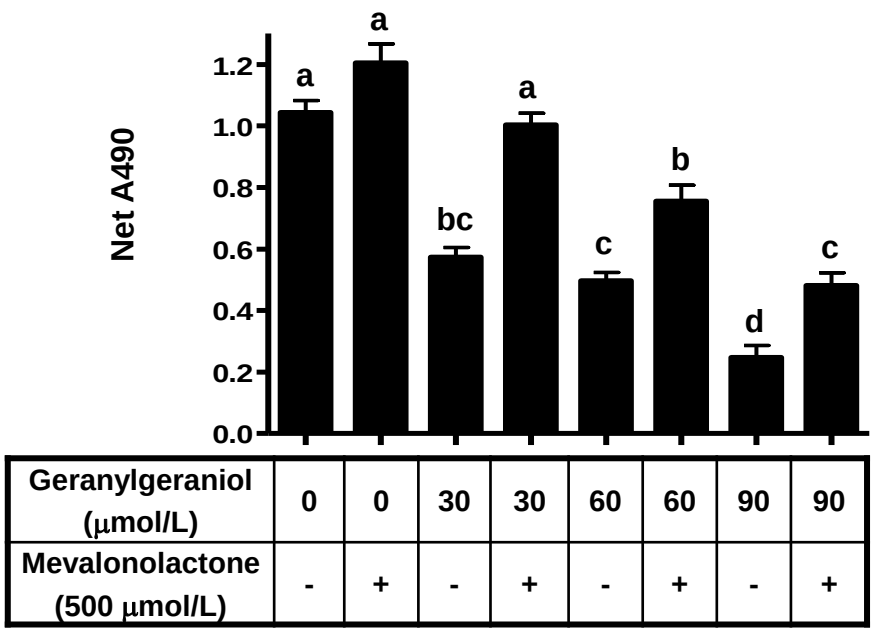

Figure 2. Mevalonolactone (500 μmol/L) attenuates the geranylgeraniol-mediated growth suppression in murine B16 melanoma cells following a 48-h incubation with 0, 30, 60 and 90 μmol/L of geranylgeraniol. Values for net growth measured by net absorbance at 490 nm are mean±SD, n=6. There were significant effects of geranylgeraniol concentration (P<0.001), mevalonolactone supplementation (P<0.001) and their interaction (P<0.05) based on two-way ANOVA. All geranylgeraniol groups without mevalonolactone were significantly different from their mevalonolactone-free control (Tukey's, P<0.05). With mevalonolactone supplementation, groups with 60 and 90 μmol/L geranylgeraniol were different from their control (Tukey's, P<0.05). Groups with blends of geranylgeraniol and mevalonolactone were different from their respective mevalonolactone-free groups (Tukey's, P<0.05).

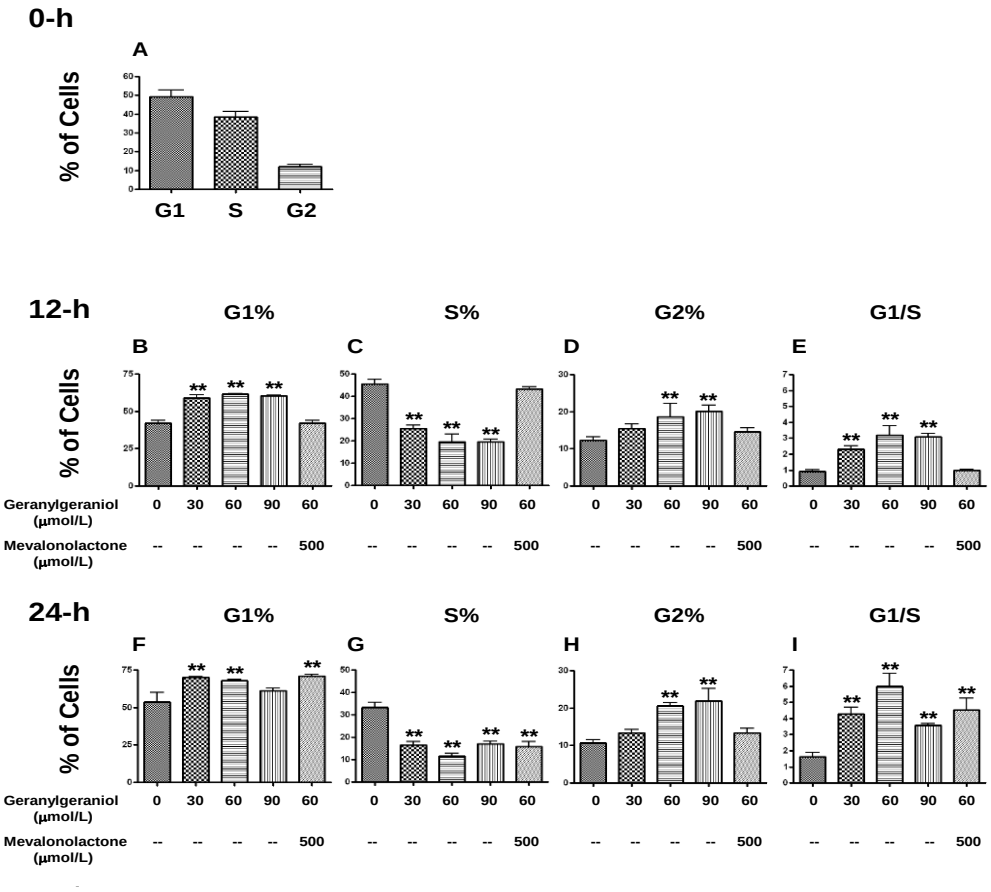

Figure 3. The impact of geranylgeraniol on the cell cycle distribution of murine B16 melanoma cells. The percentages of murine B16 melanoma cells in G1 (B & F), S (C & G), and G2 (D & H) phases of the cell cycle and the G1/S ratio (E & I) of B16 cells following 0- (A), 12- (B-E) and 24- (F-I) h incubations with 0, 30, 60 and 90 μmol/L geranylgeraniol blended with 0 and 500 μmol/L mevalonolactone. Values are mean ± SD, n=3. Differences between treated and control (0 μmol/L) groups were analyzed by one-way ANOVA with Dunnett's post test (**P*<0.05; ***P*< 0.01).

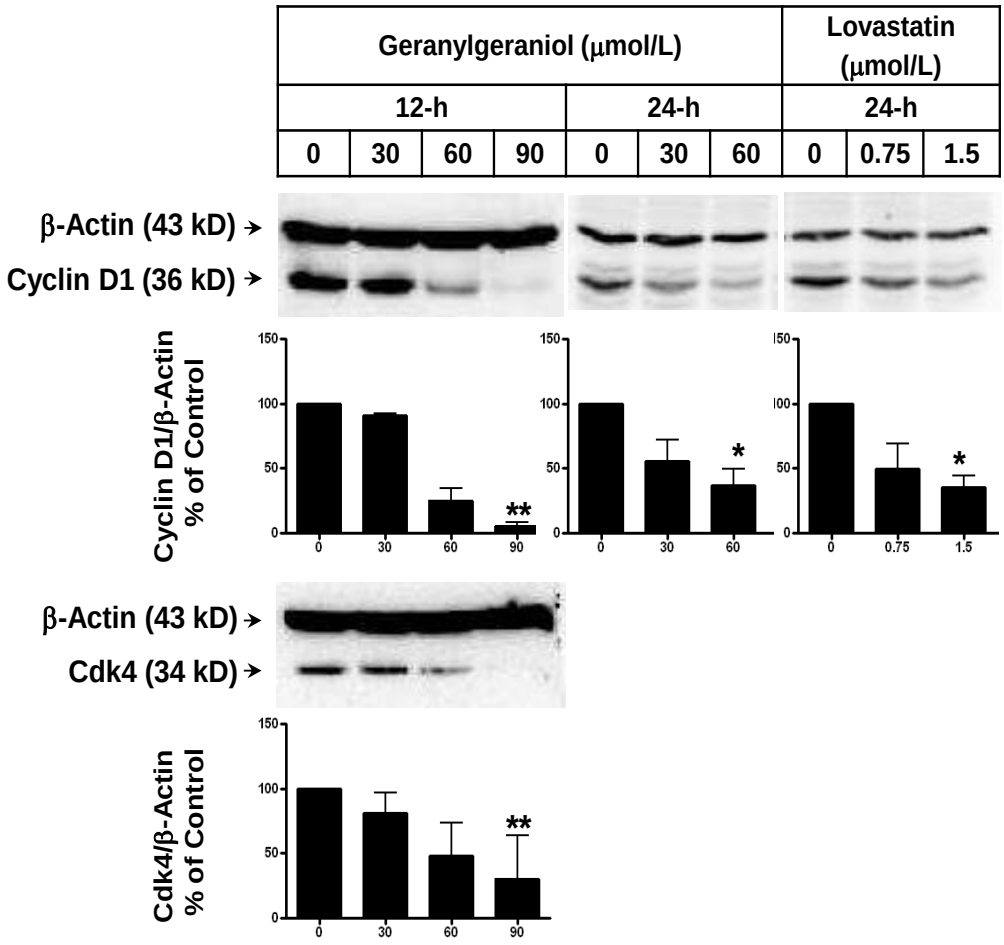

Figure 4. The impact of geranylgeraniol and lovastatin on the expression of cyclin-dependent kinase (Cdk) 4 and cyclin D1 in murine B16 melanoma cells following 12- and 24-h incubations shown in representative blots. Cell lysates were subjected to western-blot procedures and blots were detected by chemiluminescence and quantitated. The values for the ratios of Cdk4/β-actin and cyclin D1/β-actin shown in the bar graphs are median ± range, n ≥ 3. Values with * and ** are significantly different from that of control with $P<0.05$ and $P<0.01$, respectively, based on Kruskal-Wallis test followed by Dunnett's multiple comparison test.

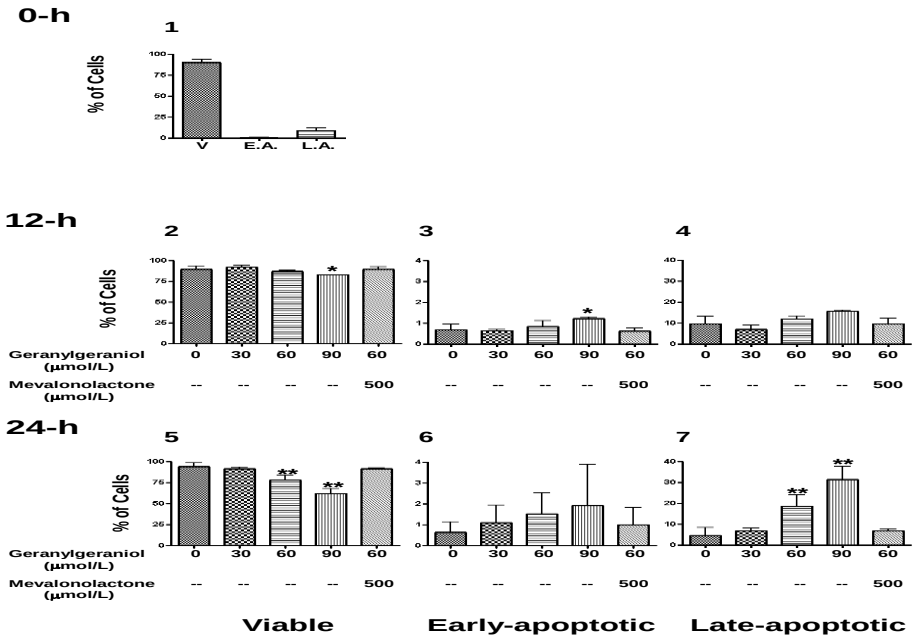

Figure 5A.

Figure 5. The impact of geranylgeraniol on the initiation of apoptosis in murine B16 melanoma cells. (A) The percentages of viable (V), early-apoptotic (E.A.), and late-apoptotic and necrotic (L.A.) B16 cells following 0- (1), 12- (2-4) and 24- (5-7) h incubations with geranylgeraniol as measured by the Guava Nexin™ assay. The percentages of V, E.A., and L.A. cells prior to geranylgeraniol incubation are shown in 1. Following a 12-h incubation with 90 μmol/L geranylgeraniol, the percentage of viable cells (2) decreased; concomitantly, the percentage of early apoptotic cells (3) increased. A 24-h incubation with 60 and 90 μmol/L geranylgeraniol led to decreased percentage of viable cells (5) and increased percentage of late apoptotic cells (7). Supplemental mevalonolactone significantly attenuated the impact of 24-h geranylgeraniol incubation on the percentages of viable (5) and late apoptotic and necrotic (7) cells. Values are mean ± SD, n = 3. Differences between treated and control (0 μmol/L) groups were analyzed by one-way ANOVA with Dunnett's post test (**P*< 0.05; ***P*<0.01). (B) Photomicrographs of murine B16 melanoma cells showing the geranylgeraniol-initiated apoptosis detected by acridine orange and ethidium bromide dual staining. B16 cells were incubated with 0 (1-4) and 75 (5-8) μmol/L geranylgeraniol for 24 h. Photomicrographs of the same fields were taken under phase-contrast microscope (1 and 5) and fluorescence microscope with a fluorescein isothiocyanate (FITC) (2 and 6) or tetramethylrhodamine isothiocyanate (TRITC) (3 and 7) filter and then merged (4 and 8). Arrows mark the red fluorescence emission from ethidium bromide staining shown in late apoptotic and necrotic cells induced by geranylgeraniol

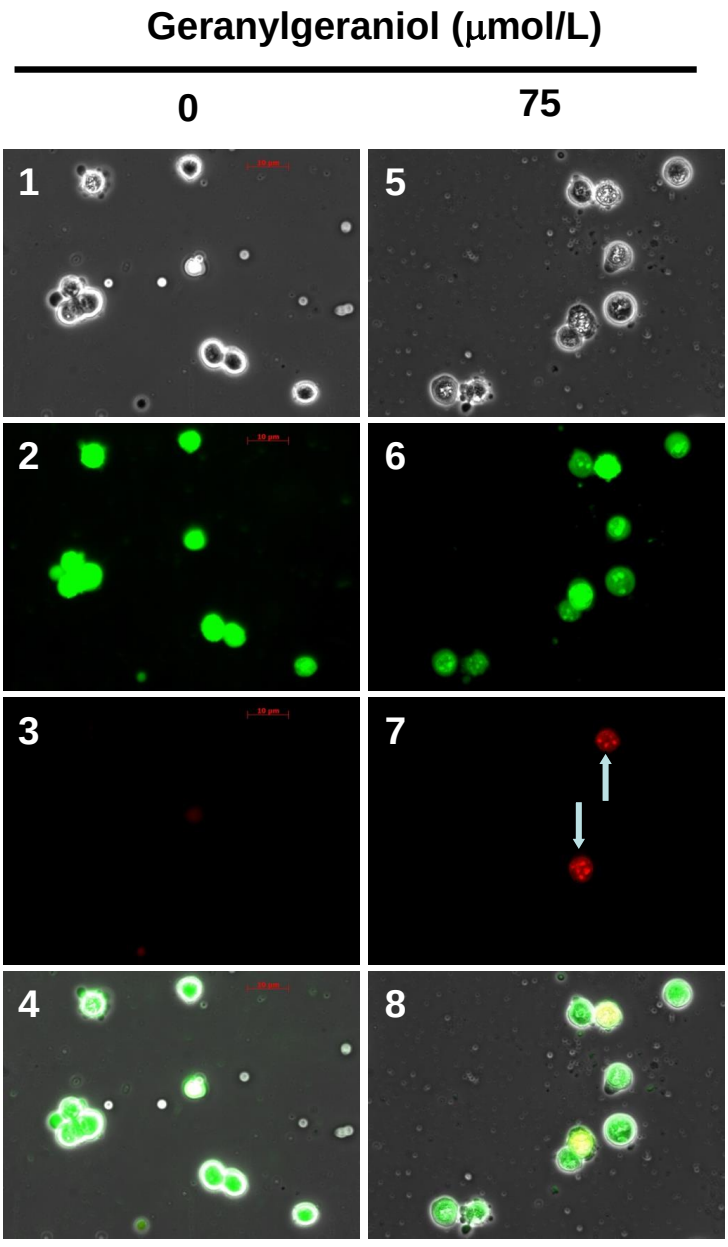

Figure 5B.

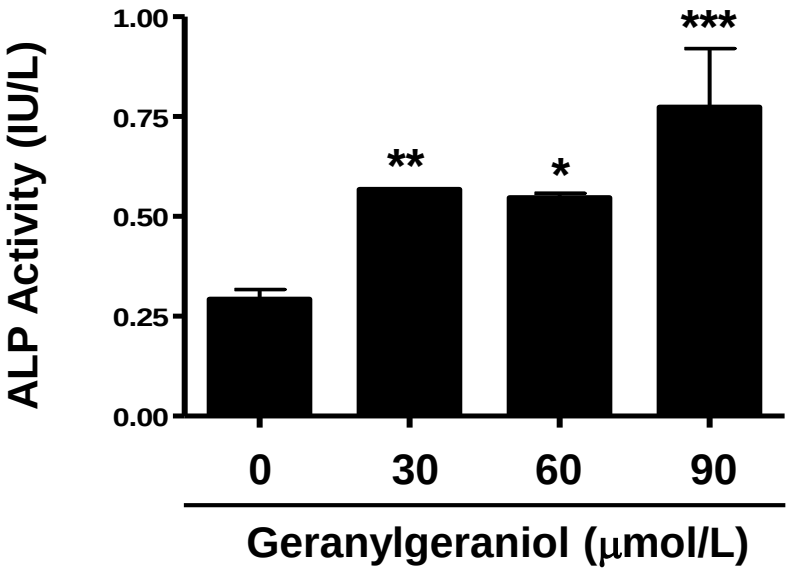

Figure 6. The impact of geranylgeraniol on alkaline phosphatase (ALP) activity in murine B16 melanoma cells. Following a 48-h incubation with 0, 30, 60, and 90 μmol/L geranylgeraniol, B16 cells were lysed and ALP activity in the supernatant was analyzed using QuantiChrom™ Alkaline Phosphatase Assay Kit as described in Materials and Methods. Values are mean ± SD, n = 3. Values with *, ** and *** are significantly different from that of control with $P<0.05$, $P<0.01$, and $P<0.001$, respectively, as determined by one-way ANOVA with Tukey's multiple comparison test.

DISCUSSION:

Diverse cell lines have a wide range of sensitivity to geranylgeraniol-mediated growth suppression, with IC50 values ranging from 10 μmol/L for human HuH-7 hepatoma cells (18) to 400 μmol/L for human H460 lung adenocarcinoma cells (16); those for other tumor cells originated from pancreas (14, 20), stomach, colon, liver, blood and ovary (14) fall somewhere in between. The IC50 value for geranylgeraniol in B16 cells evaluated herein lies in the mid-range of the reported IC50 values. The underlying mechanisms for such a wide range of sensitivities remain unknown, though they may be related to culture conditions including cell density and length of treatment and potentially the differential extent of dysregulation of the mevalonate pathway in various cell lines. The cell growth assay employed in this study does not differentiate cytostatic and cytotoxic effects that could both lead to decreased cell numbers. The morphological changes induced by geranylgeraniol are reminiscent of those effected by other mevalonate suppressors including lovastatin and tocotrienols (28).

The geranylgeraniol-induced concentration-dependent impact on cell cycle distribution of B16 cells is consistent with the G1 arrest mediated by geranylgeraniol in A549 cells (17). Lovastatin (33, 34) and other isoprenoid mevalonate suppressors including the monoterpenes perillyl alcohol and geraniol (35), sesquiterpenes *trans*, *trans*-farnesol (35) and β-ionone (5, 36), and tocotrienols (5) have been shown to induce G1 arrest in tumor cells. Mevalonate attenuated the lovastatin-mediated G1 arrest in human T24 bladder carcinoma cells (37) and MCF-7 breast cancer cells (38). The geranylgeraniol-mediated down-regulation of cyclin D1 and Cdk4, two regulators of the G1 to S transition, is consistent with the upregulation of p21 and p27, two suppressors of cyclin D1 and Cdk4 (39), and down-regulation of cyclin D1 and Cdk4 induced by other mevalonate suppressors including lovastatin (40), perillyl alcohol (35), geraniol (35, 41), farnesol (35), β-ionone (41), and lycopene (42). Mevalonate attenuated the lovastatin-mediated upregulation of p21 and p27 in MDA-MB-157 tumor cells (40).

Geranylgeraniol-induced B16 cell apoptosis is consistent with previous reports in A549 lung adenocarcinoma cells (11, 17), HL-60 (12, 13, 43), K562 (12, 13), ML1, M1, P388 (43) and U937 (15, 43) leukemia cells, COLO320 DM colon adenocarcinoma cells (13), HuH-7 hepatoma cells (18), and TYK-nu ovarian cancer cells (19). Geranylgeraniol also activates caspase-3 (15, 18, 44) and PARP cleavage (44). The concentration of geranylgeraniol required to induce apoptosis in these studies (12, 13, 15, 17) falls in the 30-90 μmol/L range employed in the present study for the induction of apoptosis in B16 cells (Figure 5).

Geranylgeraniol-induced ALP activity, an indicator of B16 cell differentiation, is reminiscent of the geranylgeranylacetone-induced differentiation of human U937, ML1 and HL-60 myeloid leukemia cells (45). Consequently, menaquinone 4 (46, 47) with a geranylgeraniol moiety, rather than phylloquinone (46) with a phytol side chain, is able to induce differentiation.

Parallel to the impact of geranylgeraniol, mevalonate suppressors (48) including the monoterpenes (49), sodium phenylacetate, sodium phenylbutyrate (50), lovastatin (51, 52) and genistein (53) induce tumor cell differentiation.

Mevalonate suppressors have been shown to induce cell cycle arrest, apoptosis, and differentiation, consequent to the impaired post-translational modification of Ras (26), insulin-like growth factor 1 receptor (48) and nuclear lamins (5). These events may have collectively contributed to the geranylgeraniol-induced growth suppression. Supplemental mevalonolactone attenuated growth suppression, cell cycle arrest and apoptosis, further supporting our hypothesis that the suppression of HMG-CoA reductase activity, at least in part, mediates the impact of geranylgeraniol in B16 cells. Previous studies have shown that geranylgeraniol suppresses reductase activity in fibroblasts (9, 10), human A549 lung adenocarcinoma cells (11) and human MCF-7 breast adenocarcinoma cells (54); mevalonate attenuated the geranylgeraniol impact in MCF-7 cells (54). The IC50 value (55 μmol/L) of geranylgeraniol in suppressing the growth of B16 cells equals to that required to suppress HMG-CoA reductase by 50% in A549 cells (11) and MCF-7 cells (54) and in the current study, that required to suppress the mRNA level for HMG-CoA reductase by 50%. Consequent to HMG-CoA reductase down-regulation, gavage feeding of geranylgeraniol reduced plasma cholesterol level in Wistar rats and more prominently, reduce tumor incidence and the size of preneoplastic lesions in chemically initiated hepatocarcinogenesis (55).

Previous studies have used mevalonate at concentrations ranging from 500 μmol/L (54) to 4 mmol/L (40) to show its ability to reverse the effects of mevalonate suppressors including geranylgeraniol and lovastatin. Though at the lower end of that range, the 500 μmol/L mevalonolactone used herein far exceeds physiologically attainable levels. It is conceivable that secondary effects of the pharmaceutical level of mevalonate beyond the repletion of cellular mevalonate pool may have interfered with the impact of geranylgeraniol. *In vivo* studies may provide more direct evidence linking the reductase- and tumor- suppressive activities of geranylgeraniol. Nevertheless, the present study may have identified mevalonate depletion as a unifying mechanism for geranylgeraniol-mediated tumor suppression.

The concentration of geranylgeraniol, 100 μmol/L, employed to suppress reductase in fibroblasts (9) is twice as high as that in the A549 cells (11), MCF-7 cells (54) and the B16 cells herein. In the present study murine 3T3-L1 cells were more than 10-fold resistant than B16 cells to geranylgeraniol-mediated growth suppression, suggesting a tumor-targeting action of geranylgeraniol. Geranylgeraniol may be added to the growing list of isoprenoids with specific impact on the uniquely dysregulated HMG-CoA reductase in tumors (48). It remains unknown whether the reductase is dysregulated in B16 melanoma cells.

Blends of mevalonate suppressors synergistically suppress tumor growth (28, 29, 48). The additive effect of geranylgeraniol and *d*-δ-tocotrienol in suppressing B16 cell growth could reflect their dual impact on HMG-CoA reductase. *In vivo* and further mechanistic studies may reveal whether geranylgeraniol and a broad class of mevalonate-

derived secondary products, the pure and mixed isoprenoids with reductase-suppressive activities, have potential in cancer chemoprevention and/or therapy when applied individually and in blends.

Statement of Author Contributions and Acknowledgements

All authors participated in the design, interpretation of the studies and analysis of the data and review of the manuscript. RK, NVF, ME, DD, NM, and DLH conducted the experiments. HM, CK and DLH contributed to the conceptualization of the studies. HM wrote the manuscript.

The authors thank Dr. Heather Conrad-Webb of the Biology Department for her assistance with the BD FACSCalibur.

REFERENCES:

1. Hutchison CJ, Bridger JM, Cox LS, Kill IR. Weaving a pattern from disparate threads: lamin function in nuclear assembly and DNA replication. *J Cell Sci* 1994;**107**:3259-69
2. Crowell PL, Chang RR, Ren ZB, Elson CE, Gould MN. Selective inhibition of isoprenylation of 21-26-kDa proteins by the anticarcinogen d-limonene and its metabolites. *J Biol Chem* 1991;**266**:17679-85
3. Goldstein JL, Brown MS. Regulation of the mevalonate pathway. *Nature* 1990;**343**:425-30
4. Elson CE, Peffley DM, Hentosh P, Mo H. Isoprenoid-mediated inhibition of mevalonate synthesis: potential application to cancer. *Proc Soc Exp Biol Med* 1999;**221**:294-311
5. Mo H, Elson CE. Apoptosis and cell-cycle arrest in human and murine tumor cells are initiated by isoprenoids. *J Nutr* 1999;**129**:804-13
6. Fedeli E, Capella P, Cirimele M, Jacini G. Isolation of geranyl geraniol from the unsaponifiable fraction of linseed oil. *J Lipid Res* 1966;**7**:437-41
7. Myers CE, Trepel J, Sausville E, Samid D, Miller A, Curt G. Monoterpenes, sesquiterpenes and diterpenes as cancer therapy. United States Patent 5,602,184, 1997.
8. Mors WB, dos Santos Filho MF, Monteiro HJ, Gilbert B, Pellegrino J. Chemoprophylactic agent in schistosomiasis: 14,15-epoxygeranylgeraniol. *Science* 1967;**157**:950-1
9. Sever N, Song BL, Yabe D, Goldstein JL, Brown MS, DeBose-Boyd RA. INSIG1-dependent ubiquitination and degradation of mammalian 3-hydroxy-3-methylglutaryl-CoA reductase stimulated by sterols and geranylgeraniol. *J Biol Chem* 2003;**278**:52479-90
10. Houten SM, Schneiders MS, Wanders RJ, Waterham HR. Regulation of isoprenoid/cholesterol biosynthesis in cells from mevalonate kinase-deficient patients. *J Biol Chem* 2003;**278**:5736-43
11. Miquel K, Pradines A, Favre G. Farnesol and geranylgeraniol induce actin cytoskeleton disorganization and apoptosis in A549 lung adenocarcinoma cells. *Biochem Biophys Res Commun* 1996;**225**:869-76
12. Ohizumi H, Masuda Y, Yoda M, Hashimoto S, Aiuchi T, Nakajo S, Sakai I, Ohsawa S, Nakaya K. Induction of apoptosis in various tumor cell lines by geranylgeraniol. *Anticancer Res* 1997;**17**:1051-7
13. Ohizumi H, Masuda Y, Nakajo S, Sakai I, Ohsawa S, Nakaya K. Geranylgeraniol is a potent inducer of apoptosis in tumor cells. *J Biochem (Tokyo)* 1995;**117**:11-3
14. Shibayama-Imazu T, Sakairi S, Watanabe A, Aiuchi T, Nakajo S, Nakaya K. Vitamin K(2) selectively induced apoptosis in ovarian TYK-nu and pancreatic MIA PaCa-2 cells out of eight solid tumor cell lines through a mechanism different from geranylgeraniol. *J Cancer Res Clin Oncol* 2003;**129**:1-11

15. Masuda Y, Nakaya M, Nakajo S, Nakaya K. Geranylgeraniol potently induces caspase-3-like activity during apoptosis in human leukemia U937 cells. *Biochem Biophys Res Commun* 1997;**234**:641-5
16. Joo JH, Liao G, Collins JB, Grissom SF, Jetten AM. Farnesol-induced apoptosis in human lung carcinoma cells is coupled to the endoplasmic reticulum stress response. *Cancer Res* 2007;**67**:7929-36
17. Miquel K, Pradines A, Terce F, Selmi S, Favre G. Competitive inhibition of choline phosphotransferase by geranylgeraniol and farnesol inhibits phosphatidylcholine synthesis and induces apoptosis in human lung adenocarcinoma A549 cells. *J Biol Chem* 1998;**273**:26179-86
18. Takeda Y, Nakao K, Nakata K, Kawakami A, Ida H, Ichikawa T, Shigeno M, Kajiya Y, Hamasaki K, Kato Y, Eguchi K. Geranylgeraniol, an intermediate product in mevalonate pathway, induces apoptotic cell death in human hepatoma cells: death receptor-independent activation of caspase-8 with down-regulation of Bcl-xL expression. *Jpn J Cancer Res* 2001;**92**:918-25
19. Shibayama-Imazu T, Sonoda I, Sakairi S, Aiuchi T, Ann WW, Nakajo S, Itabe H, Nakaya K. Production of superoxide and dissipation of mitochondrial transmembrane potential by vitamin K2 trigger apoptosis in human ovarian cancer TYK-nu cells. *Apoptosis* 2006;**11**:1535-43
20. Burke YD, Stark MJ, Roach SL, Sen SE, Crowell PL. Inhibition of pancreatic cancer growth by the dietary isoprenoids farnesol and geraniol. *Lipids* 1997;**32**:151-6
21. McAnally JA, Jung M, Mo H. Farnesyl-O-acetylhydroquinone and geranyl-O-acetylhydroquinone suppress the proliferation of murine B16 melanoma cells, human prostate and colon adenocarcinoma cells, human lung carcinoma cells, and human leukemia cells. *Cancer Lett* 2003;**202**:181-92
22. Fernandes N, Jung M, Daoud A, Mo H. Biphenylalkylacetylhydroquinone ethers suppress the proliferation of murine B16 melanoma cells. *Anticancer Res* 2008;**28**:1005-12
23. Hussein D, Mo H. *d*-δ-Tocotrienol-mediated suppression of the proliferation of human PANC-1, MIA PaCa2 and BxPC-3 pancreatic carcinoma cells. *Pancreas* 2009;**38**:e124-36
24. de Jonge HJ, Fehrmann RS, de Bont ES, Hofstra RM, Gerbens F, Kamps WA, de Vries EG, van der Zee AG, te Meerman GJ, ter Elst A. Evidence based selection of housekeeping genes. *PLoS One* 2007;**2**:e898
25. Massague J. G1 cell-cycle control and cancer. *Nature* 2004;**432**:298-306
26. Fernandes NV, Guntipalli PK, Mo H. *d*-δ-Tocotrienol-mediated cell cycle arrest and apoptosis in human melanoma cells. *Anticancer Res* 2010;**30**:4937-44
27. Yamada T, Ohwada S, Saitoh F, Adachi M, Morishita Y, Hozumi M. Induction of Ley antigen by 5-aza-2'-deoxycytidine in association with differentiation and apoptosis in human pancreatic cancer cells. *Anticancer Res* 1996;**16**:735-40
28. McAnally JA, Gupta J, Sodhani S, Bravo L, Mo H. Tocotrienols potentiate lovastatin-

mediated growth suppression *in vitro* and *in vivo*. *Exp Biol Med (Maywood)* 2007;**232**:523-31
29. Tatman D, Mo H. Volatile isoprenoid constituents of fruits, vegetables and herbs cumulatively suppress the proliferation of murine B16 melanoma and human HL-60 leukemia cells. *Cancer Lett* 2002;**175**:129-39
30. Parker RA, Pearce BC, Clark RW, Gordon DA, Wright JJ. Tocotrienols regulate cholesterol production in mammalian cells by post-transcriptional suppression of 3-hydroxy-3-methylglutaryl-coenzyme A reductase. *J Biol Chem* 1993;**268**:11230-8
31. Song BL, DeBose-Boyd RA. INSIG1-dependent ubiquitination and degradation of 3-hydroxy-3-methylglutaryl coenzyme a reductase stimulated by δ- and γ-tocotrienols. *J Biol Chem* 2006;**281**:25054-61
32. Mo H, Elson CE. Role of the mevalonate pathway in tocotrienol-mediated tumor suppression. In: Watson RR, Preedy VR, Eds. *Tocotrienols: vitamin E beyond tocopherols*. Boca Raton: CRC Press,2008: p185-207.
33. Rao S, Lowe M, Herliczek TW, Keyomarsi K. Lovastatin mediated G1 arrest in normal and tumor breast cells is through inhibition of CDK2 activity and redistribution of p21 and p27, independent of p53. *Oncogene* 1998;**17**:2393-402
34. Park C, Lee I, Kang WK. Lovastatin-induced E2F-1 modulation and its effect on prostate cancer cell death. *Carcinogenesis* 2001;**22**:1727-31
35. Wiseman DA, Werner SR, Crowell PL. Cell cycle arrest by the isoprenoids perillyl alcohol, geraniol, and farnesol is mediated by p21(Cip1) and p27(Kip1) in human pancreatic adenocarcinoma cells. *J Pharmacol Exp Ther* 2007;**320**:1163-70
36. He L, Mo H, Hadisusilo S, Qureshi AA, Elson CE. Isoprenoids suppress the growth of murine B16 melanomas *in vitro* and *in vivo*. *J Nutr* 1997;**127**:668-74
37. Jakobisiak M, Bruno S, Skierski JS, Darzynkiewicz Z. Cell cycle-specific effects of lovastatin. *Proc Natl Acad Sci U S A* 1991;**88**:3628-3238. Keyomarsi K, Sandoval L, Band V, Pardee AB. Synchronization of tumor and normal cells from G1 to multiple cell cycles by lovastatin. *Cancer Res* 1991;**51**:3602-9
39. Sherr CJ. Mammalian G1 cyclins. *Cell* 1993;**73**:1059-65
40. Gray-Bablin J, Rao S, Keyomarsi K. Lovastatin induction of cyclin-dependent kinase inhibitors in human breast cells occurs in a cell cycle-independent fashion. *Cancer Res* 1997;**57**:604-9
41. Duncan RE, Lau D, El-Sohemy A, Archer MC. Geraniol and β-ionone inhibit proliferation, cell cycle progression, and cyclin-dependent kinase 2 activity in MCF-7 breast cancer cells independent of effects on HMG-CoA reductase activity. *Biochem Pharmacol* 2004;**68**:1739-47
42. Palozza P, Colangelo M, Simone R, Catalano A, Boninsegna A, Lanza P, Monego G, Ranelletti FO. Lycopene induces cell growth inhibition by altering mevalonate pathway and Ras signaling in cancer cell lines. *Carcinogenesis* 2010;**31**:1813-21
43. Masuda Y, Yoda M, Ohizumi H, Aiuchi T, Watabe M, Nakajo S, Nakaya K. Activation of protein kinase C prevents induction of apoptosis by geranylgeraniol in human leukemia HL60 cells. *Int J Cancer* 1997;**71**:691-7

44. Au-Yeung KK, Liu PL, Chan C, Wu WY, Lee SS, Ko JK. Herbal isoprenols induce apoptosis in human colon cancer cells through transcriptional activation of *Ppar*gamma. *Cancer Invest* 2008;**26**:708-17
45. Sakai I, Tanaka T, Osawa S, Hashimoto S, Nakaya K. Geranylgeranylacetone used as an antiulcer agent is a potent inducer of differentiation of various human myeloid leukemia cell lines. *Biochem Biophys Res Commun* 1993;**191**:873-9
46. Sakai I, Hashimoto S, Yoda M, Hida T, Ohsawa S, Nakajo S, Nakaya K. Novel role of vitamin K2: a potent inducer of differentiation of various human myeloid leukemia cell lines. *Biochem Biophys Res Commun* 1994;**205**:1305-10
47. Takami A, Nakao S, Ontachi Y, Yamauchi H, Matsuda T. Successful therapy of myelodysplastic syndrome with menatetrenone, a vitamin K2 analog. *Int J Hematol* 1999;**69**:24-6
48. Mo H, Elson CE. Studies of the isoprenoid-mediated inhibition of mevalonate synthesis applied to cancer chemotherapy and chemoprevention. *Exp Biol Med (Maywood)* 2004;**229**:567-85
49. Shi W, Gould MN. Induction of differentiation in neuro-2A cells by the monoterpene perillyl alcohol. *Cancer Lett* 1995;**95**:1-6
50. Melichar B, Ferrandina G, Verschraegen CF, Loercher A, Abbruzzese JL, Freedman RS. Growth inhibitory effects of aromatic fatty acids on ovarian tumor cell lines. *Clin Cancer Res* 1998;**4**:3069-76
51. Maltese WA. Induction of differentiation in murine neuroblastoma cells by mevinolin, acompetitive inhibitor of 3-hydroxy-3-methylglutaryl coenzyme A reductase. *Biochem Biophys Res Commun* 1984;**120**:454-60
52. Dimitroulakos J, Thai S, Wasfy GH, Hedley DW, Minden MD, Penn LZ. Lovastatin induces a pronounced differentiation response in acute myeloid leukemias. *Leuk Lymphoma* 2000;**40**:167-78
53. Record IR, Broadbent JL, King RA, Dreosti IE, Head RJ, Tonkin AL. Genistein inhibits growth of B16 melanoma cells *in vivo* and *in vitro* and promotes differentiation *in vitro*. *Int J Cancer* 1997;**72**:860-4
54. Raikkonen J, Monkkonen H, Auriola S, Monkkonen J. Mevalonate pathway intermediates downregulate zoledronic acid-induced isopentenyl pyrophosphate and ATP analog formation in human breast cancer cells. *Biochem Pharmacol* 2010;**79**:777-83
55. de Moura Espindola R, Mazzantini RP, Ong TP, de Conti A, Heidor R, Moreno FS. Geranylgeraniol and β-ionone inhibit hepatic preneoplastic lesions, cell proliferation, total plasma cholesterol and DNA damage during the initial phases of hepatocarcinogenesis, but only the former inhibits NF-κB activation. *Carcinogenesis* 2005;**26**:1091-9

APPENDIX C
A Book Chapter in Tocotrienols: Vitamin E Beyond Tocopherols

Mevalonate-suppressive tocotrienols for cancer chemoprevention and adjuvant therapy

Mo H, Elfakhani M., Shah A, Yeganehjoo H. (2013) Mevalonate-suppressive tocotrienols for cancer chemoprevention and adjuvant therapy, in *Tocotrienols: vitamin E beyond tocopherols*. 2nd ed., eds B. Tan, R.R. Watson & V.R. Preedy. CRC Press, Boca Raton, FL. Page 135-149.

Acknowledgments

This work was partially supported by the Agriculture and Food Research Initiative Grant 2009-02941 from the USDA National Institute for Food and Agriculture, Texas Department of Agriculture Food and Fiber Research Program, and Texas Woman's University Research Enhancement Program.